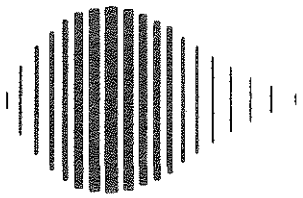

NATIONAL CENTER FOR EARTHQUAKE
ENGINEERING RESEARCH
State University of New York at Buffalo

AUTOMATED SEISMIC DESIGN OF REINFORCED CONCRETE BUILDINGS

by

Y. S. Chung and M. Shinozuka
Department of Civil Engineering and Operations Research
Princeton University
Princeton, New Jersey 08544

and

C. Meyer
Department of Civil Engineering and Engineering Mechanics
Columbia University
New York, New York 10027-6699

Technical Report NCEER-88-0024

July 5, 1988

This research was conducted at Princeton University and Columbia University and was partially supported by the National Science Foundation under Grant No. ECE 86-07591.

NOTICE

This report was prepared by Princeton University and Columbia University as a result of research sponsored by the National Center for Earthquake Engineering Research (NCEER). Neither NCEER, associates of NCEER, its sponsors, Princeton University, Columbia University, nor any person acting on their behalf:

a. makes any warranty, express or implied, with respect to the use of any information, apparatus, method, or process disclosed in this report or that such use may not infringe upon privately owned rights; or

b. assumes any liabilities of whatsoever kind with respect to the use of, or for damages resulting from the use of, any information, apparatus, method or process disclosed in this report.

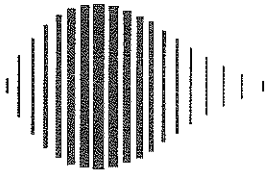

AUTOMATED SEISMIC DESIGN OF REINFORCED CONCRETE BUILDINGS

by

Y.S. Chung[1], C. Meyer[2] and M. Shinozuka[3]

July 5, 1988

Technical Report NCEER-88-0024

NCEER Contract Number 86-3033

NSF Master Contract Number ECE 86-07591

1 Research Associate, Dept. of Civil Engineering and Operations Research, Princeton University
2 Associate Professor, Dept. of Civil Engineering, Columbia University
3 Professor, Dept. of Civil Engineering and Operations Research, Princeton University

NATIONAL CENTER FOR EARTHQUAKE ENGINEERING RESEARCH
State University of New York at Buffalo
Red Jacket Quadrangle, Buffalo, NY 14261

PREFACE

The National Center for Earthquake Engineering Research (NCEER) is devoted to the expansion of knowledge about earthquakes, the improvement of earthquake-resistant design, and the implementation of seismic hazard mitigation procedures to minimize loss of lives and property. The emphasis is on structures and lifelines that are found in zones of moderate to high seismicity throughout the United States.

NCEER's research is being carried out in an integrated and coordinated manner following a structured program. The current research program comprises four main areas:

- Existing and New Structures
- Secondary and Protective Systems
- Lifeline Systems
- Disaster Research and Planning

This technical report pertains to Program 1, Existing and New Structures, and more specifically to Reliability Analysis and Risk Assessment.

The long term goal of research in Existing and New Structures is to develop seismic hazard mitigation procedures through rational probabilistic risk assessment for damage or collapse of structures, mainly existing buildings, in regions of moderate to high seismicity. This work relies on improved definitions of seismicity and site response, experimental and analytical evaluations of systems response, and more accurate assessment of risk factors. This technology will be incorporated in expert systems tools and improved code formats for existing and new structures. Methods of retrofit will also be developed. When this work is completed, it should be possible to characterize and quantify societal impact of seismic risk in various geographical regions and large municipalities. Toward this goal, the program has been divided into five components, as shown in the figure below:

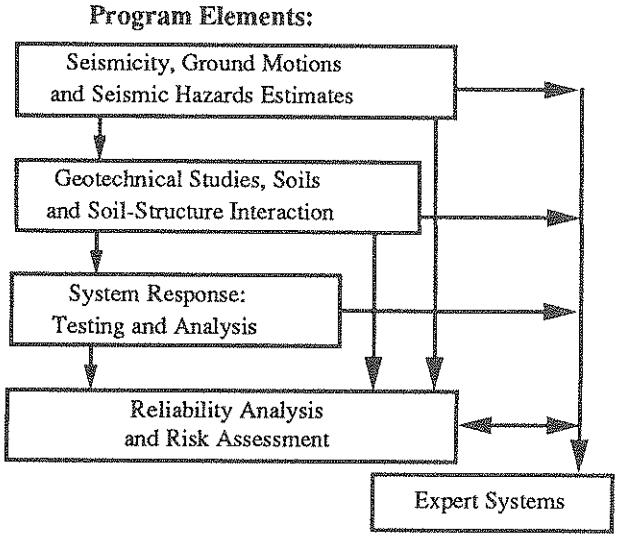

Reliability Analysis and Risk Assessment research constitutes one of the important areas of Existing and New Structures. Current research addresses, among others, the following issues:

1. Code issues - Development of a probabilistic procedure to determine load and resistance factors. Load Resistance Factor Design (LRFD) includes the investigation of wind vs. seismic issues, and of estimating design seismic loads for areas of moderate to high seismicity.
2. Response modification factors - Evaluation of RMFs for buildings and bridges which combine the effect of shear and bending.
3. Seismic damage - Development of damage estimation procedures which include a global and local damage index, and damage control by design; and development of computer codes for identification of the degree of building damage and automated damage-based design procedures.
4. Seismic reliability analysis of building structures - Development of procedures to evaluate the seismic safety of buildings which includes limit states corresponding to serviceability and collapse.
5. Retrofit procedures and restoration strategies.
6. Risk assessment and societal impact.

Research projects concerned with Reliability Analysis and Risk Assessment are carried out to provide practical tools for engineers to assess seismic risk to structures for the ultimate purpose of mitigating societal impact.

ABSTRACT

This report presents a new automatic method for the seismic design of reinforced concrete frame buildings. A new damage index is briefly reviewed, which serves as a measure of a member's residual energy dissipation capacity and thus is suitable as a control parameter in an automated design method. The method proposed herein aims for a uniform energy dissipation throughout the building frame, as measured by the individual member damage indices.

The new damage index is modeled on the low-cycle fatigue phenomenon exhibited by reinforced concrete members subjected to strong inelastic cyclic loads. It accounts for the observed stiffness and strength deterioration, includes a modified Miner's Rule for variable amplitude loading, and considers the effect of load history. These features make the damage index a useful measure of a member's capacity to resist further cyclic loading.

The automatic design method is based on a thorough study of the effects of three important design variables, the longitudinal reinforcement, the confinement steel, and member depth. Design rules derived from the large number of numerical studies allow an iterative improvement of a preliminary design until the distribution of damage indices has reached a user-specified degree of uniformity. The usefulness of this design method, which incorporates aspects of a knowledge-based expert system, is demonstrated with a typical four-story three-bay office building.

Acknowledgements

This research was supported by the National Science Foundation under Grant No. ECE 86-07591 through the National Center for Earthquake Engineering Research, under Grant No. SUNYRF NCEER-86-3033. The support is gratefully acknowledged.

TABLE OF CONTENTS

LIST OF FIGURES

LIST OF FIGURES

LIST OF FIGURES

LIST OF TABLES

1. Introduction

Probably the most difficult task in designing reinforced concrete buildings to withstand strong earthquake ground motions is to devise an acceptable mechanism for dissipating the large amounts of energy imparted upon the building by an earthquake. Short of resorting to unusual technologies such as base isolation, frictional dampers, active or passive control mechanisms, it has been accepted practice in recent years to dissipate the earthquake energy through inelastic action of some components of the structure. There are basically two different approaches to achieve this goal.

1. A number of structural members are deliberately selected to act as "fuses", i.e. weak spots in the structure assigned to develop plastic hinges and to dissipate energy under tightly controlled conditions. The designer has to detail the selected structural elements very carefully to assure that the energy dissipation demand can be met without prior failure. A frequently cited example is the solution of Park and Paulay for the coupling beams of coupled shear walls (10).
2. All or most structural elements are called upon to equally share in the task of energy dissipation so that the resulting damage is uniformly distributed over all elements in question, thus assuring a minimum average damage level. In the design of ductile moment-resistant frames it is accepted practice to use strong columns and weak beams. Thus the energy dissipation duty is limited to the beams.

It is the objective of this research to develop an automatic design procedure for reinforced concrete frames, in which a preliminary design is modified iteratively until the damage has reached a preselected distribution. That means, the chosen design approach utilizes the second of the two options just mentioned. The general procedure consists of the following steps, Fig 1.1.

1. Perform a preliminary design of a frame to satisfy the static lateral load requirements of the Uniform Building Code (19). At this point, the engineer is expected to perform this task by hand.
2. Perform a nonlinear dynamic analysis of the frame for seismic ground shaking of specified intensity, duration and spectral content.
3. Compute for both ends of each frame member the damage index as defined in Chapter 2. The random nature of the ground motion requires a Monte Carlo simulation, the output of which consists of mean value and variance of the member damage indices.
4. Evaluate the damage distribution by comparing it with an acceptable distribution as specified by the engineer.
5. If the damage is unacceptable, automatically introduce certain design changes on the basis of design rules incorporated in the program.
6. Repeat step 2 through 5 until the level of the frame damage is acceptable for the specified intensity of ground motion.

It is obvious that the concept of damage plays a key role in the entire design procedure. In Ref (4,5), a new damage model had been introduced, which is structured after a modified Miner's rule and is based on the hypothesis that damage of a structural member is closely related to the amount of energy dissipated, relative to the member's total energy dissipation capacity. In Chapter 2, this damage model will be briefly reviewed.

Chapter 3 describes the generation of artificial ground motion histories which is based on the Monte Carlo simulation of a non-stationary random process developed by Shinozuka (17).

The most difficult aspect of the design methodology is the formulation of de-

sign rules which guarantee convergence towards an acceptable damage distribution. Chapter 4 summarizes a comprehensive parameter study, wherein the influences of various small design changes on the damage distribution in a 4-story example office building frame are studied and evaluated in detail. The design parameters considered in this study are the longitudinal steel ratio, the confinement steel ratio, and the section depth of a member.

In Chapter 5, some design rules are synthesized from the preceding parameter studies and incorporated into the computer program. It will be interesting to expand this design method with some of the rules inherent in the capacity design concept of Paulay (12) in a future study. The usefulness of this automatic design method is demonstrated by applying it to various preliminary designs. Chapter 6 concludes this work with some general observations, a summary of the important conclusions and recommendations for further study.

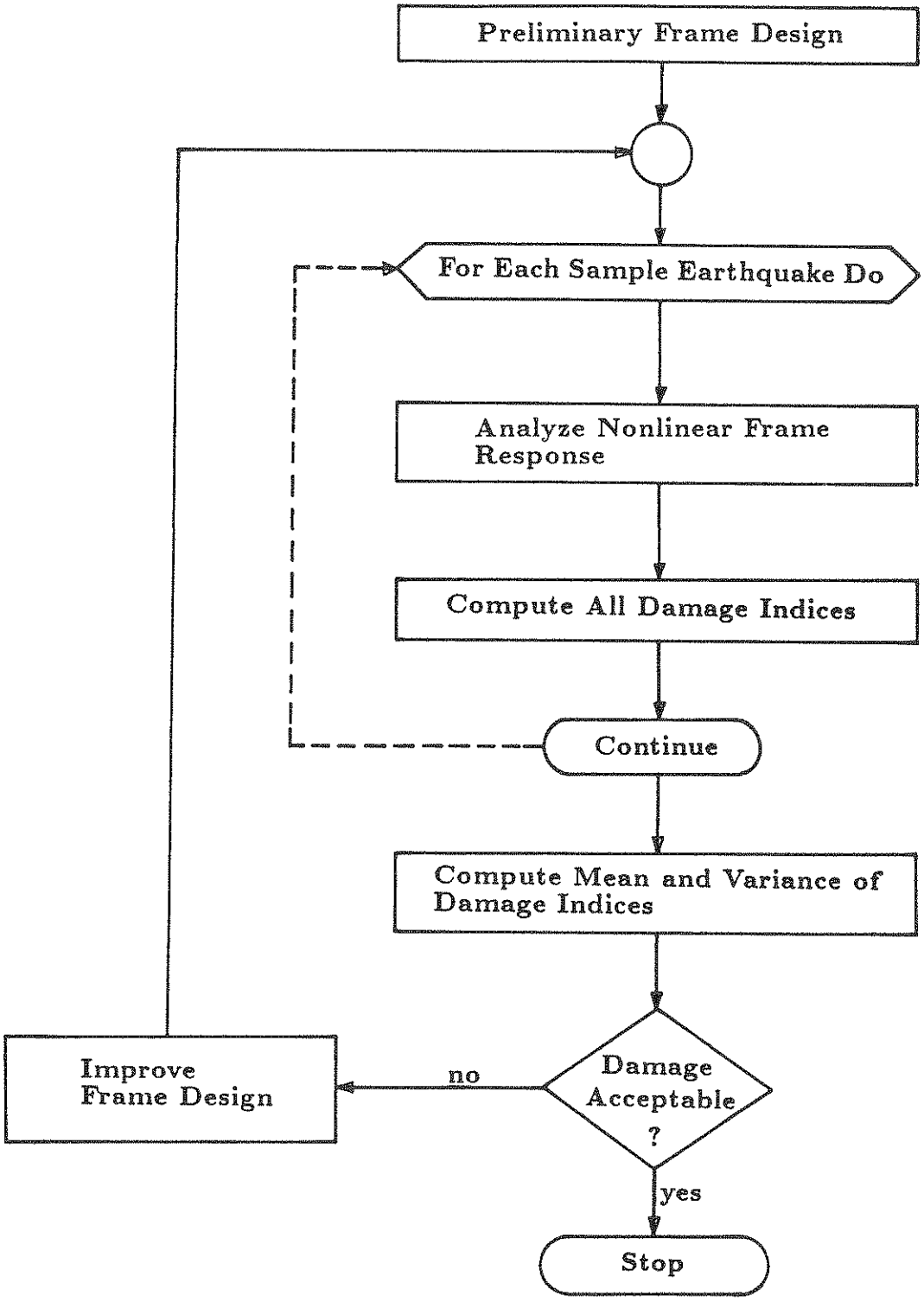

Fig 1.1 - Automated Design Method

2. A New Damage Model

Experience from past strong earthquakes and laboratory investigations has shown that damage sustained by reinforced concrete structures is the result of a combination of level of exposure and the number of exposures or load cycles, a phenomenon generally known as low-cycle fatigue. Thus, a rational damage model for reinforced concrete members has to take into account not only the load severity, but also the number of load cycles, or better, the amount of dissipated energy, relative to the member's total energy dissipation capacity.

An earlier study (5) has critically evaluated numerous models, which had been proposed to represent damage of concrete members. It was concluded that none of these prior models is well suited to describe the residual strength and stiffness of damaged structural members and thus permit an acceptably accurate prediction of response to subsequent cyclic loading. It was the recognized need for such a model that had prompted the development of a new damage model, which was described in detail in Ref (4,5). Herein, only a brief review of the model shall suffice.

2.1 Definition of Failure

It is common to express damage in the form of a damage index, which remains zero as long as the member's yield capacity is not exceeded, and is assigned a value of 1.0 when the member fails. This representation thus requires a definition of failure. Some investigators have proposed to define a member as having failed when its strength(moment) has dropped below 75% of the initial yield strength(moment) (3,6,9). But if a member which, according to this definition, has already failed, is subsequently loaded up to further displacement or curvature, its moment can be observed to increase well above the 75% level, Fig 2.1. For this reason it is necessary to relate the definition of a failure moment level to the member's actual strength

reserve or residual strength, which is a function of the experienced loading history, and maximum experienced curvature ϕ.

In Fig 2.2, the failure moment is plotted as a function of the normalized curvature level, given by

$$M_{fi} = M_f \cdot \frac{2\Phi_i}{\Phi_i + 1.0} \tag{2.1}$$

where

M_{fi} : failure moment for given curvature level ϕ_i

M_f : failure moment for monotonic loading

$\Phi_i = \dfrac{\phi_i}{\phi_f}$: curvature ratio

ϕ_f : failure curvature for monotonic loading

Fig 2.2 illustrates the fact that the level of failure moment should be a function of the loading level. For low curvature levels (i.e. ϕ exceeds ϕ_y by a small amount), the strength drop expected in a single load cycle is small. Also, the strength reserve activated when this load level is exceeded is relatively large. This means that a larger number of cycles is needed to reach the failure moment level M_{fi} for a small ϕ_i than for a larger ϕ_i. A constant failure moment level $M_{fi} = 0.75M_y$ does not appear to be very meaningful.

2.2 New Damage Index

The new damage model proposed in Ref (4,5), takes into consideration the nonlinear relationship between maximum displacement and dissipated energy, the strength deterioration rate and the number of load cycles to failure. The proposed damage index D_e is expressed in the form of a modified Miner's Rule. It contains damage modifiers, which reflect the effect of the loading history, and it considers the fact that RC members typically respond differently to positive and negative

moments:

$$D_e = \sum_i \left(\alpha_i^+ \frac{n_i^+}{N_i^+} + \alpha_i^- \frac{n_i^-}{N_i^-} \right) \tag{2.2}$$

where

i : indicator of different displacement or curvature levels

$N_i = \dfrac{M_i - M_{fi}}{\Delta M_i}$: number of cycles up to curvature level i to cause failure

ΔM_i : strength drop in one load cycle up to curvature level i, Fig 2.3

n_i : number of cycles up to curvature level i actually applied

α_i : damage modifier

$+, -$: indicator of loading sense

$(M_i - M_{fi})$ and ΔM_i denote the strength drops at curvature level i, up to the failure moment and in a single subsequent load cycle, respectively.

2.3 Damage Modifiers

The loading history effect is captured by including the damage modifier α_i, which, for positive moment loading, is defined as

$$\alpha_i^+ = \frac{\frac{1}{n_i^+} \sum_{j=1}^{n_i^+} k_{ij}^+}{\overline{k_i}^+} \cdot \frac{\phi_i^+ + \phi_{i-1}^+}{2\phi_i^+} \tag{2.3}$$

where

$$k_{ij}^+ = \frac{M_{ij}^+}{\phi_i^+} \tag{2.4}$$

is the stiffness during the j-th cycle up to load level i, Fig 2.4,

$$\overline{k_i}^+ = \frac{1}{N_i^+} \sum_{j=1}^{N_i^+} k_{ij}^+ \tag{2.5}$$

is the average stiffness during N_i^+ cycles up to load level i. Denoting with

$$M_{ij}^+ = M_{i1}^+ - (j-1)\Delta M_i^+ \tag{2.6}$$

the moment reached after j cycles up to load level i, Fig 2.4, the damage modifier α_i^+ can be expressed as

$$\alpha_i^+ = \frac{M_{i1}^+ - \frac{(n_i^+ - 1)\Delta M_i^+}{2}}{M_{i1}^+ - \frac{(N_i^+ - 1)\Delta M_i^+}{2}} \cdot \frac{\phi_i^+ + \phi_{i-1}^+}{2\phi_i^+} \tag{2.7}$$

As Fig 2.4 illustrates, the energy that can be dissipated during a single cycle up to a given load level i decreases for successive cycles. That means the damage increments also decrease. In a constant-amplitude loading sequence, the first load cycle will cause more damage than the last one, and the α_i-factor decreases as load cycling proceeds. This has been considered by incorporating the stiffness ratio into the damage modifier. The factor $\frac{\phi_i^+ + \phi_{i-1}^+}{2\phi_i^+}$ has been introduced to normalize the damage increments in the case of changing load amplitudes, Fig 2.5. For negative loading, "+" superscripts are replaced by "−" superscripts. For further details refer to Ref (4,5).

2.4 Structural Damage Index

Important decisions concerning the residual strength and safety of a damaged building are most conveniently based on a single structural or global damage index. A comprehensive survey of such damage indices can be found in Ref (14). Some of these were also reviewed in Ref (5). Final decisions on repair or demolition will have to take into account the building's use (e.g. warehouse, residence, school, hospital). The choice of an appropriate importance factor is not part of this study.

A structural damage index can be composed of individual story damage indices (11), each of which is a weighted average of the damage indices of all potential plastic hinges in the story under consideration,

$$D_{S_k} = \frac{\sum_{i=1}^{n_k} D_i^k \cdot E_i^k}{\sum_{i=1}^{n_k} E_i^k} \tag{2.8}$$

where

D_{S_k} : damage index for kth story

D_i^k : damage index of joint i in story k

n_k : number of potential plastic hinges in kth story

($2 \times$ number of elements in story k)

E_i^k : energy dissipated in joint i of story k

Then, the structural damage index will be defined as,

$$D_g = \sum_{k=1}^{N} D_{S_k} I_k \tag{2.9}$$

where

D_{S_k} : damage index for story k

N : total number of stories

$I_k = \dfrac{N+1-k}{N}$ = weighting factor for story k

The weighting factors express the greater importance of the lower stories of a building ($I_k = 1$ for $k = 1$). It is noteworthy that a structural damage index such as the one defined above cannot reflect the structure's increased vulnerability under further loading, if one or more critical elements have been severely damaged or have failed altogether. Only in some cases the story damage indices might preserve this crucial information, if appropriate additional weighting factors are employed, which, for example, would emphasize the importance of columns. By combining the detailed damage information of an entire frame into a single number (D_g), too much information is lost to make this single structural damage index a useful estimator of the structure's residual strength and capacity to withstand further loading. For

other applications, for example, for insurance risk evaluations, such a single number may be appropriate. But any rational evaluation of a structure's reliability can only be meaningful if the mechanical deterioration process of all significant structural members are accurately accounted for. For this reason, only individual element damage indices will be considered in the remainder of this report.

2.5 Numerical Examples

The damage model described above has been programmed and incorporated into the computer program, SARCF (Seismic Analysis of Reinforced Concrete Frames), described in the Appendix. The hysteretic response of frame members is simulated by a nonlinear element model developed at Columbia University, which takes into account the finite size of plastic hinge regions and reproduces the stiffness and strength degradation of RC frame elements (15). The accuracy of this model had been demonstrated through the simulation of numerous experimental test results (5).

The damage model cannot be similarly validated with experimental data, because test data are generally not quantifiable as to be comparable to our damage index. Indirectly, however, our member model simulates the member deterioration as a function of damage accumulation. Thus, satisfactory agreement between theoretical and experimental hysteretic response by itself is an indication that the accumulated damage is represented correctly. Moreover, it is possible to determine from the reported test results the dissipated energies and compare these with the numerical results.

Table 2.1 summarizes the cumulative dissipated energies of specimens, which had been tested by Hwang (6) and Bertero and Popov (9,13). The terminal experimental values listed are those given by Hwang. Intermediate values were obtained

from the recorded load-displacement curves by use of a planimeter. Some of the results thus obtained appear to be questionable, either because of errors in the reported response plots or in the measuring procedure employed herein. In spite of these discrepancies, which are most serious in the early load cycles of some of the specimens, the total energies dissipated by the time the tests were terminated show very good agreement between theory and experiment.

Table 2.2 contains the cumulative damage indices computed for the same specimens covered by Table 2.1. It is noteworthy that in all but the last case the damage index computed after test termination correlates reasonably well with 1.0, which corresponds to our definition of failure. In some cases, the testing proceeded well beyond this point, e.g. Specimen S22. This means that testing had continued beyond the point of (artificially defined) failure. Other specimens, most notably B35, appear not to have failed at the time the test was terminated.

Table 2.1 Experimental and Numerical Cumulative Dissipated Energies (kips-in)

Nos of Cycles	Specimen									
	S12	S14	S22	S23	S24	S32	S33	S34	R5	B35
1	44.7 (32.6)	39.6 (34.2)	41.5 (17.7)	13.7 (8.2)	46.8 (19.1)	42.3 (23.4)	15.1 (9.0)	47.3 (24.0)	10.4 (16.5)	93.5 (115.6)
2	76.0 (67.1)	71.4 (70.3)	69.1 (39.0)	23.8 (18.5)	72.1 (42.4)	76.6 (46.7)	24.9 (18.3)	82.4 (47.2)	17.4 (34.5)	158.8 (234.1)
3	103.1 (97.7)	78.3 (83.0)	90.0 (59.2)	60.0 (38.9)	77.9 (52.0)	96.9 (67.7)	59.9 (38.2)	88.6 (55.9)	37.8 (59.8)	375.9 (498.4)
4	127.4 (129.3)	83.0 (93.3)	106.9 (79.0)	92.7 (60.8)	81.0 (58.9)	113.3 (87.2)	87.1 (58.2)	92.7 (62.3)	64.9 (102.6)	630.9 (800.0)
5	150.0 (159.5)	107.7 (120.9)	119.7 (97.9)	97.5 (70.8)	104.9 (77.2)	126.4 (104.8)	92.7 (65.6)	116.3 (81.4)	90.1 (141.9)	1182.9 (1377.2)
6	172.1 (188.4)	132.6 (150.2)	129.8 (115.6)	100.1 (78.4)	123.3 (97.2)	136.9 (120.0)	96.8 (71.3)	133.9 (100.7)	114.7 (180.6)	
7	194.0 (215.9)	136.2 (161.1)	138.6 (131.9)	122.7 (96.4)	126.2 (105.5)	146.4 (132.4)	116.7 (88.4)	137.5 (106.8)	177.0 (217.9)	
8	213.9 (241.8)	138.8 (169.1)	146.4 (146.8)	142.2 (115.8)	128.3 (111.3)	155.0 (141.7)	135.1 (106.1)	140.6 (112.2)	226.5 (255.6)	
9	232.4 (265.7)	158.0 (189.8)	153.4 (160.0)	144.4 (124.3)	140.4 (126.2)		138.2 (112.3)	155.4 (117.3)	277.4 (313.9)	
10	250.4 (286.8)	179.5 (209.5)	160.0 (171.5)	145.7 (130.7)	151.0 (142.4)		141.2 (117.2)	168.5 (131.5)	333.6 (371.5)	
11	267.6 (304.4)	182.3 (216.3)		159.6 (145.1)			157.0 (131.0)	170.2 (145.2)	383.1 (418.1)	
12	283.8 (318.6)	184.4 (221.1)		171.0 (160.0)			170.6 (144.8)	171.5 (151.0)	418.5 (492.9)	
13	297.9 (329.4)	201.8 (232.4)					173.0 (149.8)	178.0 (154.9)		
14	311.4 (337.2)	219.0 (241.7)					175.0 (153.5)			
15	323.5 (342.4)	220.5 (244.4)					185.9 (163.7)			
16	333.6 (345.6)	221.8 (246.1)					196.0 (173.4)			
17	343.0 (348.0)	236.0 (249.1)								
18		248.0 (250.8)								

Note : 44.7 - Experiment (32.6) - Theory

Table 2.2 Numerical Cumulative Damage Indices

Nos of	Specimen									
Cycles	S12	S14	S22	S23	S24	S32	S33	S34	R5	B35
1	0.0254	0.0569	0.0797	0.0210	0.0664	0.0722	0.0059	0.0461	0.0041	0.0234
2	0.1250	0.2227	0.2597	0.0685	0.2278	0.2537	0.0225	0.1846	0.0154	0.0697
3	0.2485	0.2644	0.4513	0.1808	0.2863	0.4601	0.0870	0.2234	0.0389	0.1733
4	0.3740	0.2937	0.6422	0.3546	0.3262	0.6545	0.1956	0.2494	0.1043	0.3379
5	0.4871	0.4589	0.8220	0.4089	0.4763	0.8313	0.2156	0.3863	0.1876	0.5816
6	0.5963	0.6439	0.9956	0.4513	0.6453	1.0003	0.2303	0.5445	0.2745	
7	0.7016	0.6794	1.1557	0.5957	0.6959	1.1436	0.3271	0.5746	0.3605	
8	0.8019	0.7040	1.3018	0.7499	0.7296	1.2613	0.4360	0.5993	0.4509	
9	0.9035	0.8326	1.4336	0.7971	0.8552		0.4533	0.6226	0.6354	
10	0.9935	0.9718	1.5552	0.8336	0.9943		0.4661	0.7271	0.8524	
11	1.0721	0.9978		0.9565			0.5491	0.8438	1.0771	
12	1.1395	1.0156		1.0844			0.6392	0.8722	1.3877	
13	1.1960	1.1044					0.6540	0.8910		
14	1.2435	1.1976					0.6647	0.9790		
15	1.2837	1.2142					0.7307			
16	1.3215	1.2252					0.8029			
17	1.3600	1.2837								
18		1.2925								

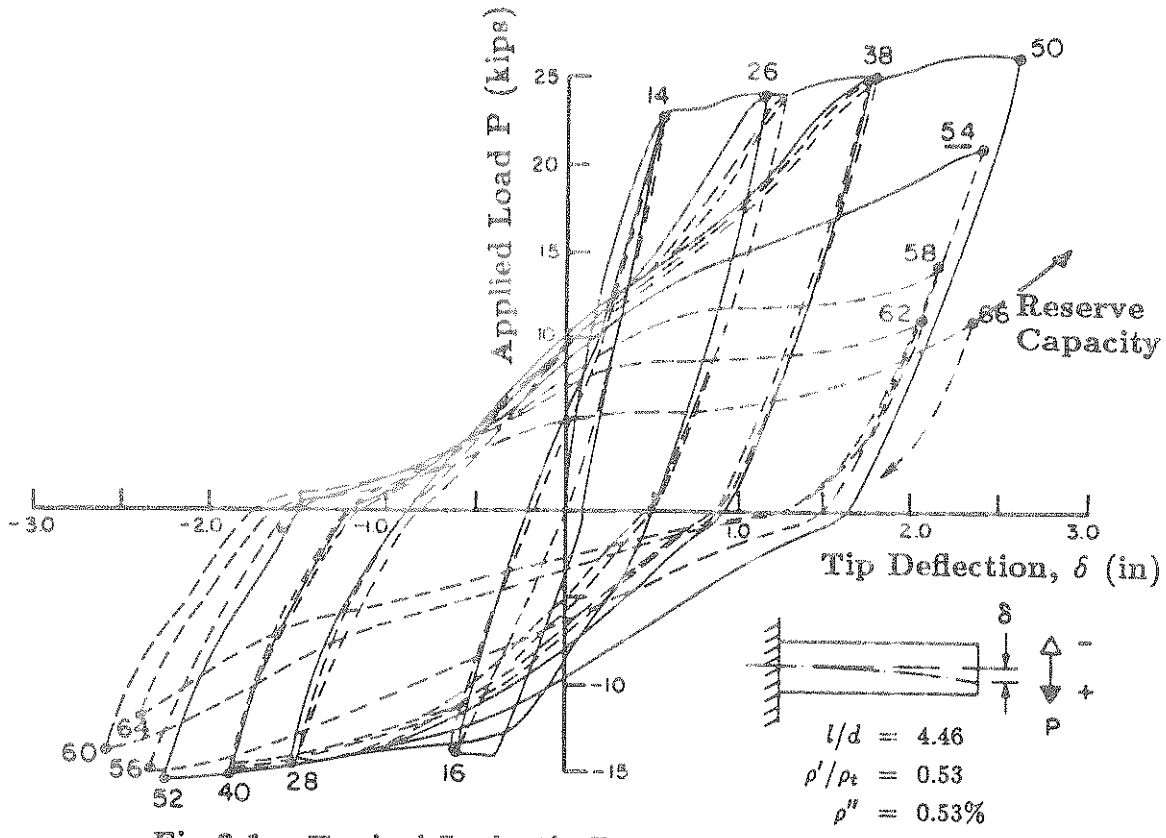

Fig 2.1 - Typical Inelastic Response of RC Member
Experiment by Ma, Bertero and Popov (Ref. 9)

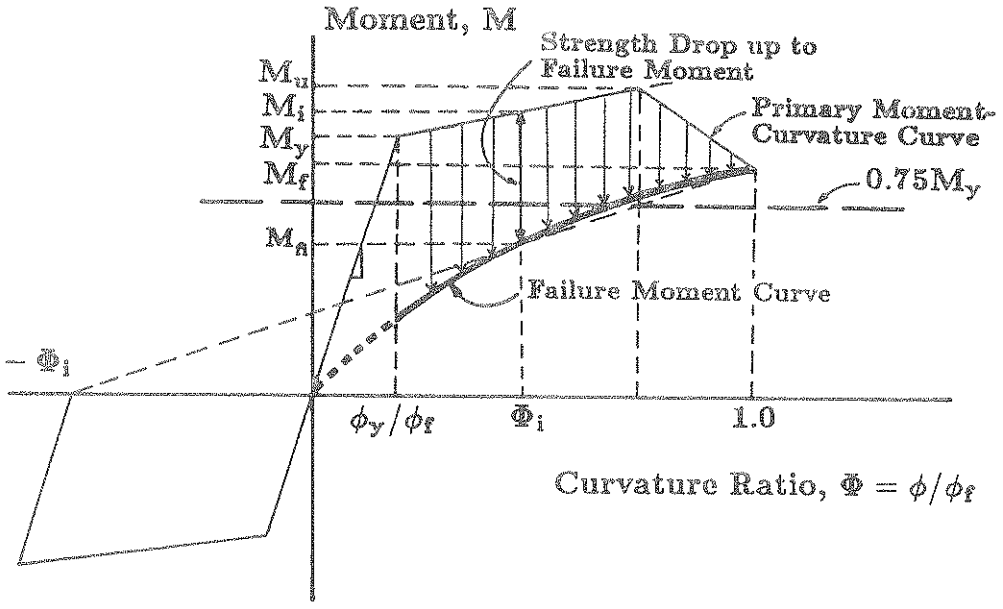

Fig 2.2 - Definition of Failure

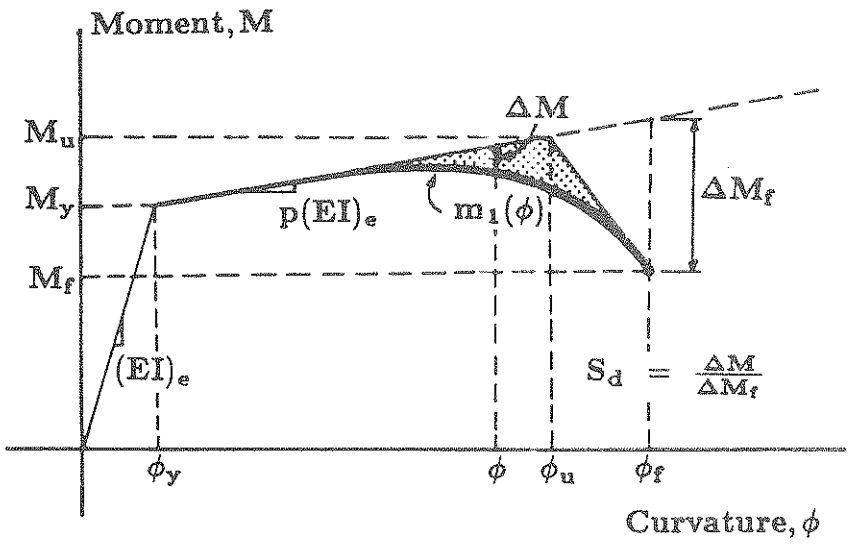

Fig 2.3 - Strength Deterioration Curve

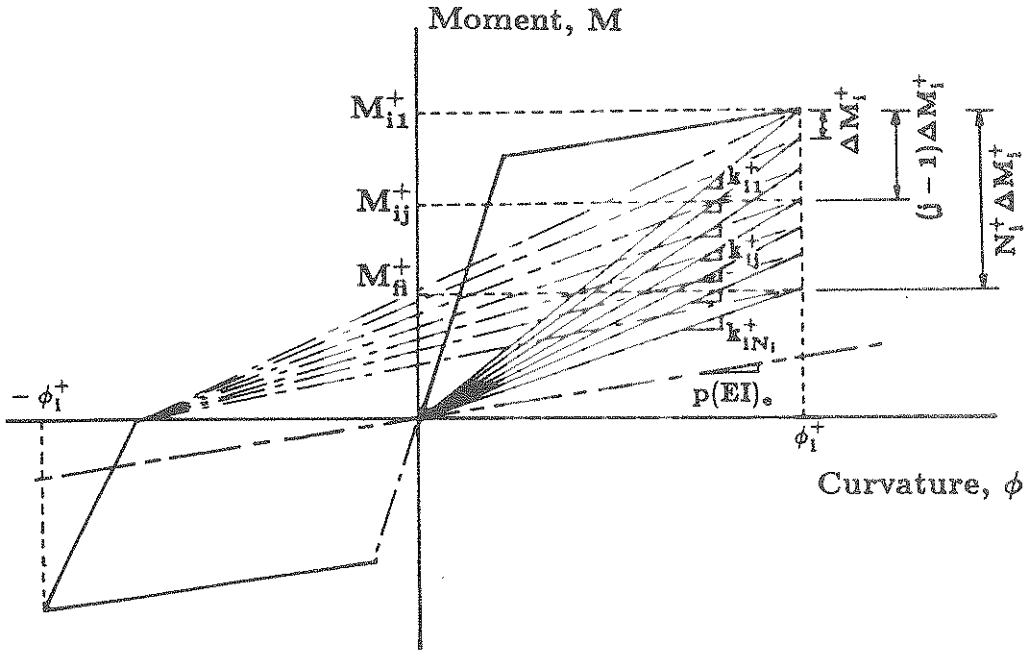

Fig 2.4 - Strength Drop Due to Cyclic Loading

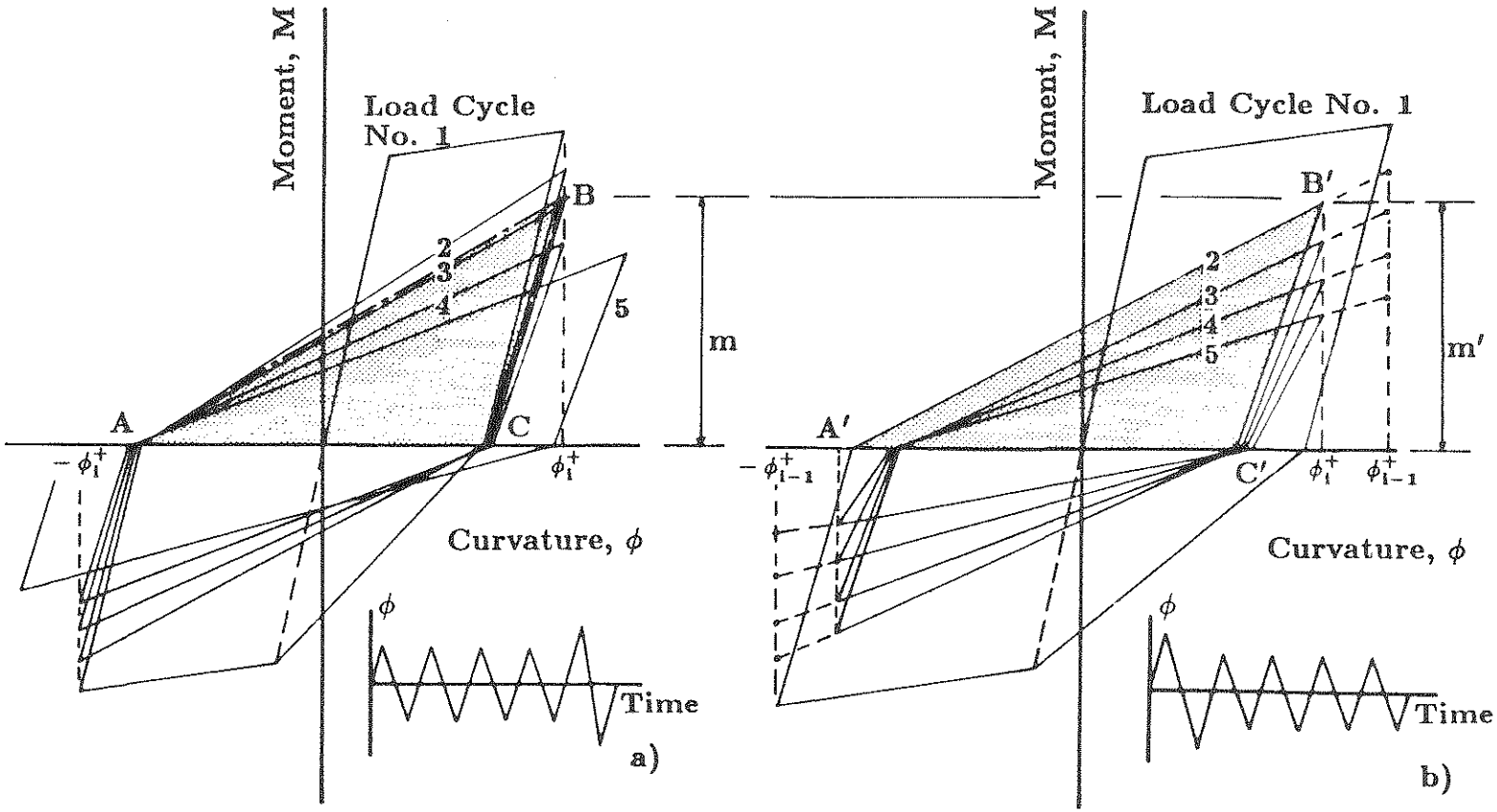

$$\frac{\Delta A'B'C'}{\Delta ABC} = \frac{\phi_1^+ + \phi_{1-1}^+}{2\phi_1^+} \quad \text{if } m = m'$$

Fig 2.5 - Energy Dissipation for Different Load Histories

3. Generation of Artificial Earthquakes

For nonlinear analysis of structures, the representation of earthquake ground motions as a stationary random process is of limited use because of the time dependency of the mean peak acceleration envelope and the duration of strong ground motion. For this study, artificial ground acceleration histories, $x(t)$, are generated by multiplying an envelope function, $s(t)$, and a stationary Gaussian process, $g(t)$,

$$x(t) = s(t) \times g(t) \tag{3.1}$$

The envelope function is here assumed to have a trapezoidal shape as shown on Fig 3.1b. Other envelope functions could be easily substituted (16). A Gaussian process, $g(t)$, can be obtained by using the Kanai-Tajimi spectrum $S(w)$, Fig 3.1a as the power spectral density function,

$$S(w) = S_o \times \frac{1 + 4\zeta_g^2(\frac{\omega}{\omega_g})^2}{[1 - (\frac{\omega}{\omega_g})^2]^2 + 4\zeta_g^2(\frac{\omega}{\omega_g})^2} \tag{3.2}$$

where

ω_g : characteristic ground frequency

ζ_g : predominant damping coefficient

S_o : intensity of Gaussian white noise over the range $-\infty < \omega < \infty$

The Gaussian process, $g(t)$, can be generated by using Monte Carlo technique (17),

$$g(t) = \sqrt{2} \sum_{k=1}^{N} \sqrt{G(\omega_k)\Delta\omega} \cdot cos(\omega_k t - \phi_k) \tag{3.3}$$

where

ϕ_k : random phase angle, uniformly distributed between 0 and 2π

ω_k : $k\Delta\omega$

$G(\omega_k) = 2S(w_k)$: one-sided power spectrum

$\omega_u = N\Delta\omega$: upper cut-off frequency

To generate an artificial earthquake, Shinozuka (18) suggested a relationship between the intensity, S_o, and the peak ground acceleration, PGA. With

$$\begin{aligned} \sigma_g^2 = E\left[\ddot{x}_g^2\right] &= \int S(\omega)\, d\omega \\ &= \frac{S_o \pi \omega_g (1 + 4\zeta_g^2)}{2\zeta_g} \end{aligned} \tag{3.4}$$

or

$$\sigma_g = \left[\pi\omega_g\left(\frac{1}{2\zeta_g} + 2\zeta_g\right)\right]^{\frac{1}{2}} \times S_o^{\frac{1}{2}} \tag{3.5}$$

the peak ground acceleration can be written as

$$PGA = \alpha_g S_o^{\frac{1}{2}} \tag{3.6}$$

where

$$\alpha_g = p_g\left[\pi\omega_g\left(\frac{1}{2\zeta_g} + 2\zeta_g\right)\right]^{\frac{1}{2}}$$

p_g : peak factor, empirically assumed to be 3.0 in this study.

The peak ground acceleration of the 1940 El Centro earthquake was $0.36g$, i.e. $PGA = 0.36g$. Therefore,

$$\begin{aligned} S_o &= \left[\frac{PGA}{\alpha_g}\right]^2 \\ &= \frac{PGA^2}{p_g^2\left[\pi\omega_g\left(\frac{1}{2\zeta_g} + 2\zeta_g\right)\right]} \end{aligned} \tag{3.7}$$

For firm soil conditions, the empirical parameters are $\omega_g = 9\pi\ (rad/sec)$ and $\zeta_g = 0.6$, which gives $S_o = 0.0827\ ft^2/sec^3$.

In this study, ground acceleration histories with peak accelerations of either $0.5g$ or $1.0g$ are generated, the latter one representing an upper bound for credible earthquake ground motion.

Because of the random nature of earthquake acceleration histories it is more meaningful to consider structure response quantities (such as damage indices)

formed as averages for an ensemble of sample input functions, rather than responses to individual functions. In order to determine the minimum number of sample functions necessary to give useful mean response values, the running mean values of damage indices computed for eight different structural elements of a frame are plotted in Fig 3.2 as functions of the number of sample earthquake input functions. As can be seen, all mean values have more or less stabilized after the accumulation of about 10 earthquake input functions. Thus the majority of the parameter studies presented below involved 10 sample functions for each case.

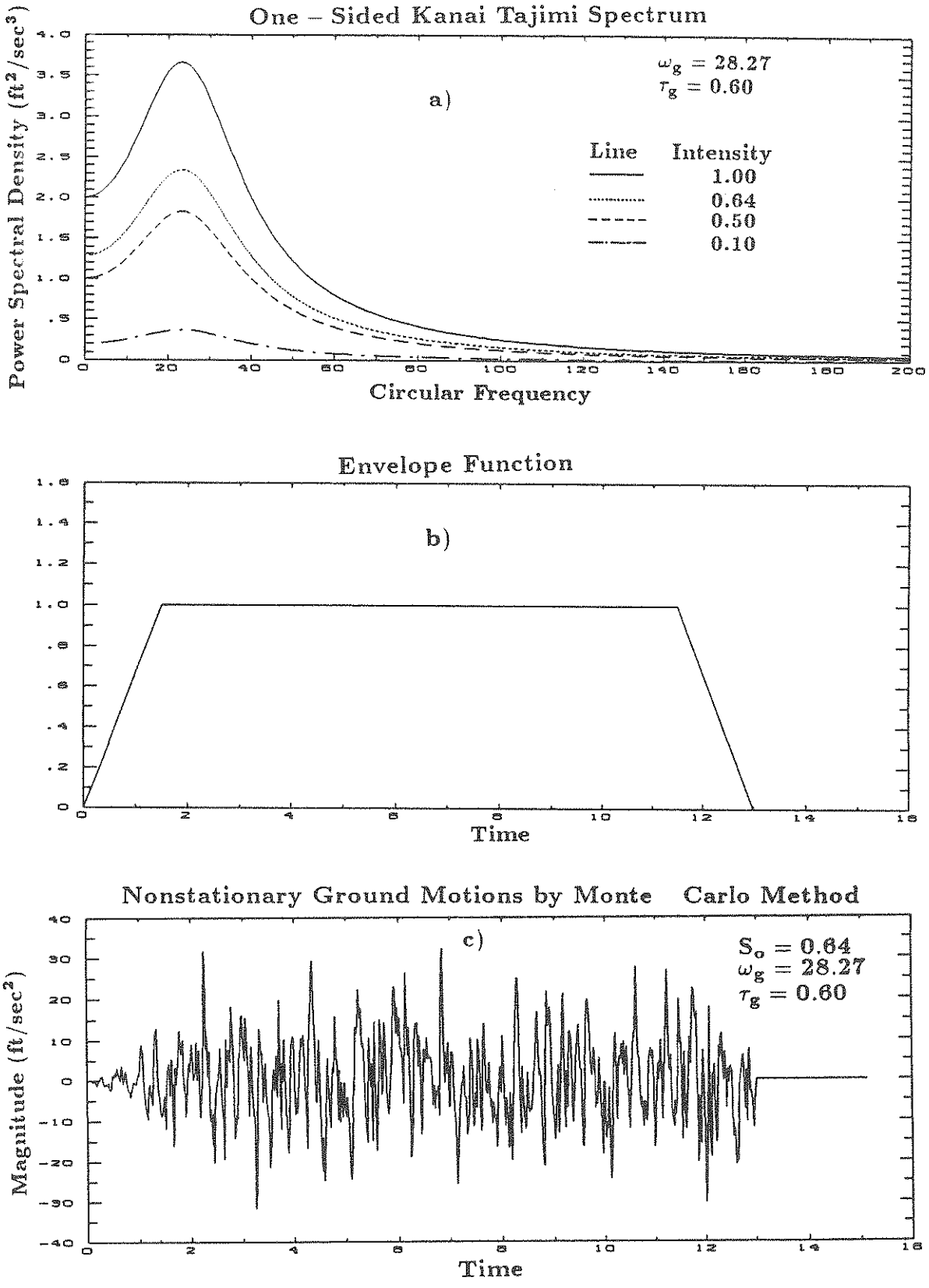

Fig 3.1 - Simulation of Nonstationary Ground Acceleration Histories

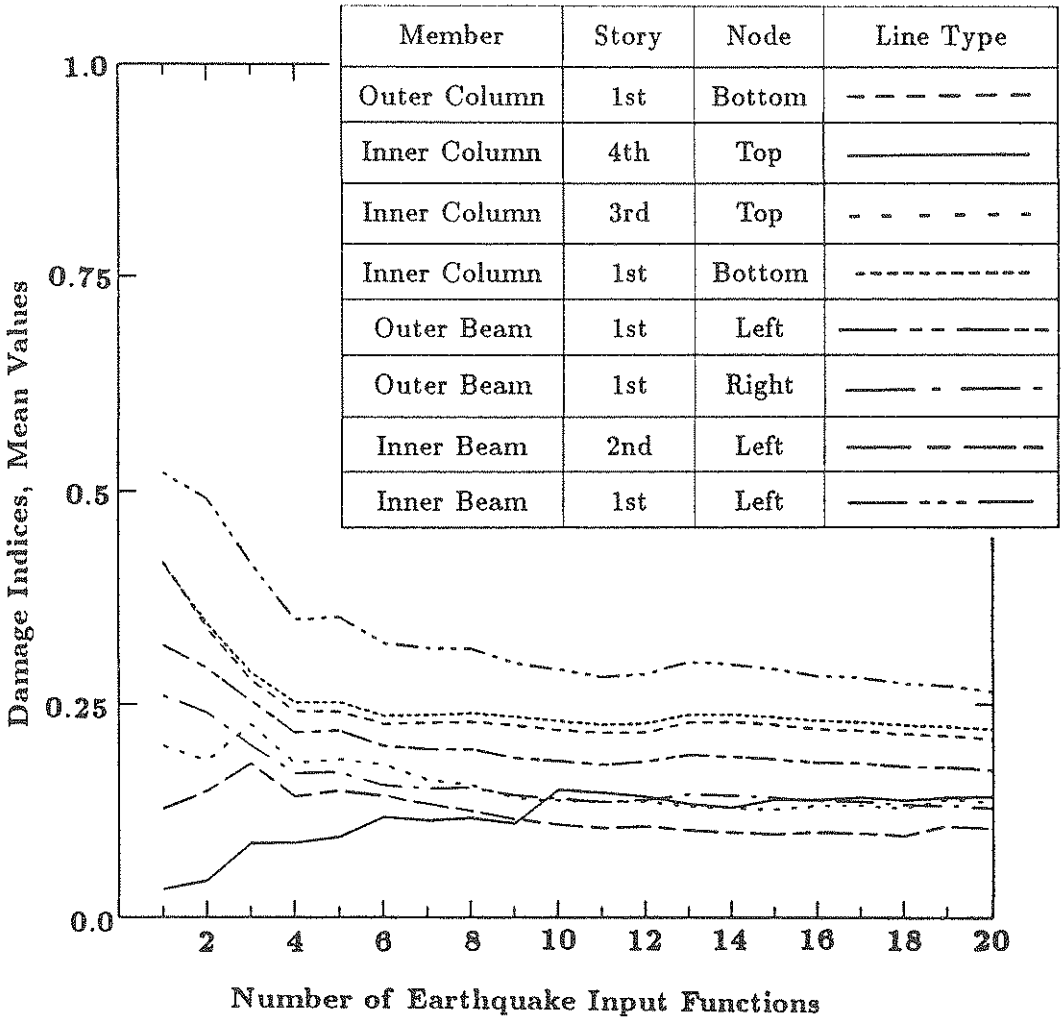

Fig 3.2 - Variation of Running Mean Values of Damage Indices with Number of Earthquake Input Functions

4. Numerical Experiments

In order to develop an automatic design procedure which guarantees convergence towards an acceptable design, it is necessary to understand and predict the consequences of certain small design modifications. Three design parameters were singled out for their impact on frame response to strong ground motions: 1) the longitudinal steel ratio, 2) the confinement steel ratio, and 3) the depth of severely stressed frame members. (This selection implies that sufficient shear reinforcement is provided to preclude shear failures. Also, bond failures due to cyclic loadings are not considered herein.) To fully appreciate the influence of these three design parameters on the frame response, a large number of parameter studies have been conducted. Since the damage indices are of prime interest, the effect of a single design parameter can be studied by changing only this one parameter in one member by a small amount and then plotting the resulting changes of all member damage indices. Such a plot can be interpreted as an influence surface. A careful study of such influence surfaces permits the drawing of important conclusions, which can be synthesized into more or less generally valid design rules.

Section 4.1 describes the details of the example frame used for the numerical experiments. The testing program is briefly described in Section 4.2. In Section 4.3, the results of the parameter studies are presented in detail. The most significant observations and conclusions are summarized in Section 4.4.

4.1 Example Office Building

A four-story three-bay concrete frame for a typical office building has been designed to serve as a model for numerical experiments. Details of this frame model are shown in Fig 4.1. It has been designed according to the ACI 318-83 Code (1), to resist the equivalent static lateral loads specified in the Uniform Building

Code (19). The design base shear is given as:

$$V = ZIKCSW \tag{4.1}$$

where in our case,

Z = 1.0 for seismic zone 4

I = 1.0 for occupancy importance factor

K = 0.67 for ductile moment–resisting space frame

CS = 0.14 for numerical coefficient for site–structure and soil

W = 658.38 *kips* for dead weight (see Table 4.1 for details)

Thus, the base shear is

$$V = 0.67 \times 0.14 \times 658.38 = 61.76 \ kips \tag{4.2}$$

to be distributed over the frame according to

$$F = \sum_{i=1}^{N} F_i + F_t \tag{4.3}$$

Since the fundamental period is estimated to be less than 0.7 *sec*, we can assume $F_t = 0.0$. Thus, the total lateral load is distributed over the building height as tabulated in Table 4.2. Based on these lateral loads, the preliminary design of Fig 4.1 resulted. The fundamental natural frequency and the natural period of this frame have been computed to be $f_1 = 1.1907 \ Hz$ and $T = 0.840 \ sec$, respectively, using the moments of inertia of the cracked reinforced concrete sections. The maximum roof displacement for the static code lateral loads is $\Delta = 2.119 \ inch$.

A mathematical model of this example frame was analyzed by program SARCF for two different artificial ground acceleration histories, one with a peak acceleration of *0.5g*, and one with *1.0g*. In this and all subsequent analyses, use of symmetry

was made by analyzing only one-half of the frame, in order to reduce the computational effort. Even though the axial forces in the columns vary considerably as functions of time, Fig 4.2, thereby affecting their yield moments, it was felt that the strong-column weak-beam design concept justifies this assumption of symmetry, since plastic hinges in columns were rare occurrences, except at the foundations.

The mean damage indices obtained for ten sample input functions for each of the two analyses are summarized in Fig 4.3. They permit the following observations:

1) Even for the earthquake with *1.0g* peak acceleration, the damage indices are surprisingly small (maximum 0.3377). This indicates a well-designed strong frame.

2) Except for the bottom of the first-story columns, all columns remain elastic in the *0.5g* earthquake. Even in the *1.0g* event, the damage indices computed for the columns are very small compared with those for the beams. This indicates that the frame was designed correctly according to the strong-column weak-beam principle.

3) In the *1.0g* earthquake, damage appears to be heavily concentrated in the beams of the lower stories, indicating that these contribute an overproportional share to the energy dissipation of the frame. It would be desirable to distribute this energy dissipation and resulting damage more evenly over the entire frame.

4) For a given frame design a single analysis for different intensities reveals quite dissimilar damage distributions because of the random nature of the ground motion history. However, relative damage distributions for different earthquake intensities tend to become more and more similar, if damage indices are computed as mean values for ten or more sample acceleration histories.

The execution of a nonlinear dynamic analysis of the example frame requires

typically about 112.6 *sec* of CPU time on the Sun-micro computer, when 1200 time steps of size $\Delta t = 0.01$ *sec* are used.

4.2 Outline of Numerical Experiments

All parameter studies reported below were carried out on the example building frame described in Section 4.1. Table 4.3 summarizes the basic case studies together with their identifiers. It should be recalled that we are concerned only with mean values of damage indices, so that each case implies ten nonlinear dynamic time history analyses. In each case a design parameter was increased by a small amount and in a separate case decreased by an equal amount. Thus the longitudinal steel ratios were varied by $\pm 5\%$, the confinement steel ratios by $\pm 50\%$ for critical beams and $\pm 30\%$ for critical columns, and the member depths by $\pm 5\%$. In addition to these $2 \times 36 \times 10 = 720$ runs, numerous studies were performed by varying the amounts by which the design parameters were changed, and by varying design parameters in other than critical frame members.

Even though the principle of superposition does not apply to the case of highly nonlinear frame response, the necessity for accelerating design convergence suggested the inclusion of the following study: In Run A change one design parameter in only the most heavily damaged member. In Run B change the corresponding design parameter in only the second most heavily damaged member. In Run C change both members together to determine to what extent the influence surfaces can be superimposed. Increasing and decreasing a design parameter by the same amount permits the drawing of conclusions about the same phenomenon.

4.3 Results of Numerical Experiments

Figs 4.4-15 present the results for Cases I through IV, and Figs 4.16-25 contain the results of additional studies. It should be stressed that all of these Figures

show the changes of mean damage indices as the result of the indicated parameter changes.

4.3.1 Study I – Critical Columns, *1.0g* Peak Acceleration

This numerical experiment consists of 9 cases, wherein three design parameters are changed by the indicated amounts for the most critical, the second most critical, and the two most critical columns, each. The results, summarized in Figs 4.4-6 permit the following observations:

1) By increasing the longitudinal reinforcement of critical columns, Fig 4.4, the damage indices for the modified columns are consistently decreased, as one would expect. Conversely, decreasing the reinforcement always leads to an increase in damage.

2) Changes in the confinement steel ratio for the critical columns, Fig 4.5, have little effect on the damage of the structure. Moreover, the effect is inconclusive, i.e. in one case, a small increase in confinement steel increases the damage index for the affected column, in another case it reduces the damage. In any case, practical considerations impose an upper limit on the confinement ratio.

3) Reducing the depth of a critical column causes a reduction in damage for the column in question, Fig 4.6. Conversely, increasing the column depth increases the damage. Since both most highly stressed columns are located in the first story, it is not certain how these results can be generalized. However, in the case studied, changing one column depth has the most profound effect on the other column in the same story. For example, reducing the depth of the most critical column by 5% decreases the damage index in the modified column by 0.0063, but increases the damage index for the other column by 0.0326, i.e. almost 5 times as much.

4) The two critical columns are both located in the ground floor of the frame.

The effects of any parameter changes are basically confined to the beams and columns of the same ground floor. The effects on the members of the upper floors are relatively smaller.

5) In this particular case the principle of superposition appears to hold by and large, as far as the longitudinal steel is concerned. For example, increasing the longitudinal steel of either one of the two first floor columns reduces the damage of both. Thus, adding steel to both columns simultaneously leads to a damage reduction of both as well. Similarly, the damage indices of all other elements can be superimposed approximately.

6) The effect of the confinement steel is less conclusive, as far as superposition is concerned. For example, the damage index of the exterior first story column is reduced when the confinement steel of either first story column is increased. But when both columns are simultaneously more heavily confined, the damage index is inexplicably increased. In any case, the damage index changes are very small.

7) Superposition with regard to column depth variations is comparably consistent. A depth increase(decrease) always increases(decreases) the damage of the affected column, but decreases(increases) the damage of the other column in the same ground story, which has now a smaller(larger) relative stiffness and carries a correspondingly lesser(larger) share of the base shear. Increasing(decreasing) both column depths simultaneously leads to a damage increase(decrease), as one would expect. The principle of superposition applies approximately.

8) The effect of column reinforcing ratio on the critical beams is similar as that on the affected columns. That is, an increase(decrease) of either critical column steel reduces(increases) the damage of all members in the critical ground floor.

9) Increasing(decreasing) the depth of one column reduces(increases) the damage

in the other column and both beams on the same floor as well. The effect on the other first floor columns exceeds the effect on the modified column itself. As a result, reducing(increasing) the depth of both columns simultaneously worsens(improves) the damage picture of the entire first floor.

10) The cause and effect relationship is approximately linear, as far as the sign is concerned. That means, increasing a particular parameter has consistently the opposite effect of decreasing it. Only the effect of the confinement steel violates this rule occasionally.

In conclusion it is important to note that in this particular study, in which the two most heavily damaged columns are situated in the ground floor, the effects of changing the longitudinal steel or the column depth are generically superposable, e.g. by increasing the reinforcement of several critical columns in the ground floor, the damage of all first floor elements can be expected to decrease.

4.3.2 Study II – Critical Columns, *0.5g* Peak Acceleration

The results of the 9 cases in this study are summarized in Figs 4.7-9. Overall, they permit all the same observations as the results of Study I. Because of the smaller ground accelerations, the damage reference values of Fig 4.3 and the absolute values of the damage changes are considerably smaller. However, the relative damage changes are larger in the *0.5g* earthquake than in the *1.0g* case. For example, a 5% steel increase in the most heavily damaged column reduces the damage index of 0.2061 by 0.0099 or 5% in the *1.0g* earthquake. In the *0.5g* case, the damage index of 0.0162 is reduced by 0.0019 or 12%.

For the lower earthquake intensity, damage values are sometimes so small, that they are increasingly influenced by the randomness of the ground motions and therefore appear to be less conclusive.

4.3.3 Study III – Critical Beams, *1.0g* Peak Acceleration

From the results of these cases, summarized in Figs 4.10-12, the following observations can be made:

1) The effect of longitudinal reinforcing ratio in the most heavily damaged beams is very similar to that for the columns, i.e. an increase in steel in either one of the two critical beams in the first floor reduces the damage in both beams to the extent that superposition is almost linear, Fig 4.10.

2) As in Study I, the effect of the confinement ratio is inconclusive. Moreover, the damage index changes are very small. This fact lessens the value of confinement ratio as a tool for damage reduction in an automatic design algorithm.

3) On the other hand, increasing the member depth increases the damage of the same beam element, but reduces the damage of the other beam on the same floor. As a result, changing both beam depths simultaneously has barely a net effect, regardless whether the beam depths are increased or decreased.

4) As in Study I, any parameter changes of either one of the two critical beams have relatively little effects on frame elements in other floors.

5) As far as the longitudinal steel and the member depth are concerned, the principle of superposition applies approximately.

6) The effects of column parameter changes on the beams of the same floor(Study I) are comparable to the effects of beam parameter changes on the columns of the same floor(Study III), i.e. there exists a kind of reciprocity with regard to the longitudinal steel effect.

7) As in Study I, increasing a particular parameter, i.e. the longitudinal steel ratio or the member depth, has consistently the opposite effect of decreasing it.

4.3.4 Study IV – Critical Beams, *0.5g* Peak Acceleration

Figs 4.13-15 show the results of these 9 case studies. Observations are very similar to those for Study III, as far as the effects of the longitudinal steel ratio and the member depth is concerned. The effect of the confinement steel ratio is again almost nil and therefore inconclusive. The principle of superposition appears to be applicable in an approximate sense also in this study, making it an essential tool for speeding convergence of an automatic design method.

4.3.5 Study V – Larger Change of Column Reinforcement, *1.0g* Peak Acceleration

In this study, the longitudinal steel ratios of the critical first floor columns were changed by ± 10% instead of the earlier 5%. A comparison between the results shown in Fig 4.16 and the earlier results of Fig 4.4 permits the conclusion that the effect of the magnitude of steel ratio change on the damage indices is almost linear, i.e. a 10% difference in steel changes the damage indices about twice as much as a 5% difference.

4.3.6 Study VI – Top Story Beams, *1.0g* Peak Acceleration

In this study, 9 cases were analyzed to investigate the influence of design parameter changes in top story beam elements. From the results, shown in Figs 4.17-19, the following observations can be made:

1) Increasing(reducing) the longitudinal steel reinforcement of either one of the two top story beams decreases(increases) its damage index, Fig 4.17.
2) Changes of the confinement steel ratio have almost no effect on the damage of the structure, Fig 4.18.
3) Reducing(increasing) the depth of top story beams increases(decreases) the damage of the modified beams, Fig 4.19. This result is opposite to the one observed in Study III, which showed an increase of damage in a deepened

beam.

4) Unlike the results of Study III, wherein changes were confined primarily to the first floor, in which members were modified, the influence of changes in top floor beams on members in other floors is considerable. It tends to change sign between the second and third floor. For example, increasing the reinforcement in the center top beam reduces the damage in all beams of the third and fourth floors, but increases it in the two lower floors.

5) In all cases of this study, the principle of the superposition appears to hold by and large, i.e. changing two beams separately has approximately the same combined effect as changing both beams simultaneously.

6) Increasing either the longitudinal steel or member depth has consistently the opposite effect from decreasing either.

4.3.7 Study VII – Top Story Beams, *0.5g* Peak Acceleration

The changes in damage indices for these cases, Figs 4.20-22, are generally very small, but are consistent with the results observed in Study VI. As was already observed earlier, the randomness of ground motions plays an increasing role in this case, so that the results tend to become less conclusive.

4.3.8 Study VIII – Top Story Columns, *1.0g* Peak Acceleration

It was the objective of this study to investigate the effect of changing the reinforcement of the top story columns. As Fig 4.3 indicates, neither of these columns suffered any damage, i.e. neither yield moment was exceeded in the *1.0g* event. Therefore a small increase or decrease of the column steel reinforcement is not expected to have any effect on the damage picture of the frame. This expectation is borne out by the results of Fig 4.23, although in some cases, non-negligible effects in first-story members can be observed. These must be explained by the small changes

in column stiffness caused by the changes in steel.

4.3.9 Study IX – Columns and Beams in Other Stories , *1.0g* Peak Acceleration

The effect of changing the steel in top and bottom story elements has been investigated in some of the preceding studies. The effect of changing the steel in members of the second and third floor is summarized in Fig 4.24-25. The following observations can be made:

1) By increasing the longitudinal reinforcement of any element, the damage index of the modified element is consistently decreased, as one would expect.
2) The effects of reinforcement changes are generally confined to the elements in the ground floor and in the floor where the modified element is located.
3) Increasing the beam reinforcement generally causes an increase of the damage for all the elements in the ground floor. This observation is similar to the one made earlier (Study VI).
4) Increasing the column reinforcing steel also causes generally large damage increases in the ground floor elements, but less consistently than the case with changes of the beam reinforcement.

4.4 Summary and Conclusions of Numerical Experiments

The preceding studies clearly show that the spatial distribution of damage changes due to changes in beam and column reinforcement has important ramifications for an automatic design method. Table 4.4 summarizes some of these changes in matrix form. These results are extracted from Fig 4.4, 4.10, 4.17, 4.24 and 4.25. Element a_{ij} in this matrix represents the change in damage index of element i if the reinforcement ratio of element j is increased by 5%. The listing of two numbers in one box signifies the fact that separate damage indices are computed for the two ends of a member, whereas only a single reinforcement ratio is assumed for one

element. A careful analysis of this matrix permits the following conclusions to be drawn:

1. Increasing the steel in any member always reduces its damage. As a result, there are no positive numbers on the diagonal of the matrix. The earlier studies indicated that this effect is consistently reversible, i.e. a reduction of member reinforcement always increases the damage in the modified members. Some of the columns are not damaged, therefore, any additional reinforcement has no effect on their damage, i.e. the corresponding diagonal elements are zero.
2. Increasing the steel in any member reduces the damage of most other elements in the same story. This result is most consistent for modifications of (critical) elements in the first story. In other stories, there are occasional deviation from this rule, as can be seen in the 4 by 4 diagonal submatrices. Small positive off-diagonal entries can be discounted as being random effects.
3. The effect of any steel increase on the damage of elements in other stories tends to decrease and then change sign. For example, the increase of steel in any top story beam decreases the damage in top story elements, but increases the damage in ground story elements.
4. The net effect of changing beam reinforcement is that the sum of the damage improvements exceeds the sum of damage increases, with the exception of modification of the top floor beams. This conclusion results from considering the sum of all damage changes in a matrix column.
5. The net effect of changing column reinforcing steel is more consistently favorable, i.e. the sum of the damage improvements consistently exceeds the sum of the damage increases, except that in some cases these effects are very equal.
6. The matrix exhibits an interesting property of "symmetry", reflecting a generic reciprocity to the extent that the effect of a change in element j on element i

is comparable to the effect of a change in element i on element j. The signs agree in most cases, but the magnitudes may show large differences.

In addition to the conclusions that could be drawn from Table 4.4, the observation of the other studies presented herein can be summarized as follows.

1. The amount of confinement steel in zones of plastic deformations does not influence the damage distribution to any useful extent.
2. Changes of member depths do not have significant effects on the damage distribution in a frame, especially if the depths of all beams in a story are changed by the same amount. Because of this behavior, the member depth parameter is not an effective tool for an automatic design method. Moreover, architectural considerations generally place constraints on feasible member sizes.
3. The principle of linear superposition holds in an overall sense. This applies to the magnitude of a particular change, the sign of the change, and the superposition of effects caused by changes in more than one frame element.
4. Although all of these studies involved average results based on 10 sample ground accelerations histories, some of the results are influenced by the randomness of the input, especially if the absolute values of the damage changes are small.

Table 4.1 Calculation of Dead Weight of Example Office Building

No.	Structure Component	Weight (Kips)
1	Beams	143.50
2	Columns	40.88
3	Interior Walls	18.00
4	Exterior Walls	24.00
5	Floor Slabs & Ceilings	306.00
6	Roof Slab, Ceiling & Roofing	126.00
	Total,	W = 658.38

Table 4.2 Distribution of Lateral Forces

Floor	Lateral Force (Kips)
4th Floor	$0.4 \times V = 24.70$
3rd Floor	$0.3 \times V = 18.53$
2nd Floor	$0.2 \times V = 12.35$
1st Floor	$0.1 \times V = 6.18$

Note : $V = 61.76$ *kips* from Eq (4.2)

Table 4.3 Identification of Basic Case Studies

Member	Peak Acceleration	Design Parameter	Most Critical Member	Second Most Critical Member	Two Most Critical Members
Critical Columns	1.0g	Long. Steel	I-L1	I-L2	I-L3
		Confinement	I-C1	I-C2	I-C3
		Section Depth	I-M1	I-M2	I-M3
	0.5g	Long. Steel	II-L1	II-L2	II-L3
		Confinement	II-C1	II-C2	II-C3
		Section Depth	II-M1	II-M2	II-M3
Critical Beams	1.0g	Long. Steel	III-L1	III-L2	III-L3
		Confinement	III-C1	III-C2	III-C3
		Section Depth	III-M1	III-M2	III-M3
	0.5g	Long. Steel	IV-L1	IV-L2	IV-L3
		Confinement	IV-C1	IV-C2	IV-C3
		Section Depth	IV-M1	IV-M2	IV-M3

Table 4.4 Changes in Member Damage Indices Due to 5% Increase of Reinforcement , $\times 10^{-4}$ (1.0g Peak Acceleration)
(For member designations, see Fig.4.1)

Effect / Cause	Reference Damage Index	Top Story				3rd Story				2nd Story				1st Story			
		B1	B2	C1	C2	B3	B4	C3	C4	B5	B6	C5	C6	B7	B8	C7	C8
B1	74	−7	−21	6	1	−11	−6	2	7	−4	1	3	5	9	6	7	6
	92	−11	−19	−3	8	−13	−9	−2	−3	−5	−7	−1	4	11	8	6	7
B2	191	−30	−38	−2	6	−25	−12	2	5	−9	−7	2	10	21	11	14	15
C1	0	0	0	0	0	0	0	0	0	0	0	0	0	0	0	0	0
	0	0	0	0	0	0	0	0	0	0	0	0	0	0	0	0	0
C2	0	0	0	0	0	0	0	0	0	0	0	0	0	0	0	0	0
	0	0	0	0	0	0	0	0	0	0	0	0	0	0	0	0	0
B3	551	−1	0	1	2	−81	−23	7	−7	−18	−13	6	14	30	22	23	20
	394	1	−14	4	0	−65	−38	3	14	−17	−1	7	9	25	14	16	16
B4	816	0	−15	3	3	−124	−102	2	34	−28	−15	10	14	58	26	33	31
C3	0	0	0	0	0	0	0	0	0	0	0	0	0	0	0	0	0
	0	0	0	0	0	0	0	0	0	0	0	0	0	0	0	0	0
C4	122	0	9	−2	4	31	33	−4	−36	−18	−4	7	0	−1	−3	−4	−4
	14	0	1	0	−1	−3	0	−1	−3	−2	0	−1	−1	−2	−2	−1	−1
B5	1319	8	16	−6	0	−1	9	2	−18	−111	−40	13	4	16	3	16	29
	1047	−3	2	−3	−3	−12	−4	−6	−10	−122	−69	0	24	0	5	5	4
B6	2126	11	16	8	8	−3	8	3	9	−189	−143	21	82	43	28	29	29
C5	29	1	2	1	1	7	4	2	3	14	5	−15	−13	−11	−8	−4	−2
	0	0	0	0	0	0	0	0	0	0	0	0	0	0	0	0	0
C6	151	−1	6	−2	0	17	4	0	0	54	41	−16	−49	−28	−14	−15	−16
	1	0	0	0	0	0	0	0	0	0	0	0	−1	1	1	0	0
B7	2066	5	19	−1	3	46	10	10	9	25	12	−8	−34	−156	−60	−27	−50
	1671	10	22	5	6	53	23	5	7	33	34	−5	−10	−129	−60	−25	−19
B8	3377	−7	28	−4	−15	100	24	−38	−21	72	39	−51	−60	−241	−161	−86	−54
C7	0	0	0	0	0	0	0	0	0	0	0	0	0	0	0	0	0
	2061	25	42	7	11	79	48	10	18	54	40	2	19	−7	−25	−99	−92
C8	0	0	0	0	0	0	0	0	0	0	0	0	0	1	1	0	0
	2053	7	32	4	−5	60	34	9	−15	46	20	−2	−10	−33	33	−97	−120

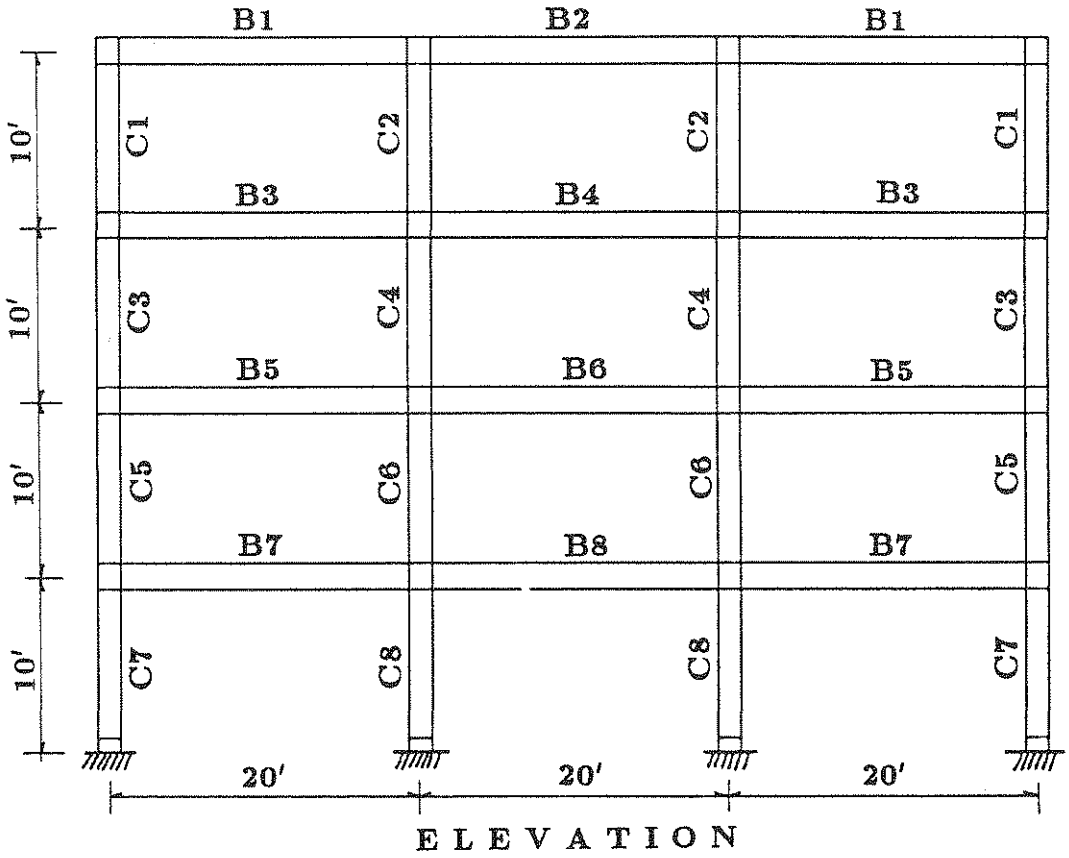

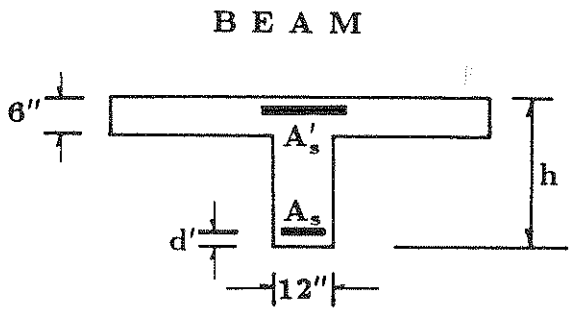

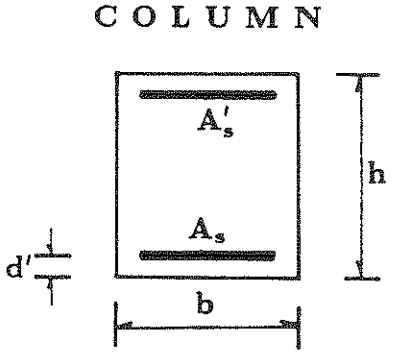

	d'	A_s	A'_s	h
	(in)	(in^2)	(in^2)	(in)
B1,B2	2.0	1.596	1.596	18.0
B3,B4	2.0	2.400	2.400	20.0
B5,B6	2.0	2.622	2.622	22.0
B7,B8	2.0	2.736	2.736	22.0

	d'	A_s	A'_s	b	h
	(in)	(in^2)	(in^2)	(in)	(in)
C1	1.500	2.160	2.160	12.0	15.0
C2,C3	1.875	2.993	2.993	12.0	18.0
C4,C5,C7	1.875	3.135	3.135	12.0	18.0
C6,C8	1.875	3.260	3.260	12.0	18.0

Fig 4.1 - Details of Example Office Building

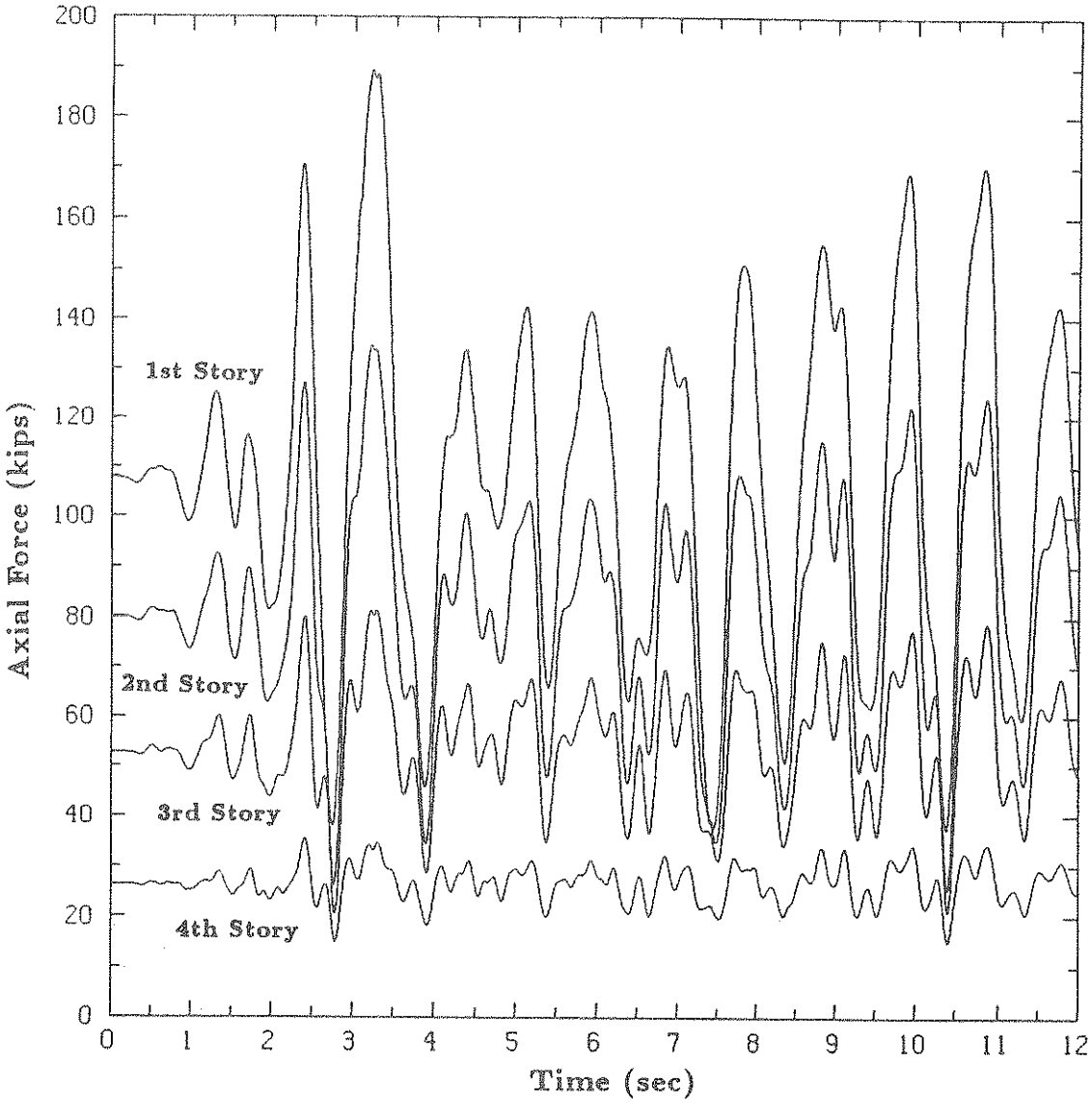

Fig 4.2 - Time Histories of Column Axial Forces

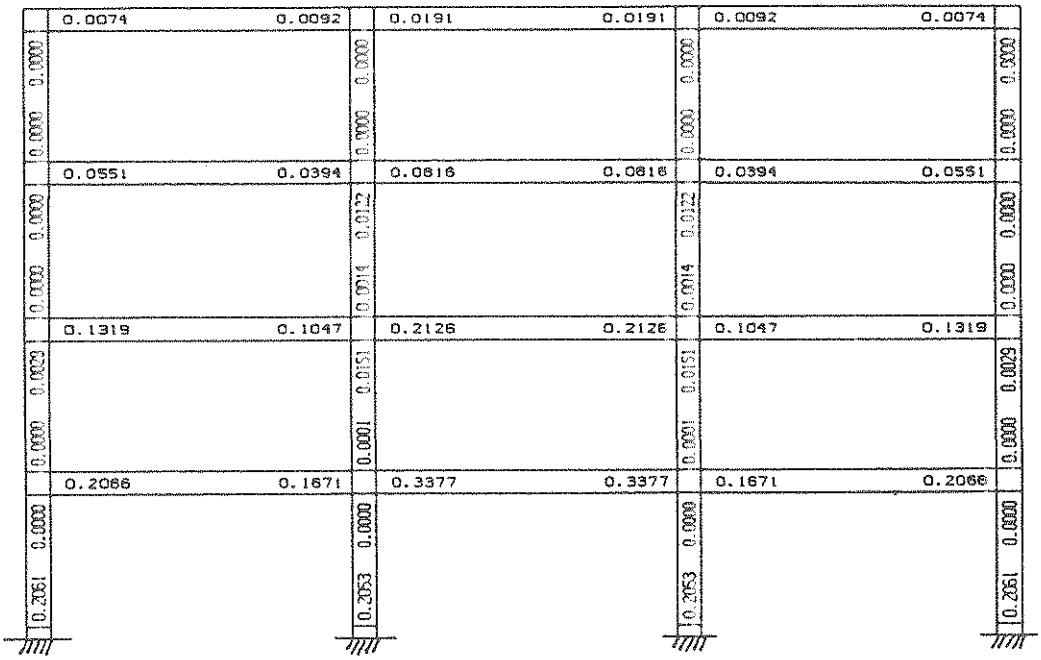

a) Earthquake with *1.0g* Peak Acceleration

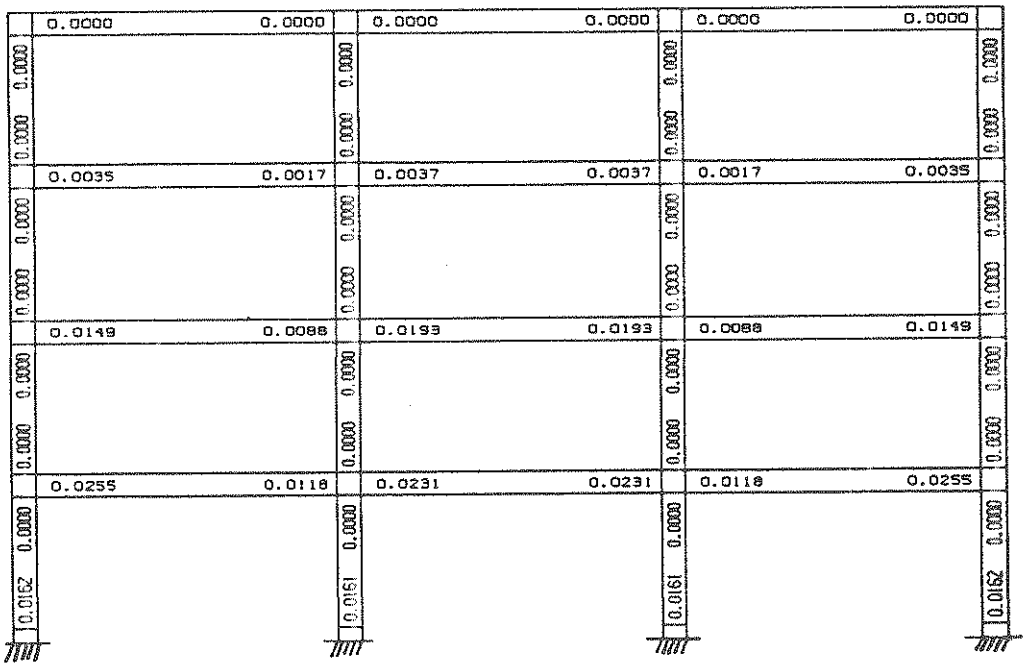

b) Earthquake with *0.5g* Peak Acceleration

Fig 4.3 - Mean Damage Indices for Example Office Building

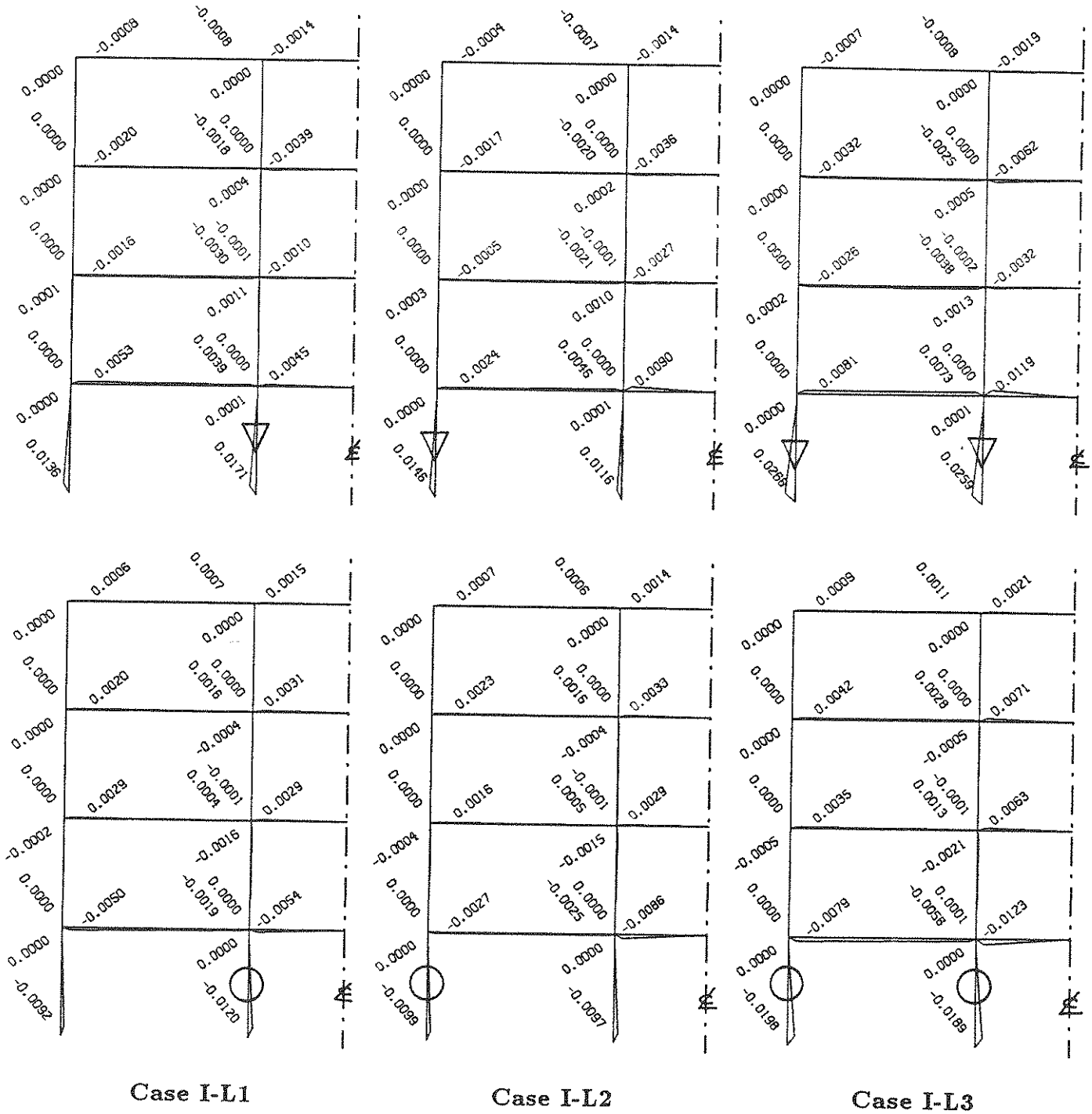

Fig 4.4 - Influence of Longitudinal Steel Ratio of Critical Columns on Frame Damage (*1.0g* Peak Acceleration)

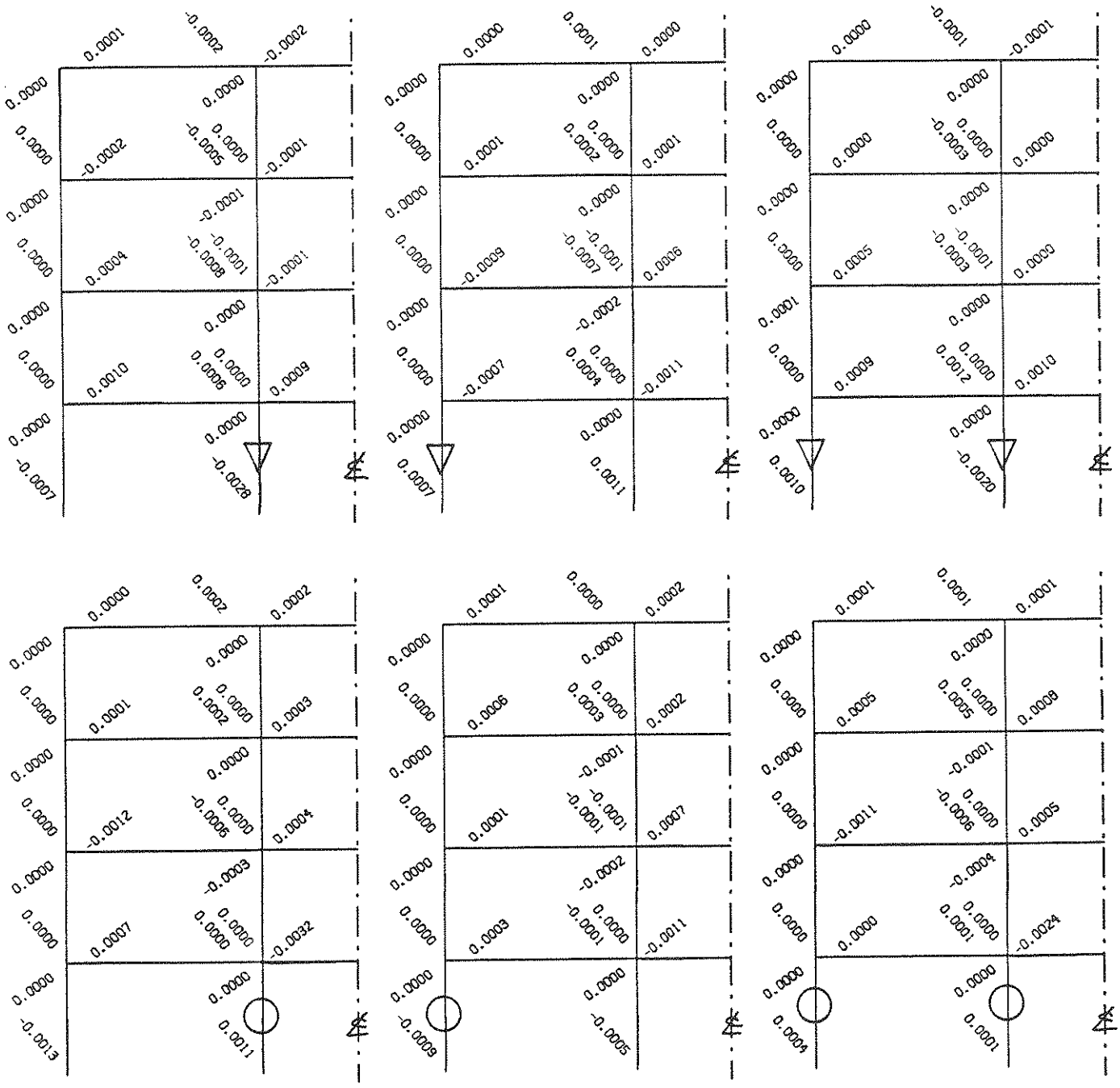

Case I-C1 Case I-C2 Case I-C3

○ – Increased +30% ▽ – Decreased -30%

Fig 4.5 - Influence of Confinement Steel Ratio of Critical Columns on Frame Damage (*1.0g* Peak Acceleration)

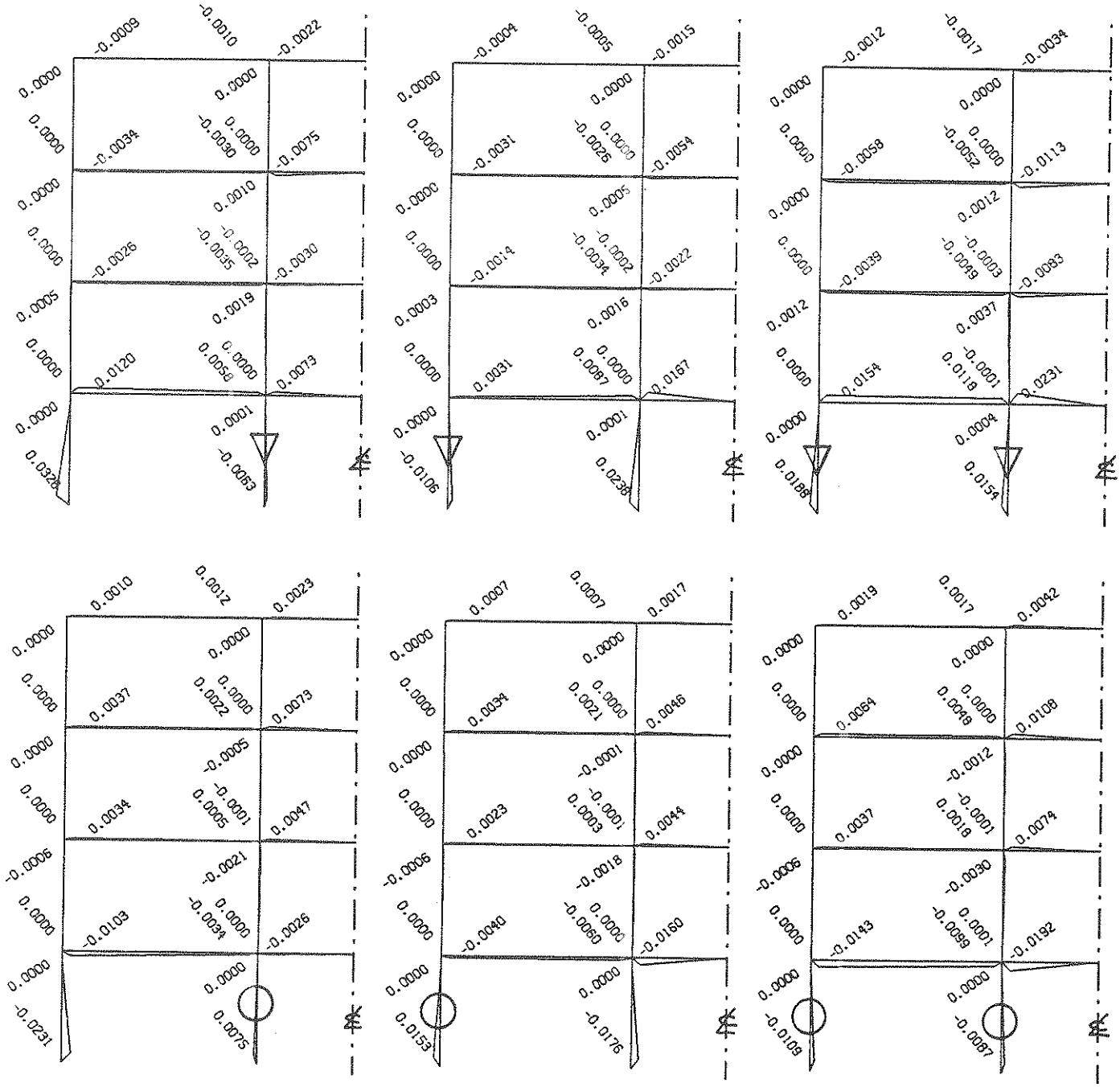

Fig 4.6 - Influence of Member Depth of Critical Columns on Frame Damage (*1.0g* Peak Acceleration)

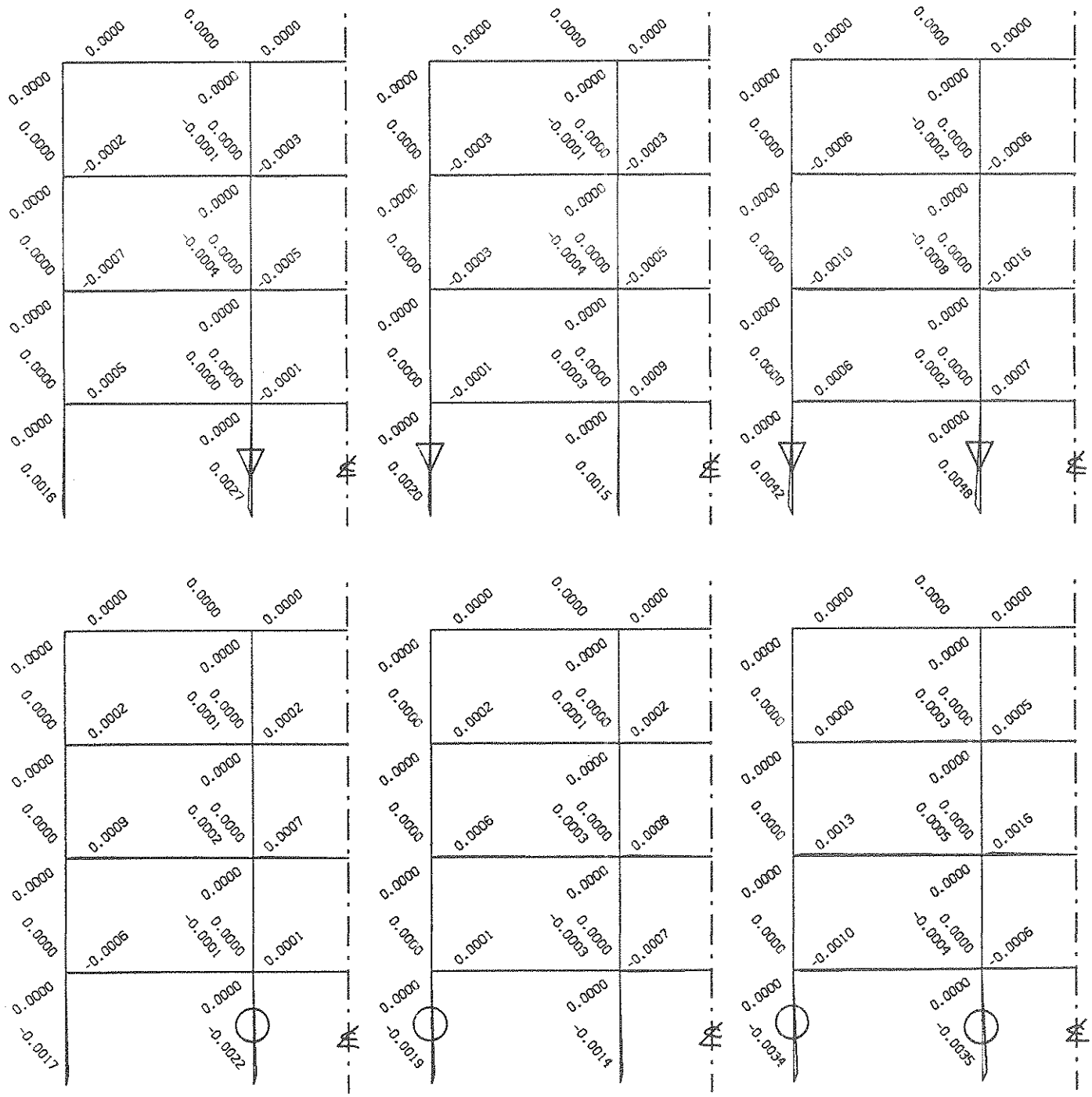

Fig 4.7 - Influence of Longitudinal Steel Ratio of Critical Columns on Frame Damage (*0.5g* Peak Acceleration)

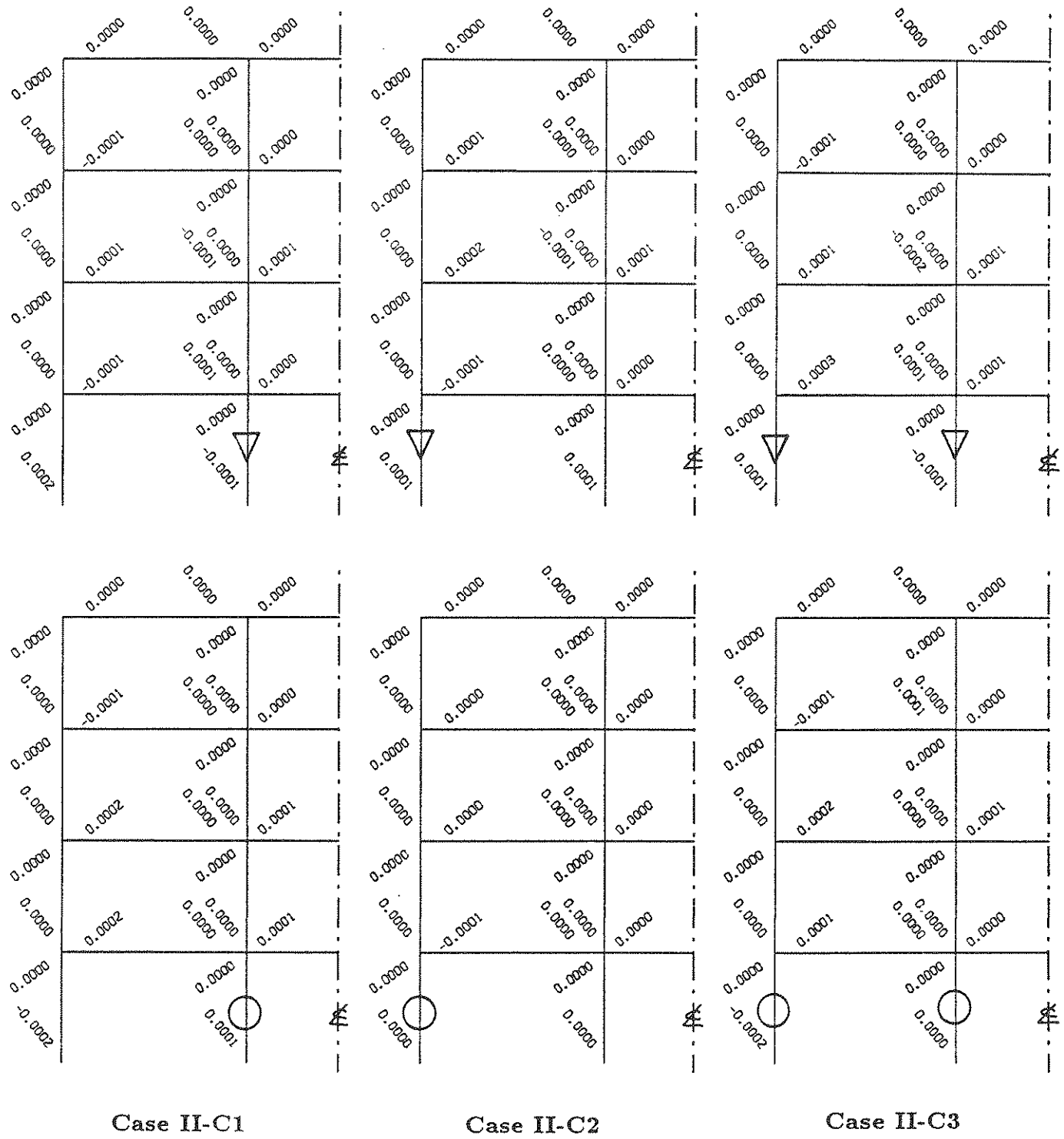

Fig 4.8 - Influence of Confinement Steel Ratio of Critical Columns on Frame Damage (*0.5g* Peak Acceleration)

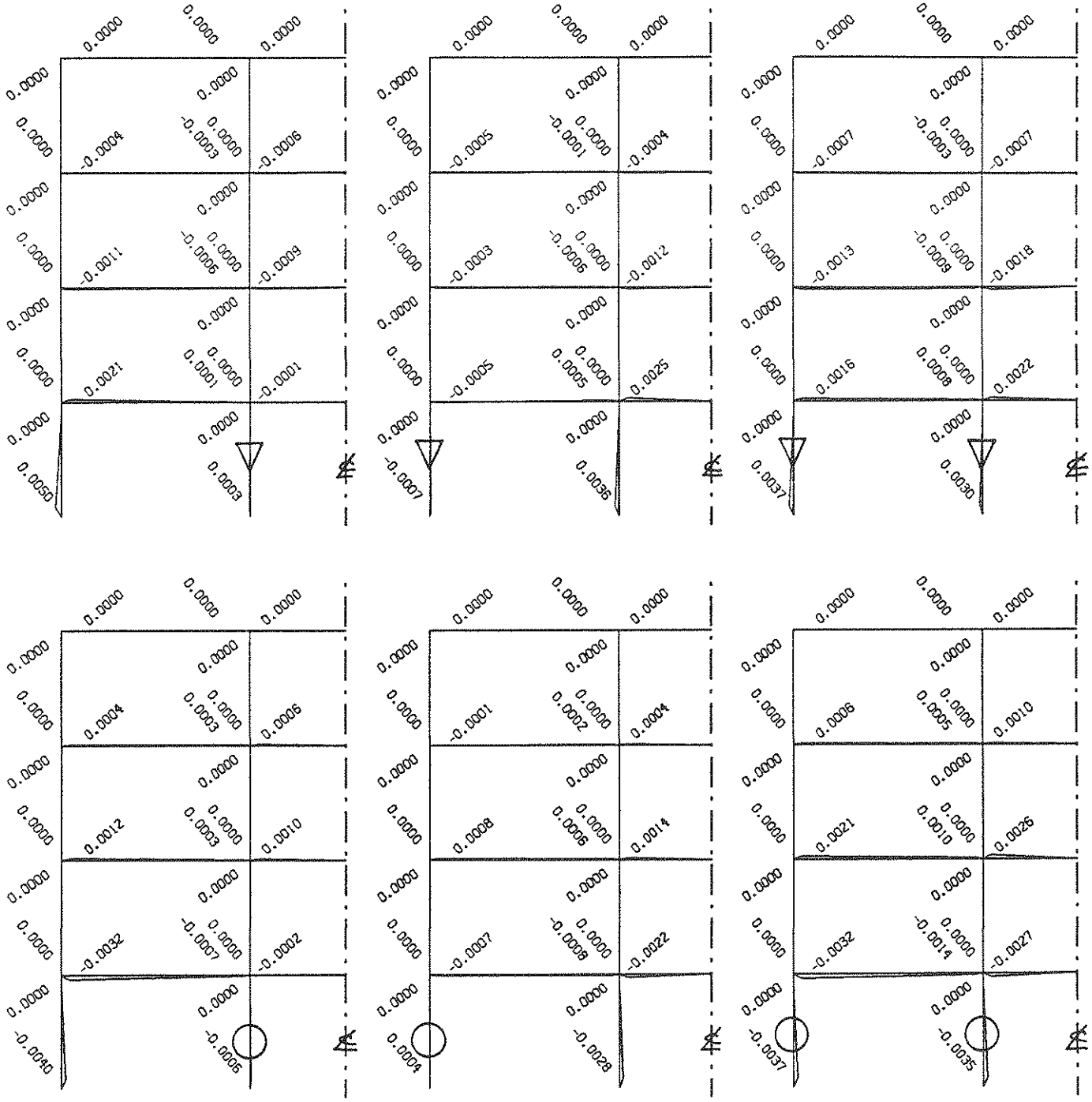

Fig 4.9 - Influence of Member Depth of Critical Columns on Frame Damage (*0.5g* Peak Acceleration)

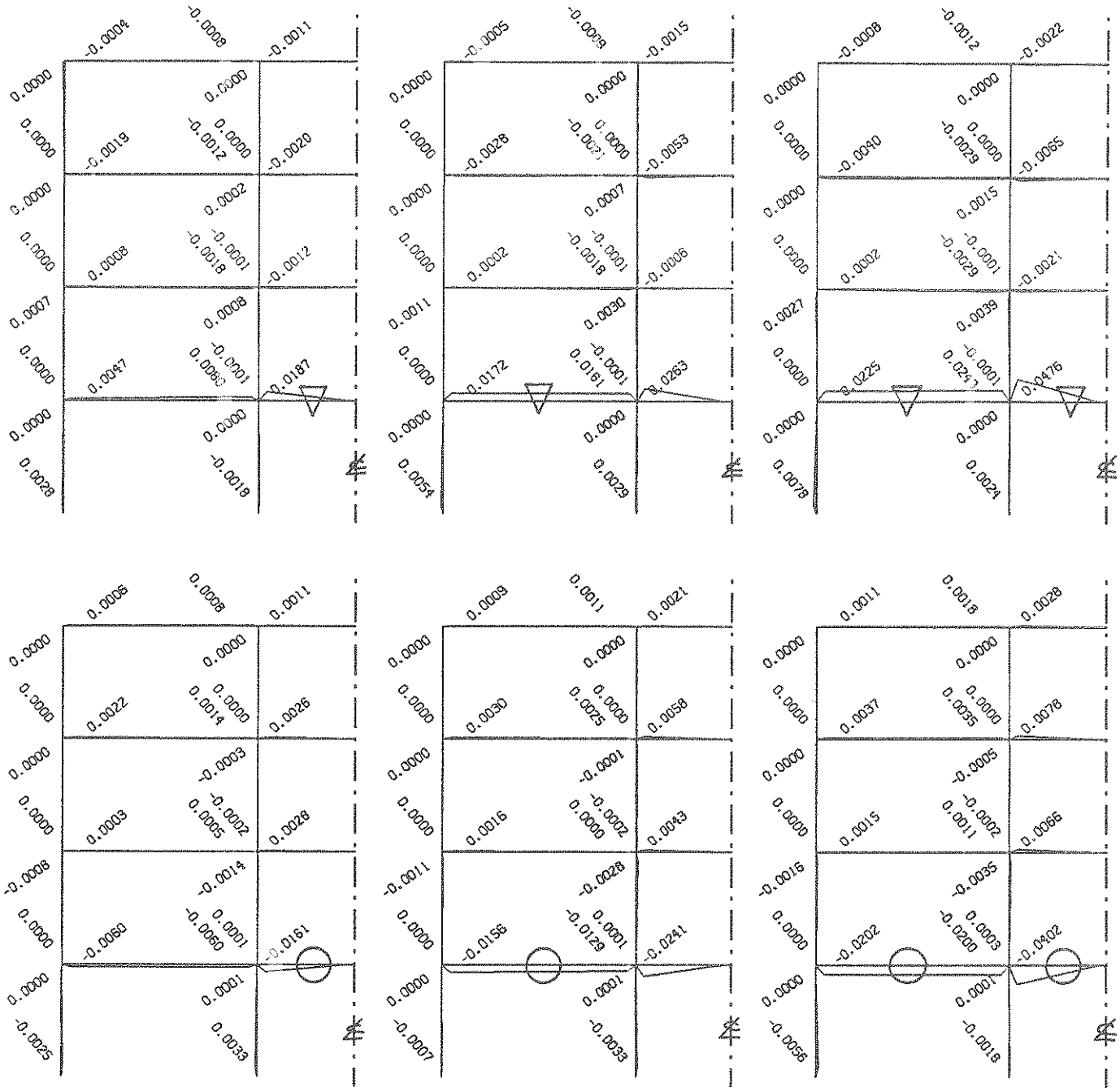

Case III-L1 Case III-L2 Case III-L3

○ – Increased +5% ▽ – Decreased -5%

Fig 4.10 - Influence of Longitudinal Steel Ratio of Critical Beams on Frame Damage (*1.0g* Peak Acceleration)

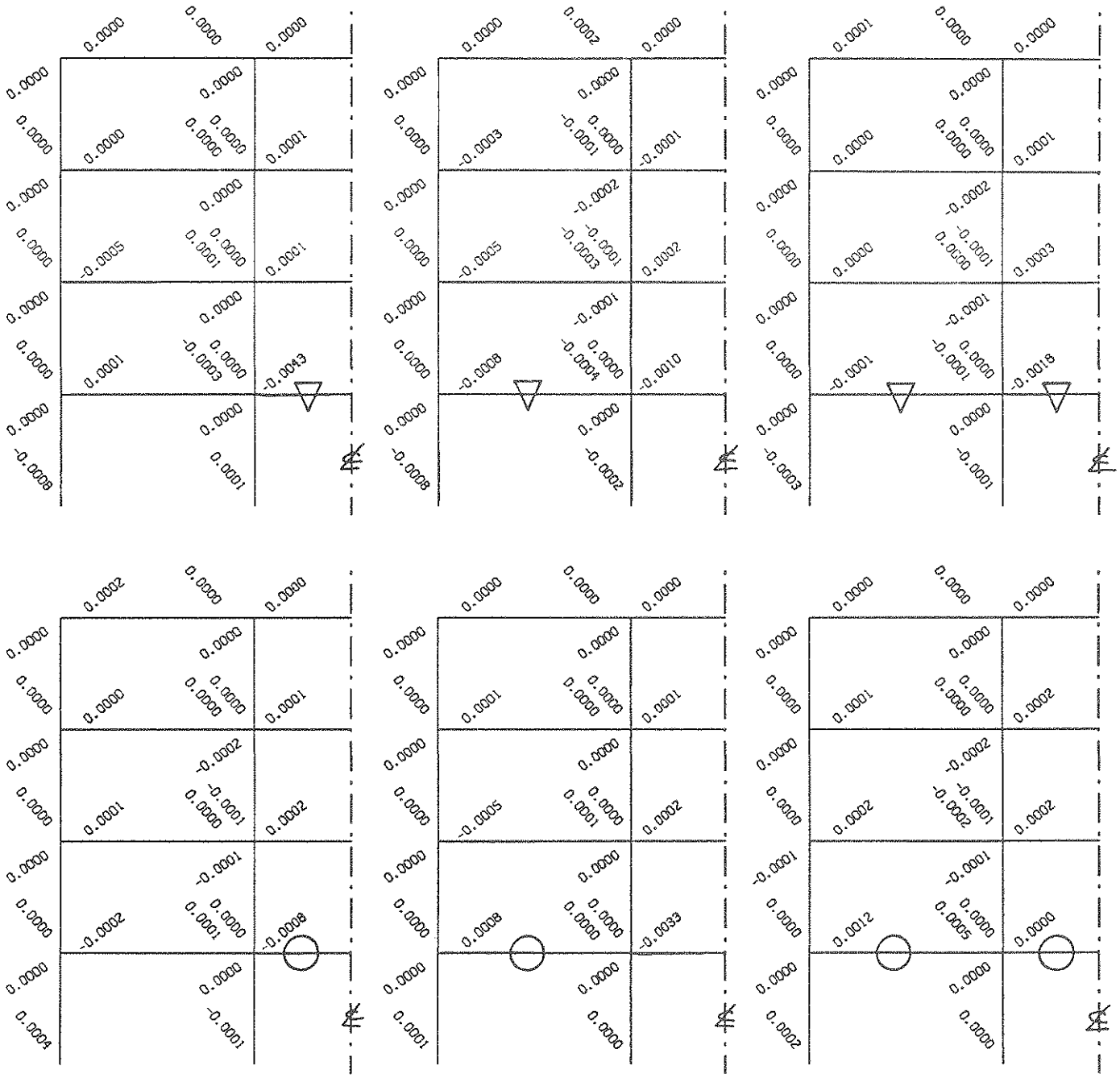

Fig 4.11 - Influence of Confinement Steel Ratio of Critical Beams on Frame Damage (*1.0g* Peak Acceleration)

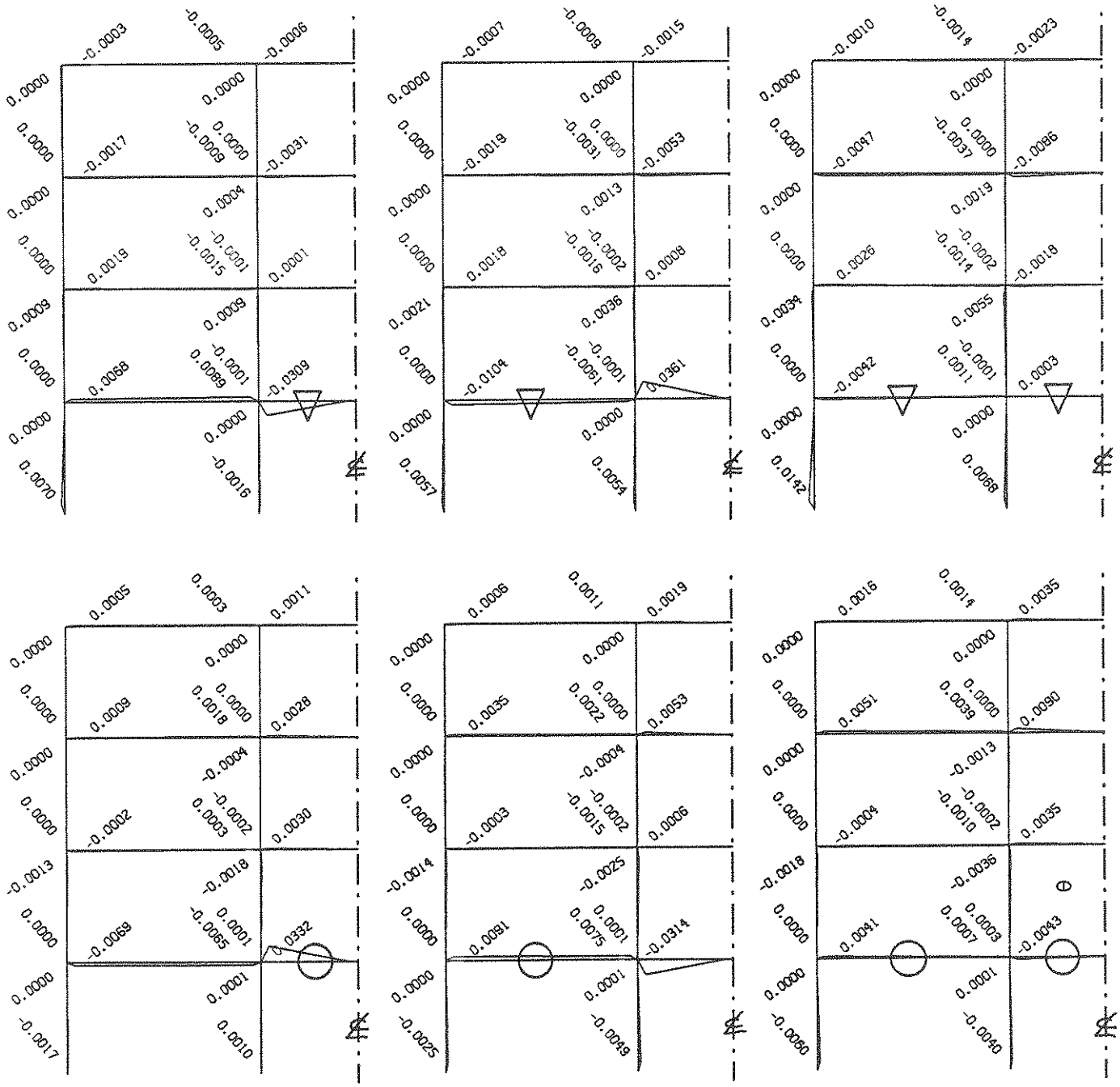

Fig 4.12 - Influence of Member Depth of Critical Beams on Frame Damage (*1.0g* Peak Acceleration)

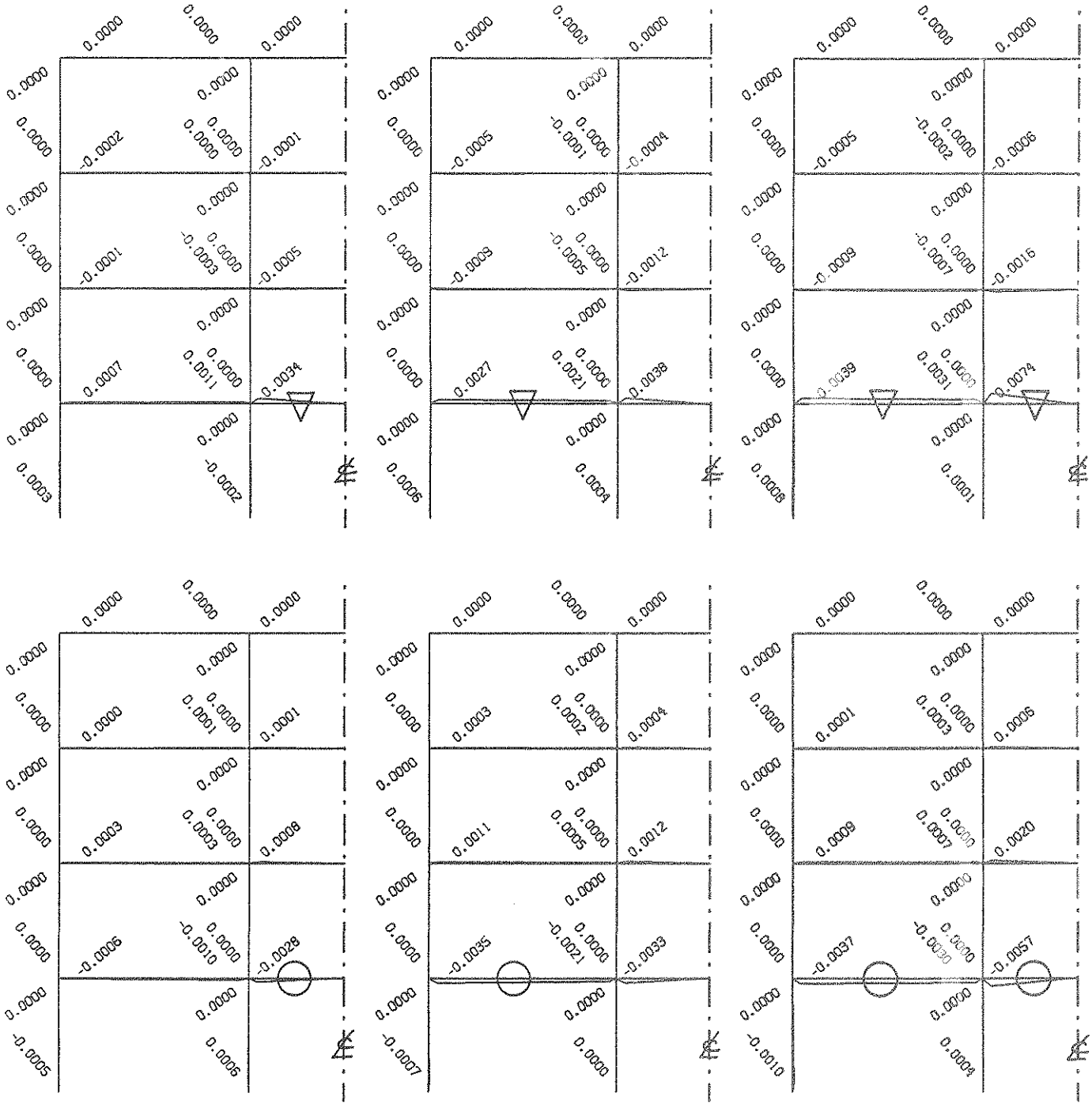

Case IV-L1 Case IV-L2 Case IV-L3

○ – Increased +5% ▽ – Decreased -5%

Fig 4.13 - Influence of Longitudinal Steel Ratio of Critical Beams on Frame Damage (*0.5g* Peak Acceleration)

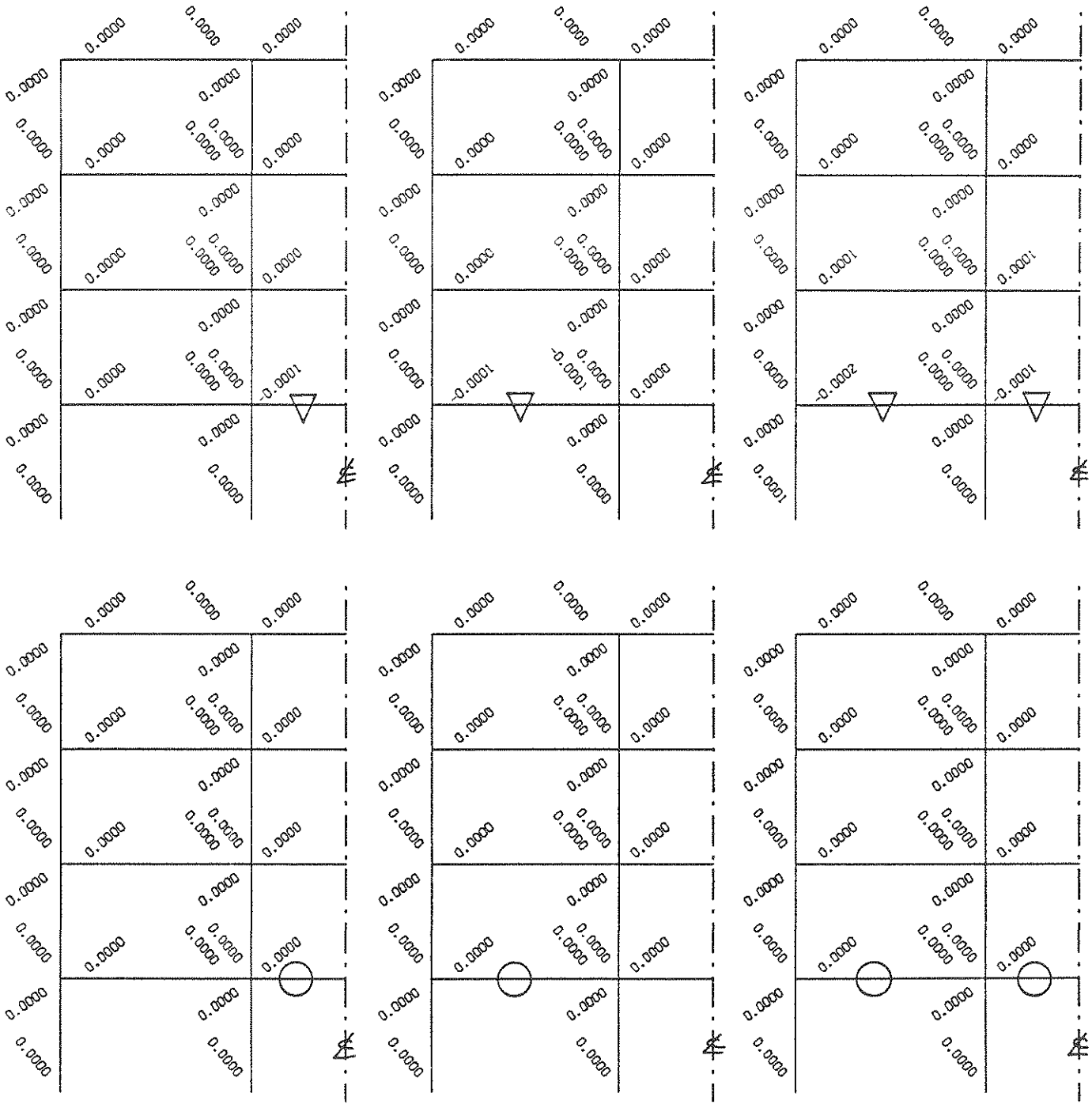

Fig 4.14 - Influence of Confinement Steel Ratio of Critical Beams on Frame Damage ($0.5g$ Peak Acceleration)

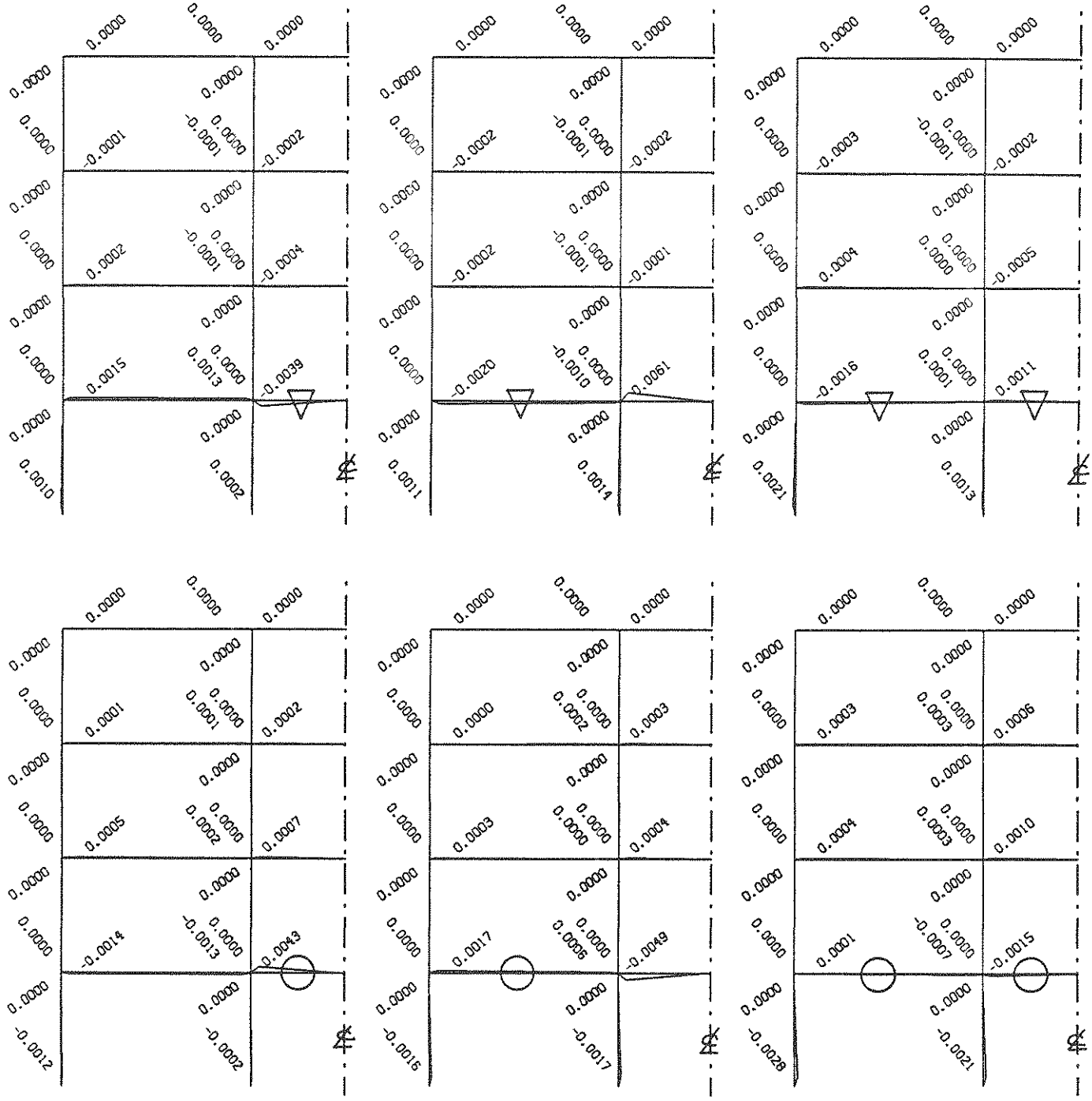

Fig 4.15 - Influence of Member Depth of Critical Beams on Frame Damage (*0.5g* Peak Acceleration)

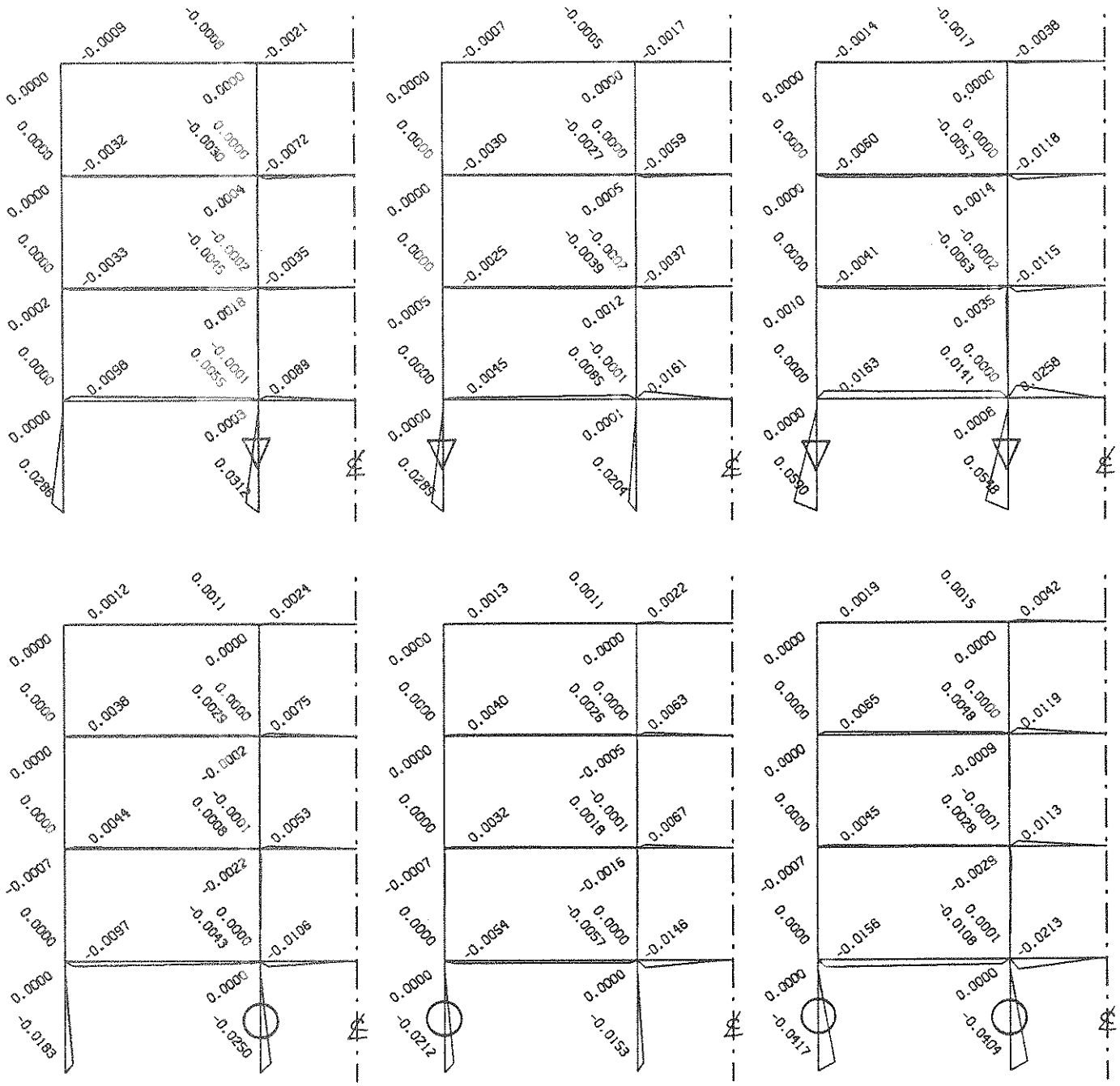

Fig 4.16 - Influence of Longitudinal Steel Ratio of Critical Beams on Frame Damage (*1.0g* Peak Acceleration)

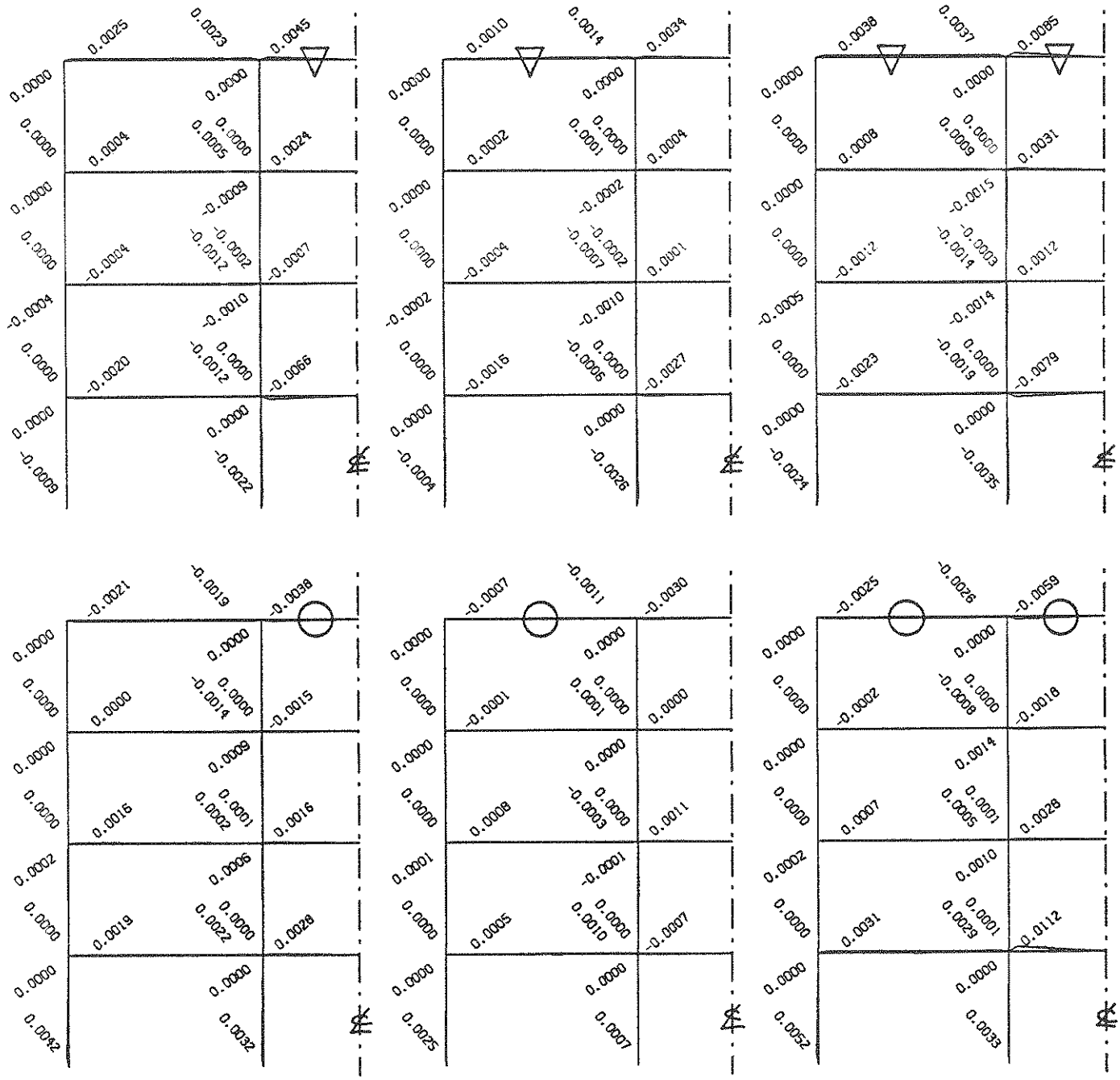

○ – Increased +5% ▽ – Decreased -5%

Fig 4.17 - Influence of Top Story Beam Reinforcement on Frame Damage (*1.0g* Peak Acceleration)

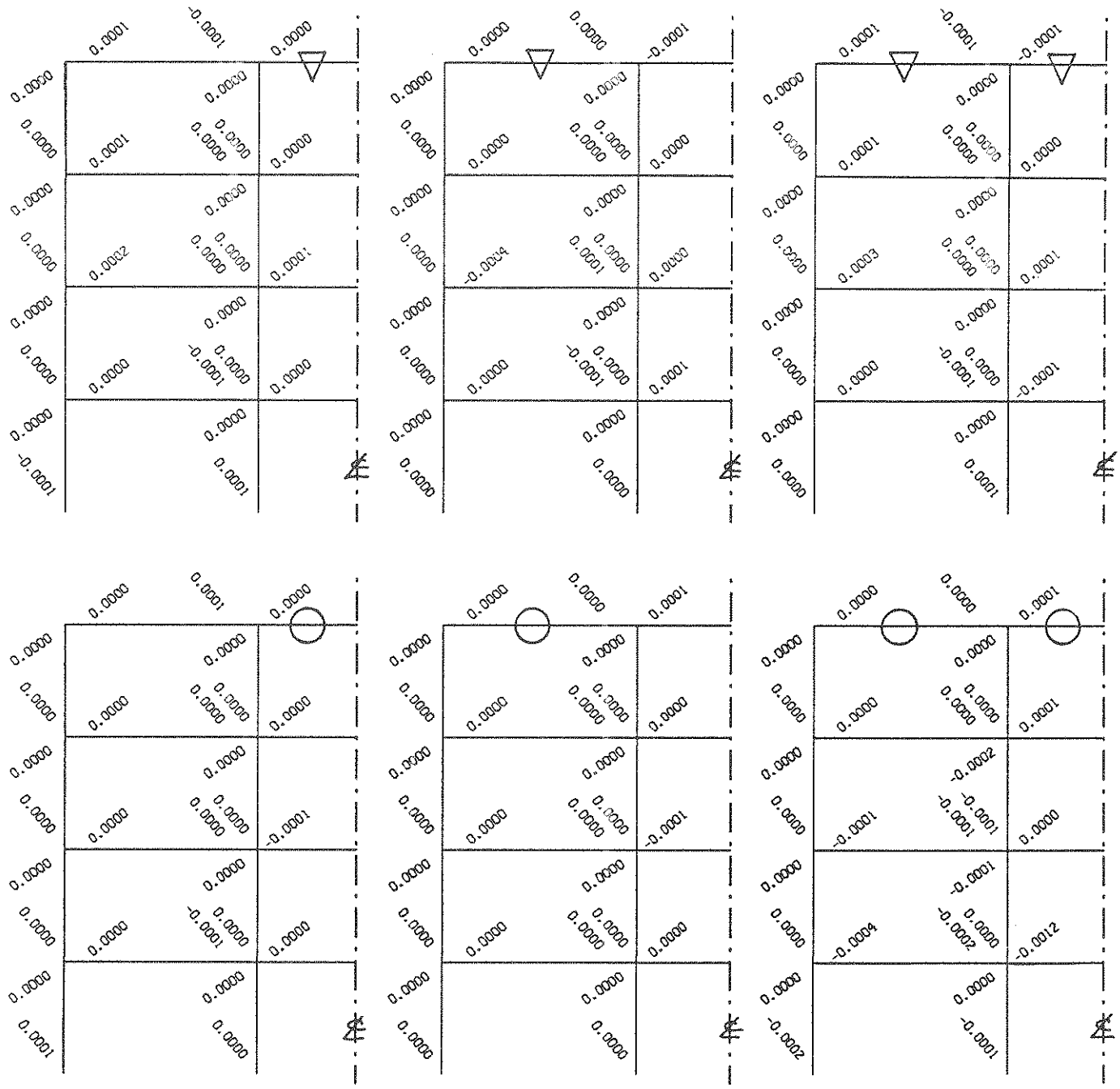

○ – Increased +50% ▽ – Decreased -50%

Fig 4.18 - Influence of Top Story Beam Confinement on Frame Damage (*1.0g* Peak Acceleration)

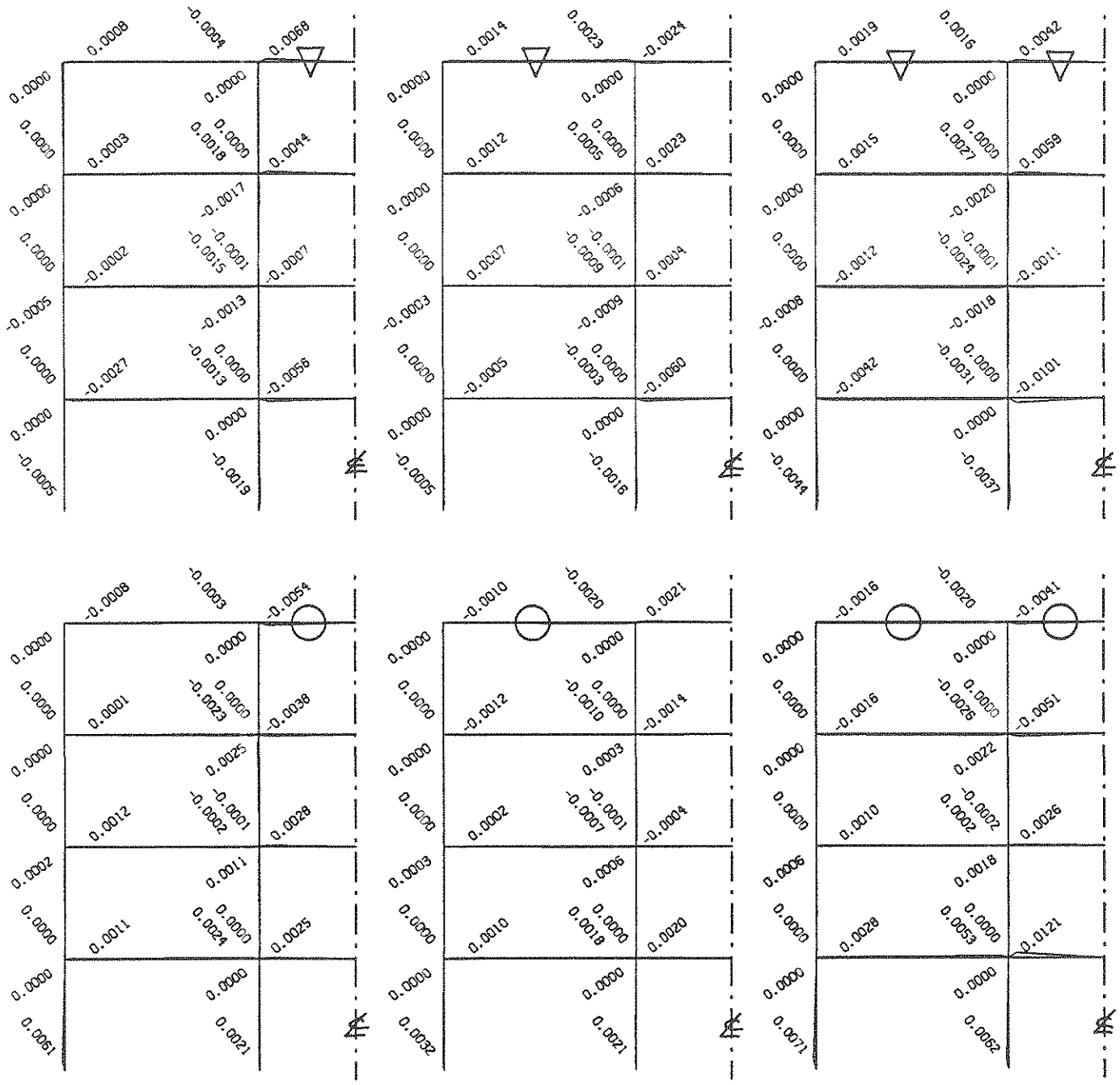

○ – Increased +5% ▽ – Decreased -5%

Fig 4.19 - Influence of Top Story Beam Depth on Frame Damage (*1.0g* Peak Acceleration)

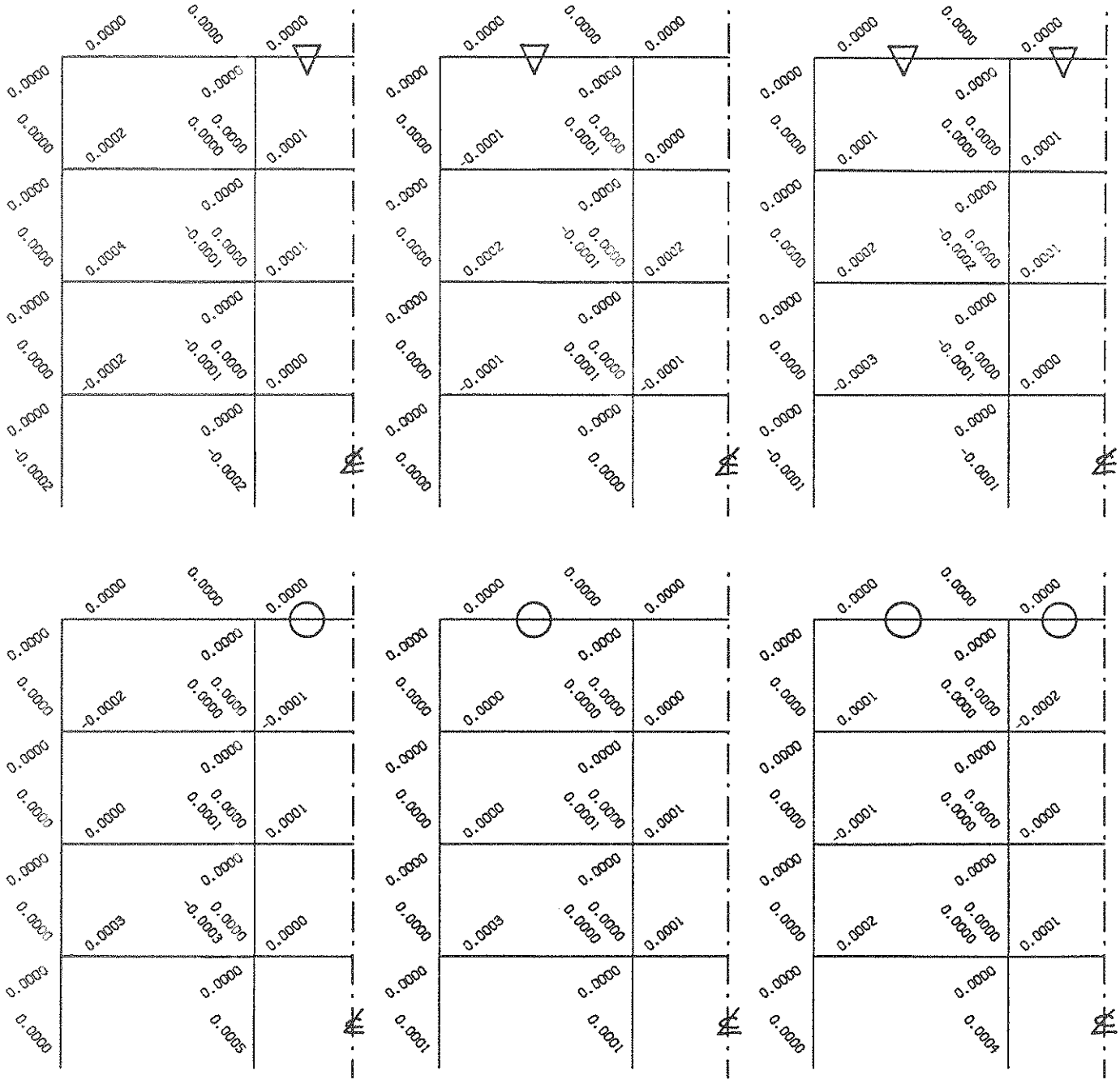

Fig 4.20 - Influence of Top Story Beam Reinforcement on Frame Damage (*0.5g* Peak Acceleration)

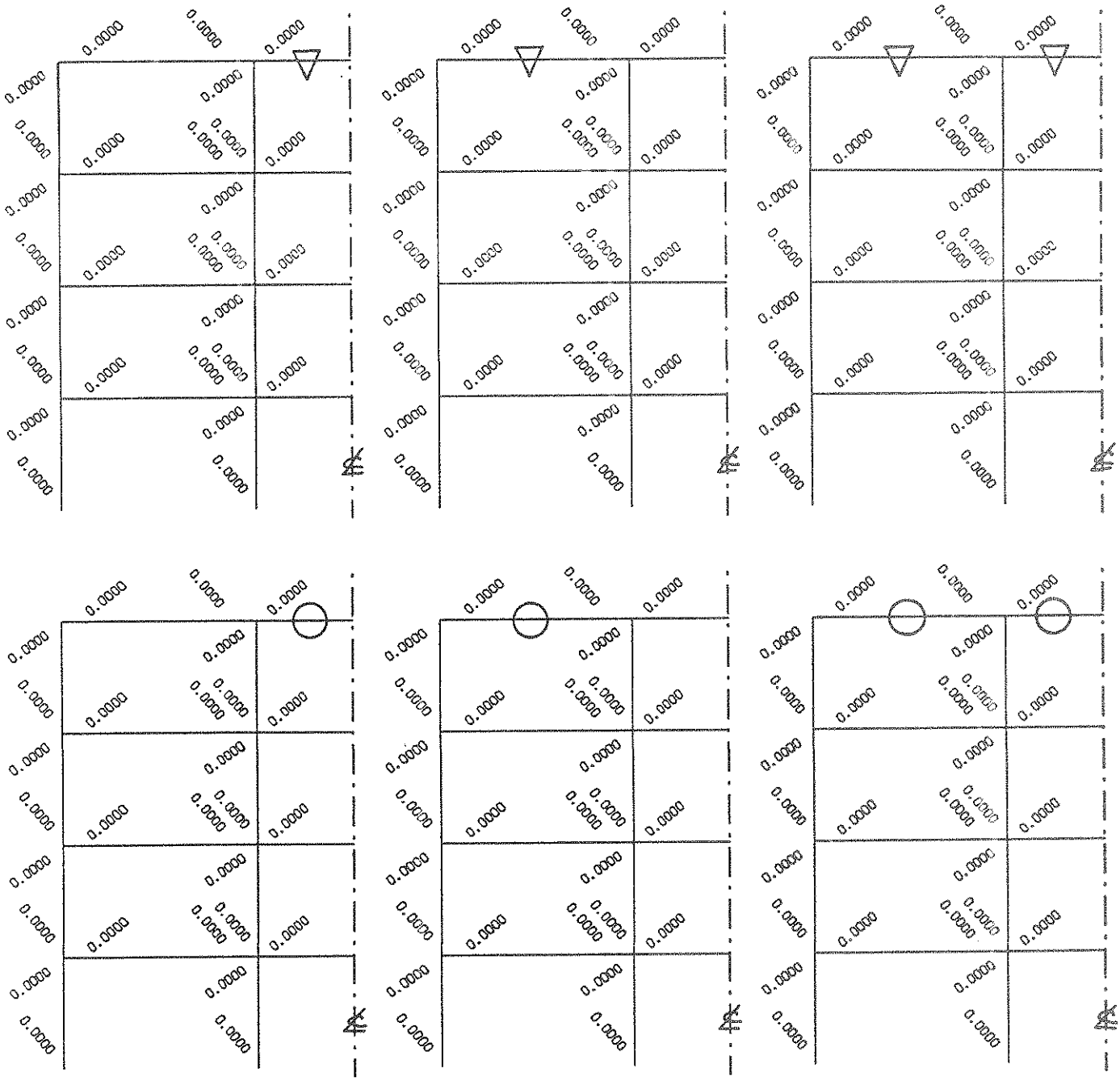

Fig 4.21 - Influence of Top Story Beam Confinement on Frame Damage (*0.5g* Peak Acceleration)

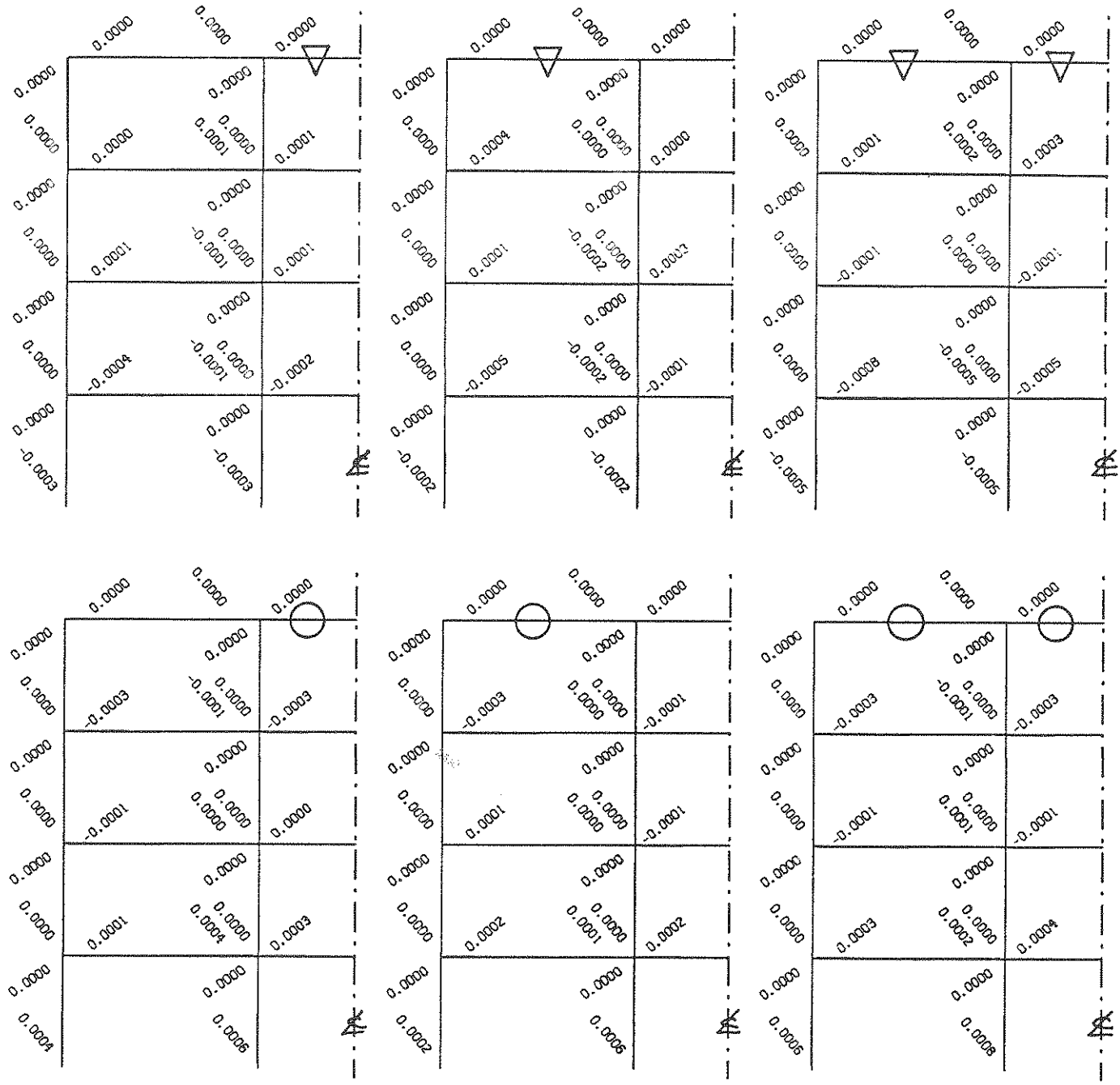

○ – Increased +5% ▽ – Decreased -5%

Fig 4.22 - Influence of Top Story Beam Depth on Frame Damage (*0.5g* Peak Acceleration)

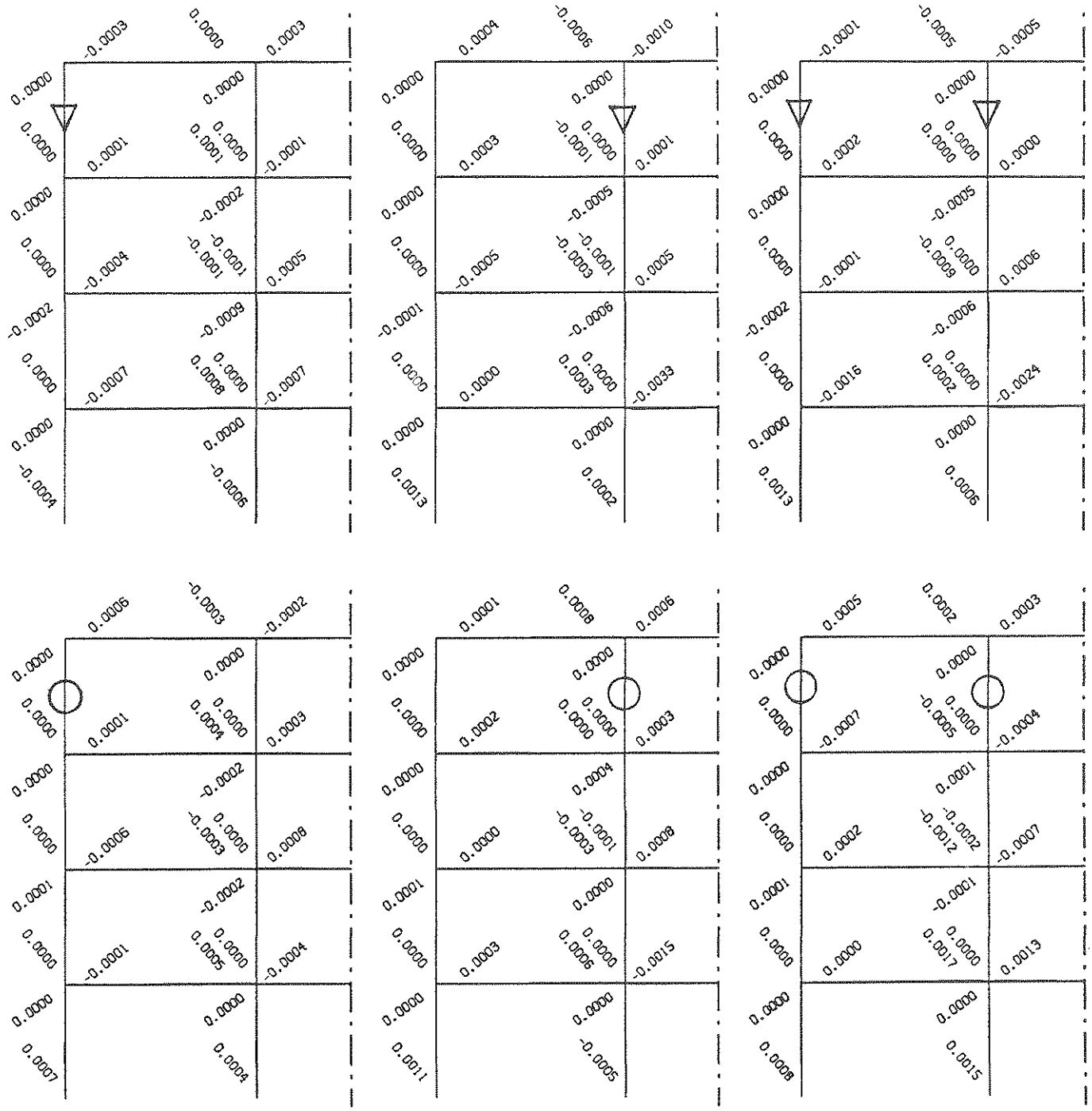

Fig 4.23 - Influence of Top Story Column Reinforcement on Frame Damage (*1.0g* Peak Acceleration)

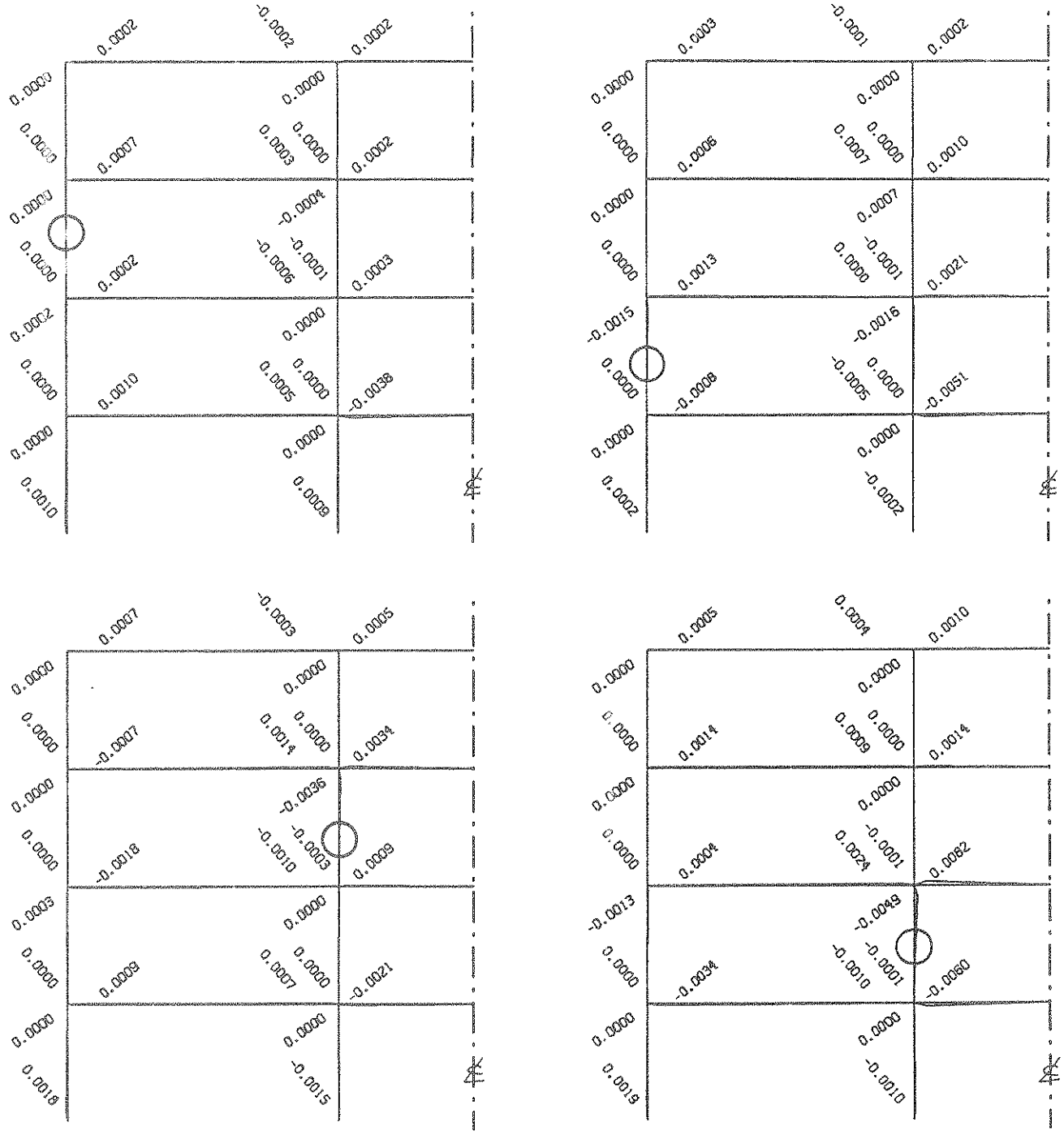

○ – Increased +5%

Fig 4.24 - Influence of Other Story Column Reinforcement on Frame Damage (*1.0g* Peak Acceleration)

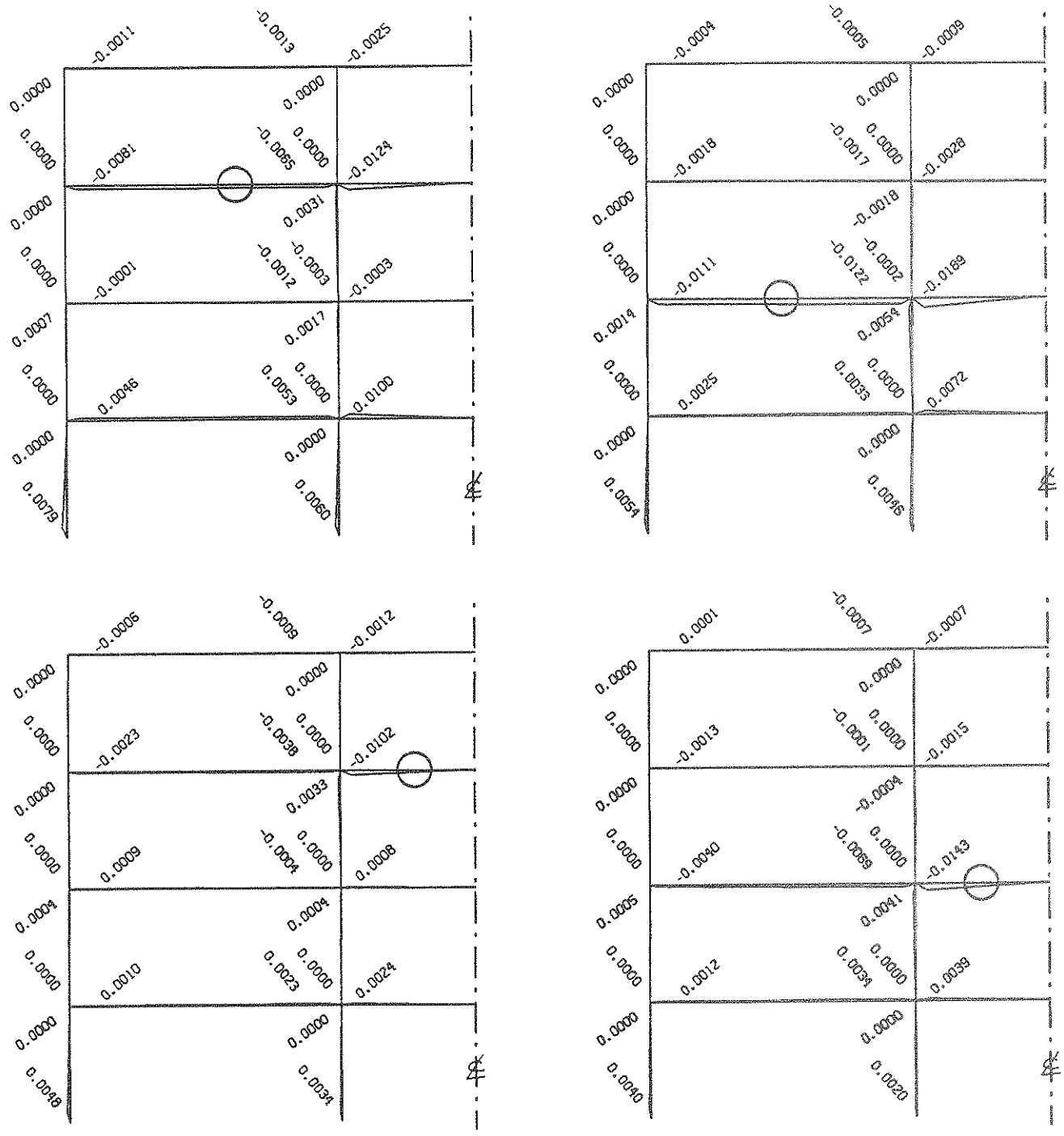

○ – Increased +5%

Fig 4.25 - Influence of Other Story Beam Reinforcement on Frame Damage (*1.0g* Peak Acceleration)

5. Automated Design Method

Conventional seismic design is typically based on equivalent static lateral loads specified in an appropriate building code. Such a simplied method, even though leading to satisfactory designs in many cases, cannot guarantee the absence of a concentration of damage in a few vulnerable structural elements. Such damage has been experienced repeatedly in recent earthquakes. On the other hand, a structure which is shown to dissipate energy uniformly in its main components can be expected to survive an earthquake of given intensity with the least amount of damage possible. It is therefore desirable that a design procedure strive for a uniform distribution of energy dissipation and damage. This goal is the objective of the automatic seismic design procedure for reinforced concrete frame buildings developed herein, Fig 1.1.

Section 5.1 describes the details of this design procedure and, in particular, the design rules that were synthesized from the parameter studies of the previous chapter. The effectiveness of the method is demonstrated with illustrative examples in Section 5.2.

5.1 Automated Design Procedure

The key components of the procedure are, 1) an algorithm to evaluate the computed damage distribution by comparing it with user-specified acceptance criteria; 2) a set of design rules which permit the automatic modification of the structure such that improved performance is guaranteed.

The damage acceptance algorithm contains the following components:

1) Damage (and plastic hinges) in columns is unacceptable, as required by the strong-column weak-beam concept. Specifically, a damage index of 0.01 or larger shall be flagged as unacceptable in any column except at the base of the first story.

2) The mean value of all beam damage indices shall not exceed a user-specified acceptance level, such as 0.1. A small tolerance such as ± 0.05 is allowed.

3) The damage index of any beam element shall not deviate from the mean value computed for all beams by more than a user-specified allowance, such as 0.05. Thus, individual beam elements may be flagged as having too much or too little damage.

If the damage index of at least one frame member is unacceptable, corrective action has to be taken, i.e. the design will have to be modified such that an improved performance in a reanalysis is guaranteed and convergence towards an acceptable design is assured.

Structural designers normally rely on their experience when designing a structure to withstand seismic loads. They can fall back on both knowledge of rational principles of structural theory and intuition. The design task is complicated by the fact that a typical reinforced concrete frame is a highly redundant structure with intricate load-resistant mechanisms. In addition, the random nature of the earthquake loading makes the design task more difficult.

There are basically two approaches one may follow to accumulate knowledge to be incorporated into an automatic design algorithm. The first approach consists of interviews with experts, that is, in our case structural engineers experienced in earthquake-resistant design. This is the approach traditionally followed by the developers of knowledge-based expert systems (2). In our work, we followed a different approach. By performing numerous numerical parameter studies, we accumulated a store of experience with this kind of building frame that structural engineers would possibly gain in years of practice. In the future, we may want to supplement the design rules synthesized from these studies with rules obtained from experts in the field. For the time being, the rules summarized below, which are contained in

program SARCF, are considered to form a useful starting point for an automatic design procedure.

1) For any beam element which showed an unacceptable level of damage in the preliminary analysis, the longitudinal steel will be increased (or decreased) by 5%,

$$\Delta A_s^1 = 0.05 \times A_s \times \text{SIGN}[D - D_{all}] \tag{5.1}$$

where A_s is the original amount of steel, D is the amount of damage determined in the preliminary analysis, and D_{all} is the allowable damage in beam elements. The steel increments (reductions) of Eq (5.1) are only trial amounts added to determine in a first design iteration the influence of these changes.

2) In a subsequent design iteration "i" , the amount of steel in any beam with unacceptable damage is changed according to,

$$\Delta A_s^i = \Delta A_s^{i-1} \times \frac{D^i - D_{all}}{D^{i-1} - D^i} \tag{5.2}$$

where ΔA_s^i denotes the additional amount of longitudinal steel required only for the element in question, ΔA_s^{i-1} denotes the steel added for the previous iteration, D^i and D^{i-1} represent damage values in the (i)th and (i-1)th iteration, respectively.

3) To adhere to the strong-column weak-beam concept, each column in the frame has to satisfy the requirement

$$M_y^{col} = 1.25 \times M_y^{beam} \tag{5.3}$$

where M_y^{col} is the yield moment of the column considered, and M_y^{beam} is the yield moment of the beam framing into the same joint. We consider here three categories of joints: 1) one beam and one column, 2) one beam and two columns, and 3) two beams and two columns. In case 3), M_y^{beam} is the average

of the two beam yield moments. Then, the reinforcing steel of each column will be increased(or decreased) linearly by the amount,

$$\Delta A_s^i = A_s \times \frac{M_y^i - M_y^{i-1}}{M_y^{i-1}} \tag{5.4}$$

where the superscript indicates the iteration number. It should be noted that the more critical capacity of the top and bottom joint of the column controls.

4) At any section of any element, the longitudinal steel ratio ρ shall not be less than the minimum required by the ACI 318-83 Code.

$$\rho = \frac{A_s}{b \cdot d} \quad \geq \quad \rho_{min} = \frac{200}{f_y} \tag{5.5}$$

where $f_y(\text{lb/in}^2)$ denotes the yield strength of the steel.

5) To ensure ductile behavior, the longitudinal steel ratio ρ shall not be greater than the maximum permitted by the ACI 318-83 Code.

$$\rho \quad \leq \quad \rho_{max} = \frac{3}{4}\rho_b + \rho' \tag{5.6}$$

where ρ_b is the balanced steel and ρ' is the compression steel.

6) For any element which does not satisfy the minimum steel requirement ($\rho < \rho_{min}$), the member depth will be reduced by:

$$\Delta d = \frac{A_s}{b \cdot (\rho_{min} - \rho)} \tag{5.7}$$

where b is the sectional width of the element in question.

7) For any element which does not satisfy the maximum steel permitted by the ACI Code ($\rho > \rho_{max}$), the member depth will be increased by:

$$\Delta d = \frac{A_s}{b \cdot (\rho - \rho_{max})} \tag{5.8}$$

8) The steel ratios of all beams with damage indices exceeding the specified limits are either increased or decreased simultaneously. Thus, full use of the superposition principle is made.

9) The analysis and redesign steps are repeated until all damage indices fall within the specified limits and all elements satisfy the reinforcing bounds, Eq (5.5) and (5.6), of the ACI Code.

Design rules 6 and 7 are subjected to practical constraints, which at this time are not yet fully implemented. Because most preliminary frame designs are expected to be "reasonable", the reinforcing limits will seldom be exceeded.

5.2 Demonstration Examples

The example office building of Fig 4.4 had been analyzed earlier, and the damage indices were summarized in Fig 4.5. Damage in the columns was very low, with a maximum value of 0.0151, not counting the base of the first story. Beam damage indices varied from 0.0074 to 0.3377, with a mean value of 0.1144, standard deviation of 0.0970 and maximum deviation of 0.2233.

In Fig 5.1 these damage values are compared with the damage expected for the same ground motions, after the frame has undergone six automatic design iterations. Program SARCF was provided with a target mean damage value of 0.1 together with a tolerance allowance of 0.05 and a maximum deviation of 0.1. As can be seen, all acceptance criteria of Section 5.1 are satisfied: 1) no column damage index exceeds 0.01, except at the base; 2) the mean value of all beam damage indices of 0.1208 is less than the target value of 0.15, including the specified tolerance; 3) no beam damage value deviates from the mean value by more than the allowed amount of 0.1.

The reinforcing steel areas for the members of the improved design are com-

pared in Table 5.1 with the original values. As can be seen, the program effected a net increase of total steel requirements of 11.1%. These changes had a negligible effect on the frame stiffness. The fundamental frequency increased from 1.19 to 1.22 *cps*.

As a further demonstration of the automatic design method, the same example frame was redesigned, with deliberately weak columns in the top story. According to Fig 5.2a, the maximum column damage index is 0.1564 in the top story, disregarding again the value obtained at the foundation. Beam damage indices vary from 0.0000 to 0.2963, with a mean value of 0.1040, standard deviation of 0.0869 and maximum deviation from the mean value of 0.1923. Fig 5.2b summarizes the damage indices of the frame after it has undergone seven automatic design iterations. Again, all damage acceptance criteria are satisfied: 1) No column damage index exceeds 0.01; 2) the mean value of all beam damage indices of 0.1186 is less than the target value 0f 0.15, including the specified tolerance; 3) the maximum deviation of any beam damage index from the mean value $(0.2147 - 0.1186 = 0.0961)$ is less than the allowable value 0.1. Table 5.2 compares the reinforcing ratios of the frame before and after the design iterations, pointing to an increase in steel requirements of 12.7%. Because of this increase in steel, the fundamental frequency increased from 1.18 to 1.21 *cps*. This example demonstrates again that the effectiveness of the automatic design method can achieve a relatively uniform distribution of damage indices over the entire frame with proper changes of the main member reinforcement.

Table 5.1 Amount of Reinforcing Steel ($A_s = A'_s$) for First Example Frame, (in^2)

Floor	Element	Original	Improved	Change
First	Outer Column	3.135	3.135	0
	Inner Column	3.260	3.260	0
	Outer Beam	2.736	2.872	0.136
	Inner Beam	2.736	3.205	0.469
Second	Outer Column	3.135	3.135	0
	Inner Column	3.260	5.709	2.449
	Outer Beam	2.622	2.622	0
	Inner Beam	2.622	3.254	0.632
Third	Outer Column	2.993	2.993	0
	Inner Column	3.135	4.957	1.822
	Outer Beam	2.400	2.161	-0.239
	Inner Beam	2.400	2.400	0
Fourth	Outer Column	2.160	2.160	0
	Inner Column	2.993	2.993	0
	Outer Beam	1.596	1.248	-0.348
	Inner Beam	1.596	1.428	-0.168

Table 5.2 Amount of Reinforcing Steel ($A_s = A'_s$) for Second Example Frame, (in^2)

Floor	Element	Original	Improved	Change
First	Outer Column	3.135	3.135	0
	Inner Column	3.260	3.260	0
	Outer Beam	2.736	2.872	0.136
	Inner Beam	2.736	3.272	0.536
Second	Outer Column	3.135	3.135	0
	Inner Column	3.260	5.516	2.256
	Outer Beam	2.622	2.622	0
	Inner Beam	2.622	3.223	0.601
Third	Outer Column	2.993	2.993	0
	Inner Column	2.993	4.635	1.642
	Outer Beam	2.400	2.166	-0.234
	Inner Beam	2.400	2.400	0
Fourth	Outer Column	2.160	2.160	0
	Inner Column	2.160	3.099	0.939
	Outer Beam	1.596	1.224	-0.372
	Inner Beam	1.596	1.422	-0.174

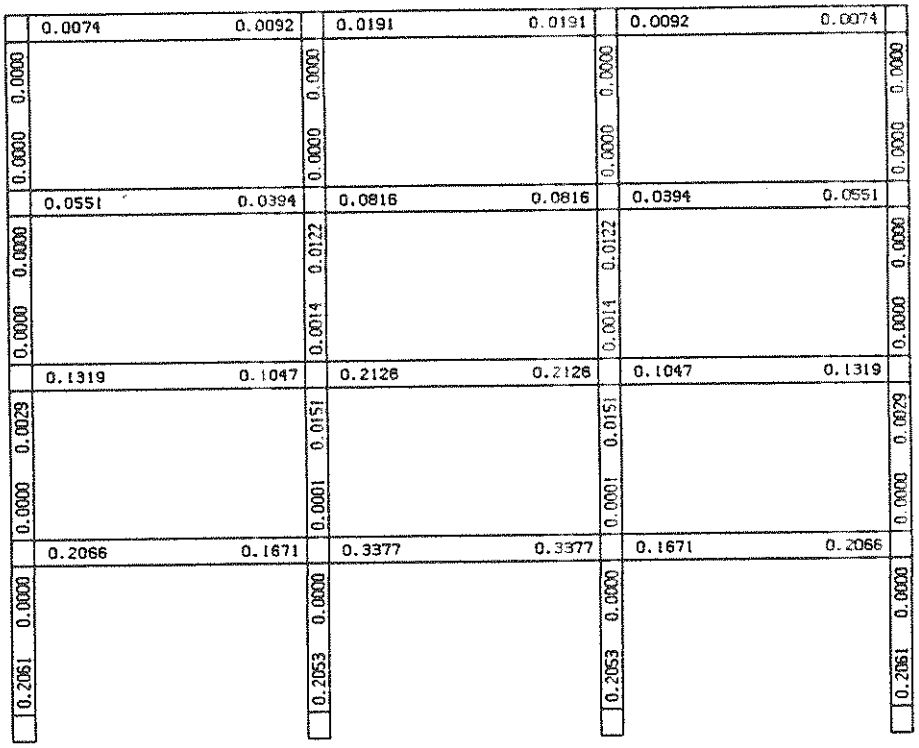

a) Original Design

$\overline{D} = 0.1144$

$\sigma_D = 0.0970$

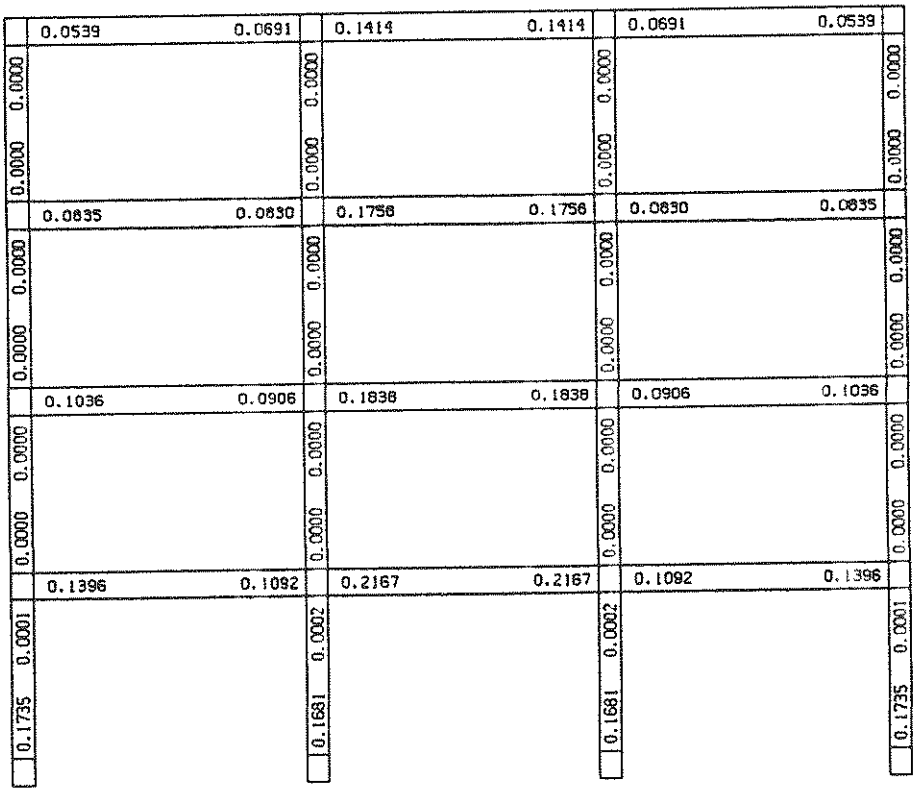

b) Revised Design

$\overline{D} = 0.1208$

$\sigma_D = 0.0485$

Fig 5.1 - Comparison of Mean Damage Indices for First Example Frame

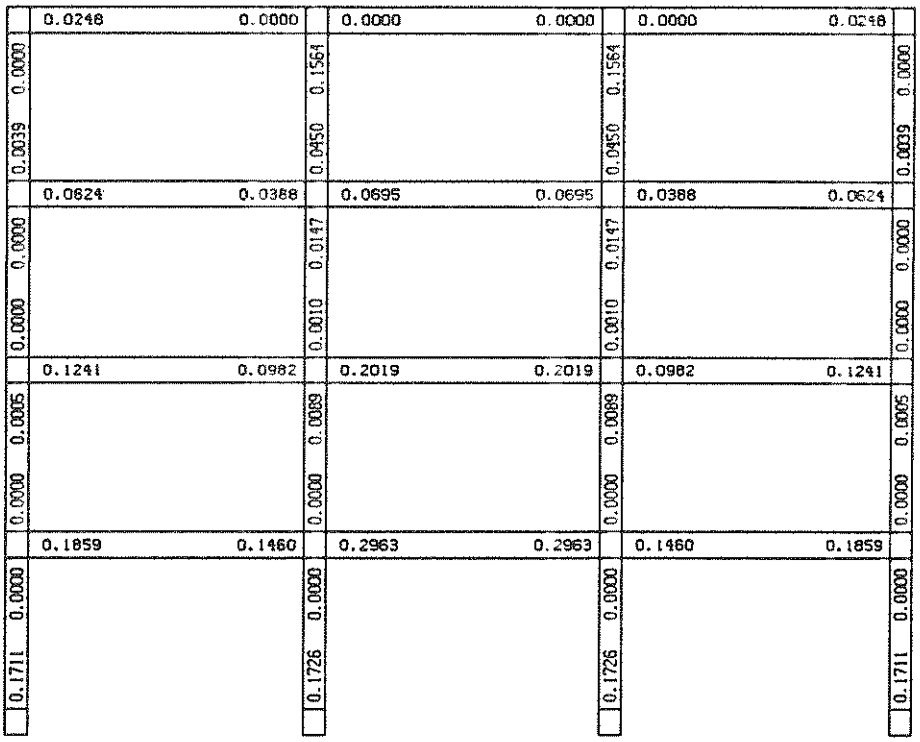

$\overline{D} = 0.1040$

$\sigma_D = 0.0869$

a) Original Design

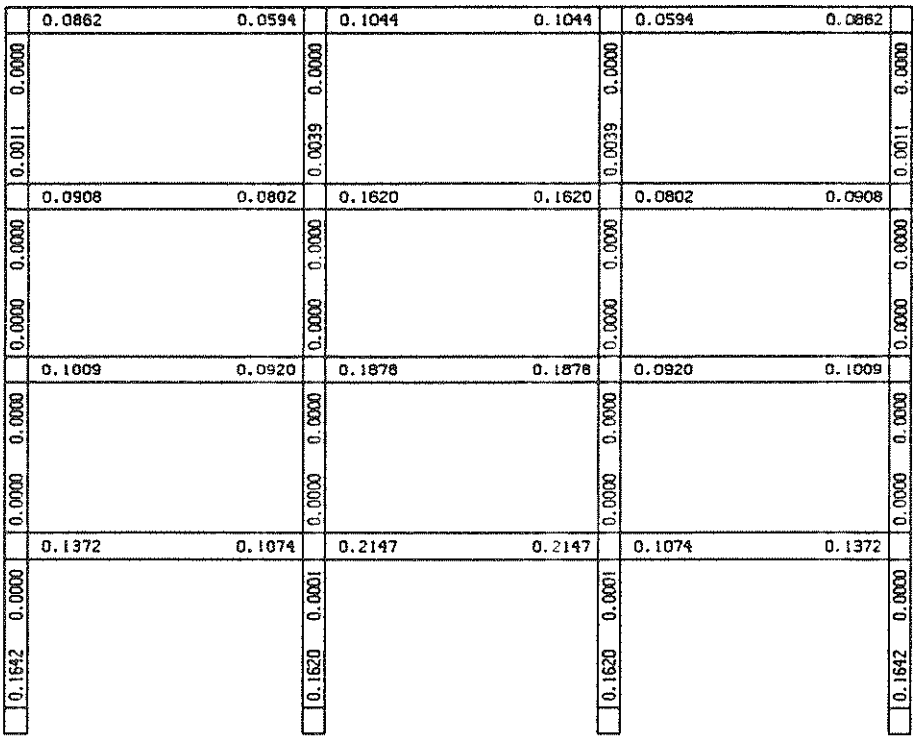

$\overline{D} = 0.1186$

$\sigma_D = 0.0451$

b) Revised Design

Fig 5.2 - Comparison of Mean Damage Indices for Second Example Frame

6. Concluding Remarks

6.1 Summary

The main objective of this study was to propose an automatic design method for reinforced concrete frame buildings subjected to strong earthquake ground motions. The design methodology consists of six main components:

1) An accurate mathematical model capable of simulating the hysteresis response of reinforced concrete members to strong cyclic loading. In earlier studies (4,5), the model of Roufaiel and Meyer was modified and refined such that it accurately reproduced many test results reported in the literature very well, particularly the stiffness and strength degradation experienced by the test specimens.

2) A useful, i.e. objective measure of damage of RC members, which can serve as an indicator of residual energy dissipation capacity and thus permit the prediction of response to further cyclic loading. The new damage index, briefly reviewed in Chapter 2, considers RC damage as a low-cycle fatigue phenomenon and takes into account the effect of load history. Even though the scarcity of experimental data made it difficult to calibrate the main model parameters, correlation studies with experimental results, as far as these were possible, were encouraging. A single structural damage index, though useful for other purposes such as insurance risk evaluations, is a poor indicator of a structure's residual strength and reliability for further loading.

3) A frame analysis program, capable of performing nonlinear dynamic analysis. In the course of this research, program SARCF was written, based on the DRAIN-2D Code (8), and enhanced with numerous features required for our studies. Further details are described in Appendix.

4) A mathematical model of the earthquake ground motion as a random process.

Since single deterministic analyses are only of limited value because of the randomness of realistic earthquake ground motions, the seismicity of a building site is represented herein by a Monte Carlo simulation, using an artificial earthquake generation algorithm due to Shinozuka.

5) An algorithm to evaluate the damage predicted for a given frame design and earthquake intensity. The user of program SARCF is expected to specify an acceptable mean damage value and a maximum deviation from this mean value which no beam elements are permitted to exceed. Columns are expected to remain essentially elastic, except at the foundations, where plastic hinges are difficult to avoid, if fixed ends are assumed.

6) A set of design rules, which permit the automatic modification of the structure such that improved performance is guaranteed. Numerous parameter studies were performed to investigate the effects on the member damage indices by small changes of the member reinforcement, the member depth, and confinement reinforcement. The evaluation of these studies led to the formulation of a few design rules. It is anticipated that these rules will be improved in time and augmented by rules synthesized from discussions with expert structural engineers. Thus, the program has features of a knowledge-based expert system.

The design methodology has been demonstrated with two four-story three-bay moment-resistant frames, typical for a medium size office building. The first frame, designed first by hand to resist equivalent static lateral loads, exhibited a damage distribution, which pointed to a disproportionate share of some beams in dissipating the earthquake energy. After six automatic design iterations, the mean value of the beam damage indices was not much different, but the standard and

maximum deviations were reduced appreciably, thus demonstrating that the beam elements can be made to participate more evenly in the dissipation of energy.

The same frame, with deliberately weak columns in the top story, was also subjected to the automatic design procedure. The damage distribution after seven design iterations was very similar to that in the first case.

The uniformity of damage distribution is thought to be a desirable goal of earthquake resistant design. Concentrations of heavy damage in some vulnerable structural members, which has led to many collapses in recent earthquakes, are avoided. It is also felt that by keeping the damage in a frame uniform, an optimum response to an earthquake of given intensity is achieved.

6.2 Future Work

The research reported herein contains several novel elements, which point to a new approach towards earthquake-resistant design of structures. Some of these components require further work, partly because of a lack of experimental data.

1. The functional relationship between load level and energy dissipation capacity is known only qualitatively. Considerable experimental work is required to furnish quantitative data to support a mathematical model.
2. The damage modifier, Eq 2.3, is based on very scarce experimental data and should be updated, as further data are made available.
3. The mathematical hysteretic model should be improved by incorporating the effect of bond and shear failure mechanisms.
4. Also, the failure moment curve of Fig 2.2 requires further experimental verification.
5. The application of Miner's rule to reinforced concrete members subjected to cyclic loading with varying amplitudes requires further substantiation.

6. In the parameter studies in Chapter 4.3, changes of the confinement steel ratio exhibit inconclusive and very small effects on the frame damage. This surprising finding requires further investigation.
7. The parameter studies of Chapter 4.3 were performed on only a single office-type building frame. Further studies are necessary to substantiate the design rules established here. Ultimately, these studies should lead to definite design rules, which guarantee fast convergence towards an acceptable design. The design rules incorporated into SARCF so far must be considered preliminary as of now.
8. It is highly desirable to interview expert structural designers and to incorporate their design rules, both rational and intuitive, into the program.

It is felt that with the enhancements to be expected from these additional studies, the proposed design methodology will prove a very effective tool for seismic design of reinforced concrete buildings.

7. References

1) ACI Committee 318-83, "Building Code Requirements for Reinforced Concrete," American Concrete Institute, 1983.

2) ASCE Special Issue, "Expert Systems in Civil Engineering," Journal of Computing in Civil Engineering, ASCE, Vol. 1, No. 4, October, 1987.

3) Atalay, M. B. and Penzien, J., "The Seismic Behavior of Critical Regions of Reinforced Concrete Components as Influenced by Moment, Shear and Axial Forces," Report No. EERC-75-19, University of California at Berkeley, CA, 1975.

4) Chung, Y. S., "Automated Seismic Analysis and Design of Reinforced Concrete Frames," Ph.D. Thesis, Department of Civil Engineering and Engineering Mechanics, Columbia University, New York, NY, 1988.

5) Chung, Y. S., Meyer, C. and Shinozuka, M., "Seismic Damage Assessment of Reinforced Concrete Members," Report No. NCEER-87-0022, National Center for Earthquake Engineering Research, Buffalo, NY, October, 1987.

6) Hwang, T. H., " Effects of Variation in Load History on Cyclic Response of Concrete Flexural Members," Ph.D. Thesis, Department of Civil Engineering, University of Illinois, Urbana, IL, 1982.

7) Hwang, T. H. and Scribner C. F., "R/C Member Cyclic Response During Various Loadings," Journal of Structural Engineering, ASCE, Vol. 110, No. 3, March 1984, pp. 477-489.

8) Kanaan, A. E. and Powell, G. H., "General Purpose Computer Program for Inelastic Dynamic Response of Plane Structures," Report No. EERC-73-6, University of California at Berkeley, CA, 1973.

9) Ma, S-Y. M., Bertero, V. V. and Popov, E. P., "Experimental and Analytical Studies on the Hysteretic Behavior of Reinforced Concrete Rectangular and T-Beams," Report No. EERC-76-2, University of California at Berkeley, CA,

1976.

10) Park, Y. J. and Ang, H-S., "A Mechanistic Seismic Damage Model for Reinforced Concrete," Journal of Structural Engineering, ASCE, Vol. 111, No.4, April 1985.

11) Park, R. and Paulay, T., "Reinforced Concrete Structures," John Wiley and Sons, Inc, New York, NY, 1975.

12) Paulay, T., "Deterministic Design Procedure for Ductile Frames in Seismic Areas," American Concrete Institute, Special Publication SP-63, Detroit, MI, 1980.

13) Popov, E. P., Bertero, V. V. and Krawinkler, H., "Cyclic Behavior of Three RC Flexural members under Large Load Reversals," Report No. EERC-72-5, University of California at Berkeley, CA, 1974.

14) Reitherman, R., "A Review of Earthquake Damage Estimation Methods," EERI, Earthquake Spectra, Vol. 1, No. 4, August 1985.

15) Roufaiel, M. S. L. and Meyer, C., "Analytical Modelling of Hysteretic Behavior of R/C Frames," Journal of Structural Engineering, ASCE, Vol. 113, No. 3, March 1987, pp. 429-444.

16) Roufaiel, M. S. L. and Meyer, C., "Reliability of Concrete Frames damaged by Earthquakes," Journal of Structural Engineering, ASCE, Vol. 113, No. 3, March 1987, pp. 445-457.

17) Shinozuka, M. and Wai, P., "Digital Simulation of Short-Crested Sea Surface Elevations," Journal of Ship Research, Vol. 23, No. 1, March 1979, pp. 76-84.

18) Shinozuka, M., Hwang, H. and Reich, M., "Reliability Assessment of Reinforced Concrete Containment Structures," Nuclear Engineering and Design, Vol. 80, 1984, pp. 247-267.

19) Uniform Building Code, "Earthquake Regulations," Chapter 23, Section 2312, 1985.

Appendix A – Computer Program for Seismic Analysis of RC Frames

As described in earlier reports (4,5), Roufaiel and Meyer's hysteretic model (15) had been adopted for nonlinear dynamic analysis of reinforced concrete frames subjected to strong earthquakes, together with certain improvements to better represent stiffness and strength degradation. This hysteretic model has been programmed for the SUN-micro and VAX-780 computer systems, which are located in the Department of Civil Engineering and Engineering Mechanics at Columbia University, and has been also incorporated into the computer program SARCF (Seismic Analysis of Reinforced Concrete Frames).

Section A.1 describes the basic procedure to simulate quasi-static experiments. Section A.2 provides some information on the program itself.

A.1 Simulation of Quasi-Static Experiments

Since most of the laboratory experiments to be simulated numerically were displacement-controlled and of quasi-static nature, the effects of inertia and damping were ignored in the analyses. Then, the nonlinear equations of motion reduce to

$$[K]\{\Delta X\} = \{\Delta P\} \tag{A.1}$$

where $[K]$ = tangent stiffness matrix, $\{\Delta X\}$ = displacement increment vector, and $\{\Delta P\}$ = load increment vector. The equations can be partitioned as:

$$\begin{bmatrix} K_{ff} & K_{fs} \\ K_{sf} & K_{ss} \end{bmatrix} \begin{Bmatrix} \Delta X_f \\ \Delta X_s \end{Bmatrix} = \begin{Bmatrix} \Delta P_f \\ \Delta P_s \end{Bmatrix} \tag{A.2}$$

where the subscripts, "s" and "f", respectively denote those degrees of freedom that are fixed to the supports and those that are not. Because $\{\Delta X_s\} = \{0\}$, the equations simplify as

$$[K_{ff}]\{\Delta X_f\} = \{\Delta P_f\} \tag{A.3}$$

These equations are again partitioned,

$$\begin{bmatrix} K_{ff_{oo}} & K_{ff_{oi}} \\ K_{ff_{io}} & K_{ff_{ii}} \end{bmatrix} \begin{Bmatrix} \Delta X_{f_o} \\ \Delta X_{f_i} \end{Bmatrix} = \begin{Bmatrix} \Delta P_{f_o} \\ \Delta P_{f_i} \end{Bmatrix} \qquad (A.4)$$

where "i" refers to those degrees of freedom for which non-zero displacements are prescribed (in a displacement-controlled test), and "o" refers to all other degrees of freedom. With $\{\Delta P_{f_o}\} = \{0\}$, Eq (A.4) leads to

$$\{\Delta X_{f_o}\} = -[K_{ff_{oo}}]^{-1}[K_{ff_{oi}}]\{\Delta X_{f_i}\} \qquad (A.5)$$

and

$$\left([K_{ff_{ii}}] - [K_{ff_{io}}][K_{ff_{oo}}]^{-1}[K_{ff_{oi}}]\right)\{\Delta X_{f_i}\} = \{\Delta P_{f_i}\} \qquad (A.6)$$

The relationships between $\{\Delta P_{f_i}\}$ and $\{\Delta X_{f_i}\}$ can be plotted and compared with the corresponding experimental results. In earlier reports (4,5), very good agreement was obtained between experimental and analytic load-deformation curves for many available experimental data.

A.2 SARCF, Seismic Analysis of Reinforced Concrete Frames

The response of reinforced concrete building to strong ground motions is sophisticated because of its nonlinear nature. In addition, the damage values associated with inelastic response of reinforced concrete buildings are of great interest and prove useful as control parameter in current seismic design.

Program SARCF has been written to perform seismic analysis of reinforced concrete frames and provides all appropriate element damage indices as well as the nonlinear response quantities of two-dimensional frames subjected to seismic motions. Based on DRAIN-2D (8), the program has incorporated the following enchancements:

1) A new hysteresis model of RC frame elements with strength and stiffness degradation (4).

2) A new damage model which serves as an indicator of residual energy dissipation capacity during cyclic loading (Chapter 2).

3) An eigenvalue solver capable of computing the natural frequencies and mode shapes of the structure with any prescribed degree of damage.

4) Generation of random artificial earthquakes based on the Kanai-Tajimi spectrum and a trapezoidal envelope function (Chapter 3). Other envelope functions could be easily substituted (6).

5) Statistical analysis of damage values based on the specified number of artificial ground motion histories. In this study, 10 histories were shown to be sufficient (Fig 3.2).

6) Automatic design procedure, Fig 1.1, to modify a preliminary design such as to produce a uniform damage distribution over the frame. The design procedure iterations continue until the user-specified target damage distribution is achieved.

The basic structure of the program is the same as that of DRAIN-2D, except that the objective of the program has been more specialized for reinforced concrete structures subjected to strong seismic motions. Some of the basic features of the SARCF are as follows:

1) The input structure has to be idealized as a planar assemblage of discrete frame elements.

2) The structure mass is assumed to be lumped at the nodes so that the mass matrix is diagonal.

3) The earthquake excitation can be generated based on Monte Carlo simulation by specifying the dominant frequency and damping ratio, the intensity function and the magnitude of the finite frequency step. Alternatively, deterministic

earthquake excitation histories can be input.

4) Input frame elements are basically of two types, beam-columns and beams.

5) The nonlinear dynamic response is determined by step-by-step integration of the equations of motion, using the constant acceleration method. The tangent stiffness of the structure is used for each step, and linear structural behavior is assumed during one step.

6) Unknown nodal displacements can be computed by the direct stiffness method. Each node possesses up to three displacement degrees of freedom, as in a typical frame analysis. However, provision is made for degrees of freedom to be deleted or combined, so that the total number of unknowns may be much less than three times the number of nodes.

7) Two nodal damage indices are computed for each element, based on the refined mathematical hysteretic model. These damage values are evaluated statistically after conclusion of each single time history analysis.

8. To implement the proposed automatic design procedure, the nodal damage indices are examined. If all damage acceptance criteria are satisfied, the computation stops. Otherwise, member properties are modified, and the analysis is repeated.

Detailed documentation of program SARCF will be found in a NCEER report currently under preparation.

Appendix B – Errata for Report No. NCEER-87-0022, October 1987

Eq (4.32) of report no. NCEER-87-0022 had contained an inaccurate notation. It's corrected form was given in this report as Eq (2.2). The inaccuracy corrections are listed below.

Report NCEER-87-0022			This report		
Eq. No	Page No	Equation	Eq. No	Page No	Equation
(4.32)	4–12	$D_e = \sum_i \sum_j \left(\alpha_{ij}^+ \frac{n_{ij}^+}{N_i^+} + \alpha_{ij}^- \frac{n_{ij}^-}{N_i^-} \right)$	(2.2)	2–3	$D_e = \sum_i \left(\alpha_i^+ \frac{n_i^+}{N_i^+} + \alpha_i^- \frac{n_i^-}{N_i^-} \right)$
(4.33)	4–13	$\alpha_{ij}^+ = \frac{k_{ij}^+}{\overline{k_i}^+} \frac{\phi_i^+ + \phi_{i-1}^+}{2\phi_i^+}$	(2.3)	2–3	$\alpha_i^+ = \frac{\frac{1}{n_i^+} \sum_{j=1}^{n_i^+} k_{ij}^+}{\overline{k_i}^+} \frac{\phi_i^+ + \phi_{i-1}^+}{2\phi_i^+}$
		$= \frac{M_{ij}^+}{\left[M_{i1}^+ - \frac{\left(N_i^+ - 1\right)\Delta M_i^+}{2} \right]} \frac{\phi_i^+ + \phi_{i-1}^+}{2\phi_i^+}$	(2.7)	2–4	$\alpha_i^+ = \frac{M_{i1}^+ - \frac{1}{2}\left(n_i^+ - 1\right)\Delta M_i^+}{M_{i1}^+ - \frac{1}{2}\left(N_i^+ - 1\right)\Delta M_i^+} \frac{\phi_i^+ + \phi_{i-1}^+}{2\phi_i^+}$

NATIONAL CENTER FOR EARTHQUAKE ENGINEERING RESEARCH
LIST OF PUBLISHED TECHNICAL REPORTS

The National Center for Earthquake Engineering Research (NCEER) publishes technical reports on a variety of subjects related to earthquake engineering written by authors funded through NCEER. These reports are available from both NCEER's Publications Department and the National Technical Information Service (NTIS). Requests for reports should be directed to the Publications Department, National Center for Earthquake Engineering Research, State University of New York at Buffalo, Red Jacket Quadrangle, Buffalo, New York 14261. Reports can also be requested through NTIS, 5285 Port Royal Road, Springfield, Virginia 22161. NTIS accession numbers are shown in parenthesis, if available.

NCEER-87-0001 "First-Year Program in Research, Education and Technology Transfer," 3/5/87, (PB88-134275/AS).

NCEER-87-0002 "Experimental Evaluation of Instantaneous Optimal Algorithms for Structural Control," by R.C. Lin, T.T. Soong and A.M. Reinhorn, 4/20/87, (PB88-134341/AS).

NCEER-87-0003 "Experimentation Using the Earthquake Simulation Facilities at University at Buffalo," by A.M. Reinhorn and R.L. Ketter, to be published.

NCEER-87-0004 "The System Characteristics and Performance of a Shaking Table," by J.S. Hwang, K.C. Chang and G.C. Lee, 6/1/87, (PB88-134259/AS).

NCEER-87-0005 "A Finite Element Formulation for Nonlinear Viscoplastic Material Using a Q Model," by O. Gyebi and G. Dasgupta, 11/2/87, (PB88-213764/AS).

NCEER-87-0006 "Symbolic Manipulation Program (SMP) - Algebraic Codes for Two and Three Dimensional Finite Element Formulations," by X. Lee and G. Dasgupta, 11/9/87, (PB88-219522/AS).

NCEER-87-0007 "Instantaneous Optimal Control Laws for Tall Buildings Under Seismic Excitations," by J.N. Yang, A. Akbarpour and P. Ghaemmaghami, 6/10/87, (PB88-134333/AS).

NCEER-87-0008 "IDARC: Inelastic Damage Analysis of Reinforced Concrete-Frame Shear-Wall Structures," by Y.J. Park, A.M. Reinhorn and S.K. Kunnath, 7/20/87, (PB88-134325/AS).

NCEER-87-0009 "Liquefaction Potential for New York State: A Preliminary Report on Sites in Manhattan and Buffalo," by M. Budhu, V. Vijayakumar, R.F. Giese and L. Baumgras, 8/31/87, (PB88-163704/AS).

NCEER-87-0010 "Vertical and Torsional Vibration of Foundations in Inhomogeneous Media," by A.S. Veletsos and K.W. Dotson, 6/1/87, (PB88-134291/AS).

NCEER-87-0011 "Seismic Probabilistic Risk Assessment and Seismic Margins Studies for Nuclear Power Plants," by Howard H.M. Hwang, 6/15/87, (PB88-134267/AS).

NCEER-87-0012 "Parametric Studies of Frequency Response of Secondary Systems Under Ground-Acceleration Excitations," by Y. Yong and Y.K. Lin, 6/10/87, (PB88-134309/AS).

NCEER-87-0013 "Frequency Response of Secondary Systems Under Seismic Excitation," by J.A. HoLung, J. Cai and Y.K. Lin, 7/31/87, (PB88-134317/AS).

NCEER-87-0014 "Modelling Earthquake Ground Motions in Seismically Active Regions Using Parametric Time Series Methods," G.W. Ellis and A.S. Cakmak, 8/25/87, (PB88-134283/AS).

NCEER-87-0015 "Detection and Assessment of Seismic Structural Damage," by E. DiPasquale and A.S. Cakmak, 8/25/87, (PB88-163712/AS).

NCEER-87-0016 "Pipeline Experiment at Parkfield, California," by J. Isenberg and E. Richardson, 9/15/87, (PB88-163720/AS).

NCEER-87-0017 "Digital Simulation of Seismic Ground Motion," by M. Shinozuka, G. Deodatis and T. Harada, 8/31/87, (PB88-155197/AS).

NCEER-87-0018 "Practical Considerations for Structural Control: System Uncertainty, System Time Delay and Truncation of Small Control Forces," J. Yang and A. Akbarpour, 8/10/87, (PB88-163738/AS).

NCEER-87-0019 "Modal Analysis of Nonclassically Damped Structural Systems Using Canonical Transformation," by J.N. Yang, S. Sarkani and F.X. Long, 9/27/87, (PB88-187851/AS).

NCEER-87-0020 "A Nonstationary Solution in Random Vibration Theory," by J.R. Red-Horse and P.D. Spanos, 11/3/87, (PB88-163746/AS).

NCEER-87-0021 "Horizontal Impedances for Radially Inhomogeneous Viscoelastic Soil Layers," by A.S. Veletsos and K.W. Dotson, 10/15/87, (PB88-150859/AS).

NCEER-87-0022 "Seismic Damage Assessment of Reinforced Concrete Members," by Y.S. Chung, C. Meyer and M. Shinozuka, 10/9/87, (PB88-150867/AS).

NCEER-87-0023 "Active Structural Control in Civil Engineering," by T.T. Soong, 11/11/87, (PB88-187778/AS).

NCEER-87-0024 "Vertical and Torsional Impedances for Radially Inhomogeneous Viscoelastic Soil Layers," by K.W. Dotson and A.S. Veletsos, 12/87, (PB88-187786/AS).

NCEER-87-0025 "Proceedings from the Symposium on Seismic Hazards, Ground Motions, Soil-Liquefaction and Engineering Practice in Eastern North America, October 20-22, 1987, edited by K.H. Jacob, 12/87, (PB88-188115/AS).

NCEER-87-0026 "Report on the Whittier-Narrows, California, Earthquake of October 1, 1987," by J. Pantelic and A. Reinhorn, 11/87, (PB88-187752/AS).

NCEER-87-0027 "Design of a Modular Program for Transient Nonlinear Analysis of Large 3-D Building Structures," by S. Srivastav and J.F. Abel, 12/30/87, (PB88-187950/AS).

NCEER-87-0028 "Second-Year Program in Research, Education and Technology Transfer," 3/8/88, (PB88-219480/AS).

NCEER-88-0001 "Workshop on Seismic Computer Analysis and Design of Buildings With Interactive Graphics," by J.F. Abel and C.H. Conley, 1/18/88, (PB88-187760/AS).

NCEER-88-0002 "Optimal Control of Nonlinear Flexible Structures," J.N. Yang, F.X. Long and D. Wong, 1/22/88, (PB88-213772/AS).

NCEER-88-0003 "Substructuring Techniques in the Time Domain for Primary-Secondary Structural Systems," by G. D. Manolis and G. Juhn, 2/10/88, (PB88-213780/AS).

NCEER-88-0004 "Iterative Seismic Analysis of Primary-Secondary Systems," by A. Singhal, L.D. Lutes and P. Spanos, 2/23/88, (PB88-213798/AS).

NCEER-88-0005 "Stochastic Finite Element Expansion for Random Media," P. D. Spanos and R. Ghanem, 3/14/88, (PB88-213806/AS).

NCEER-88-0006 "Combining Structural Optimization and Structural Control," F. Y. Cheng and C. P. Pantelides, 1/10/88, (PB88-213814/AS).

NCEER-88-0007 "Seismic Performance Assessment of Code-Designed Structures," H.H-M. Hwang, J-W. Jaw and H-J. Shau, 3/20/88, (PB88-219423/AS).

NCEER-88-0008 "Reliability Analysis of Code-Designed Structures Under Natural Hazards," H.H-M. Hwang, H. Ushiba and M. Shinozuka, 2/29/88.

NCEER-88-0009 "Seismic Fragility Analysis of Shear Wall Structures," J-W Jaw and H.H-M. Hwang, 4/30/88.

NCEER-88-0010 "Base Isolation of a Multi-Story Building Under a Harmonic Ground Motion - A Comparison of Performances of Various Systems," F-G Fan, G. Ahmadi and I.G. Tadjbakhsh, 5/18/88.

NCEER-88-0011 "Seismic Floor Response Spectra for a Combined System by Green's Functions," F.M. Lavelle, L.A. Bergman and P.D. Spanos, 5/1/88.

NCEER-88-0012 "A New Solution Technique for Randomly Excited Hysteretic Structures," G.Q. Cai and Y.K. Lin, 5/16/88.

NCEER-88-0013 "A Study of Radiation Damping and Soil-Structure Interaction Effects in the Centrifuge," K. Weissman, supervised by J.H. Prevost, 5/24/88, to be published.

NCEER-88-0014 "Parameter Identification and Implementation of a Kinematic Plasticity Model for Frictional Soils," J.H. Prevost and D.V. Griffiths, to be published.

NCEER-88-0015 "Two- and Three-Dimensional Dynamic Finite Element Analyses of the Long Valley Dam," D.V. Griffiths and J.H. Prevost, 6/17/88, to be published.

NCEER-88-0016 "Damage Assessment of Reinforced Concrete Structures in Eastern United States," A.M. Reinhorn, M.J. Seidel, S.K. Kunnath and Y.J. Park, 6/15/88.

NCEER-88-0017 "Dynamic Compliance of Vertically Loaded Strip Foundations in Multilayered Viscoelastic Soils," S. Ahmad and A.S.M. Israil, 6/17/88.

NCEER-88-0018 "An Experimental Study of Seismic Structural Response With Added Viscoelastic Dampers," R.C. Lin, Z. Liang, T.T. Soong and R.H. Zhang, 6/30/88.

NCEER-88-0019 "Experimental Investigation of Primary - Secondary System Interaction," G.D. Manolis, G. Juhn and A.M. Reinhorn, 5/27/88, to be published.

NCEER-88-0020 "A Response Spectrum Approach For Analysis of Nonclassically Damped Structures," J.N. Yang, S. Sarkani and F.X. Long, 4/22/88.

NCEER-88-0021 "Seismic Interaction of Structures and Soils: Stochastic Approach," A.S. Veletsos and A.M. Prasad, 7/21/88, to be published.

NCEER-88-0022 "Identification of the Serviceability Limit State and Detection of Seismic Structural Damage," E. DiPasquale and A.S. Cakmak, 6/15/88.

NCEER-88-0023 "Multi-Hazard Risk Analysis: Case of a Simple Offshore Structure," B.K. Bhartia and E.H. Vanmarcke, 7/21/88, to be published.

NCEER-88-0024 "Automated Seismic Design of Reinforced Concrete Buildings," Y.S. Chung, C. Meyer and M. Shinozuka, 7/5/88.